The background of the slide features a collage of two photographs of UCLA campus buildings. On the left is the iconic Campanile tower, and on the right is the Old Chapel building. The text is overlaid on this background.

Seismic Response Assessment and Protection of Bridges

Jian Zhang, Ph.D.
Assistant Professor

*Department of Civil and Environment Engineering
University of California, Los Angeles*

UCLA

Civil & Environmental Engineering Department

Henry Samueli School of Engineering and Applied Science

My Journey



2010



UCLA

My Academic Background



E-mail:

zhangj@ucla.edu

Phone:

(310) 825-7986

Office:

5731G Boelter Hall
CEE Department
UCLA

Education

- ❑ B.E. (Civil Engineering), Nanjing University of Technology
- ❑ M.E. (Geotechnical Engineering), Southeast University
- ❑ M.S. & Ph.D. (Structural Engineering & Mechanics), University of California at Berkeley

Academic Experience

- ❑ University of Illinois, Urban-Champaign (UIUC), 10/02-06/05
- ❑ University of California, Los Angeles, 7/05-present

Professional Services

- ❑ Associate Editor, ASCE Journal of Bridge Engineering
- ❑ Vice Chair, ASCE/SEI Performance-Based Design for Structures Committee; ASCE/SEI Structural Control Committee
- ❑ Member, ASCE/SEI Seismic Effects Committee; NEEScomm Simulation Steering Committee;
- ❑ Member of ASCE, EERI, NEES, CUREE

University of California, Los Angeles (UCLA)



Royce Hall



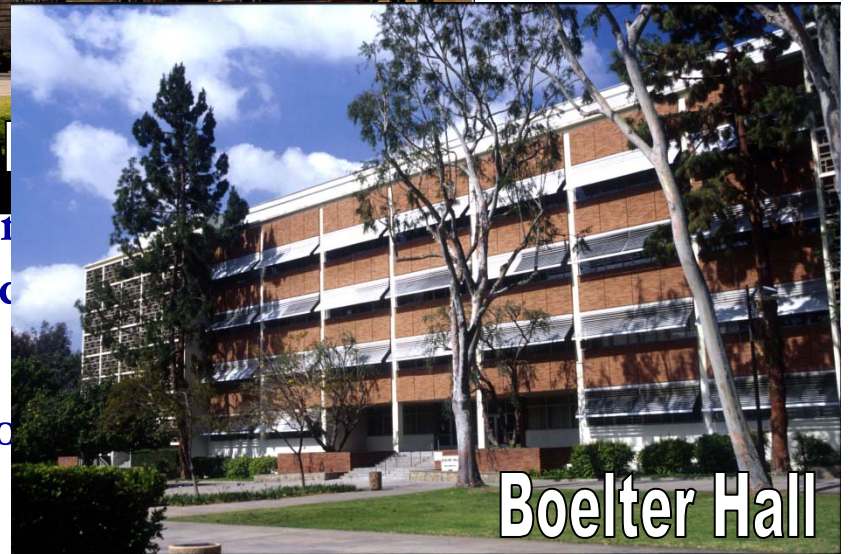
Santa Monica



UCLA
BRUINS



Powell



Boelter Hall

CEE Department – Structure Group



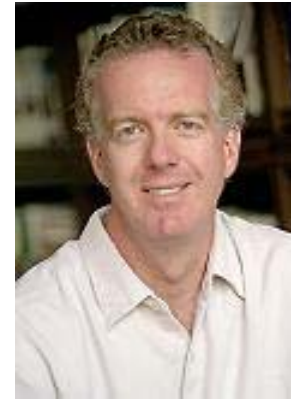
JS Chen



Woody Ju



Ertugrul Taciroglu



John Wallace



Jian Zhang



Thomas Sabol
Adjunct Prof.



Robert Nigbor
Research Eng.+



Stanley Dong
Emeritus



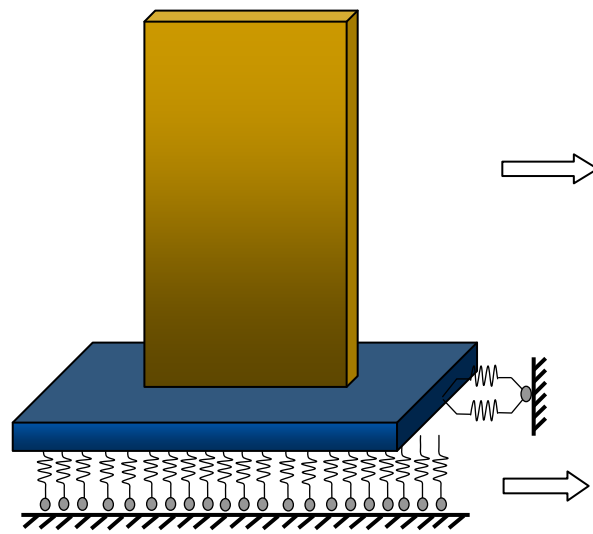
Lewis Felton
Emeritus

My Research Interests

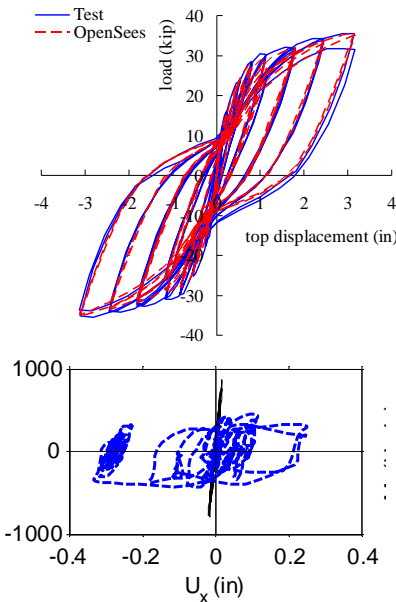
- Earthquake engineering, structural dynamics and mechanics
 - Model-Based Simulations of Seismic Response of Structures (e.g. behavior, design and analysis of complex RC wall systems; seismic simulation of bridges under multi-directional loadings; fragility functions of bridges due to liquefaction induced lateral spreading)
 - Nonlinear Model and Analysis of Structural Elements (e.g. axial-shear-flexural interactive model of RC columns; inelastic displacement demand of bridge columns)
 - Soil-Foundation-Structure Interaction (e.g. nonlinear behavior of shallow foundation; kinematic response of pile foundation, embankment, dimensional analysis of SFSI systems; 3D global dynamic analysis of liquefaction-induced lateral spreading)
 - Earthquake Hazard Mitigation Using Protective Devices (e.g. fragility functions of base isolated bridges; seismic protection of bridges considering soil-structure interaction, adaptive stiffness and damping devices)
 - Ground Motion Characteristics (e.g. near-fault ground motions; pulses)

Shear Wall Buildings

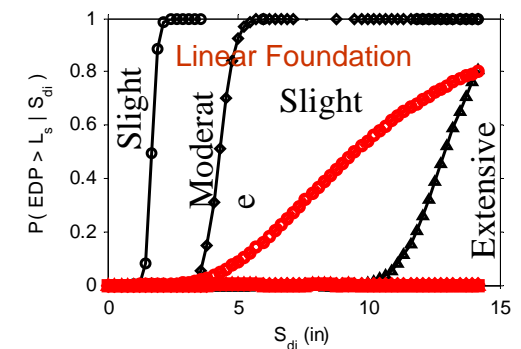
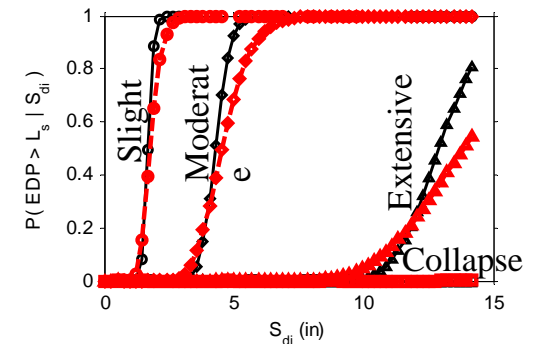
- Probabilistic seismic demand analysis of RC shear walls considering soil-structure interaction effects
 - Realistic models for shear-walls and foundations
 - Fragility functions of building systems



Shear Wall-Foundation-Soil System

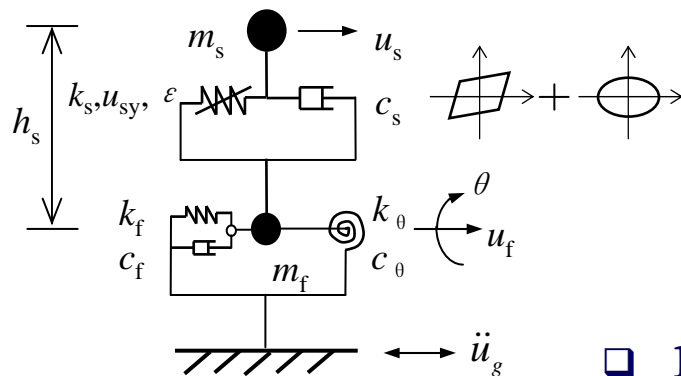
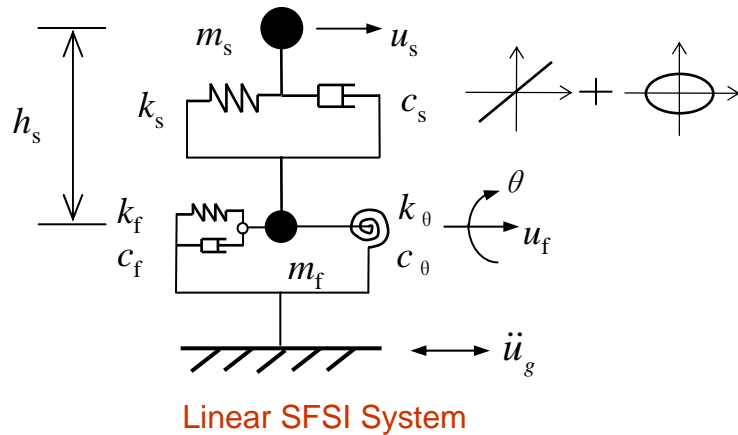


Nonlinear Modeling of Structural and Foundation Elements

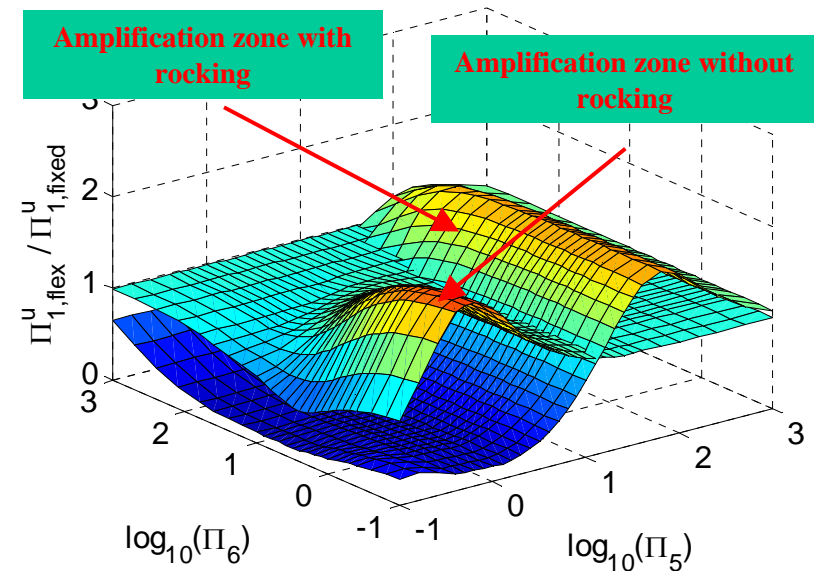


Nonlinear Foundation

Dimensional Analysis of SFSI Systems



$$\Pi_2=2, \Pi_3=0.05, \Pi_4=0.25, \Pi_7=0.2, \log_{10}(\Pi_8)=-2, \log_{10}(\Pi_9)=-2$$

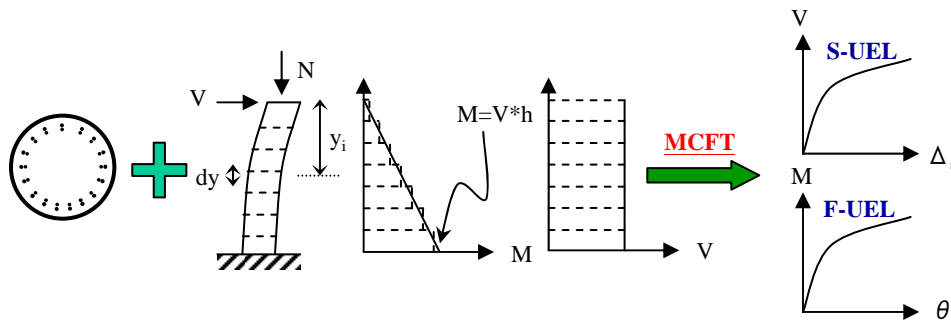


Dimensional Analysis of SFSI Systems

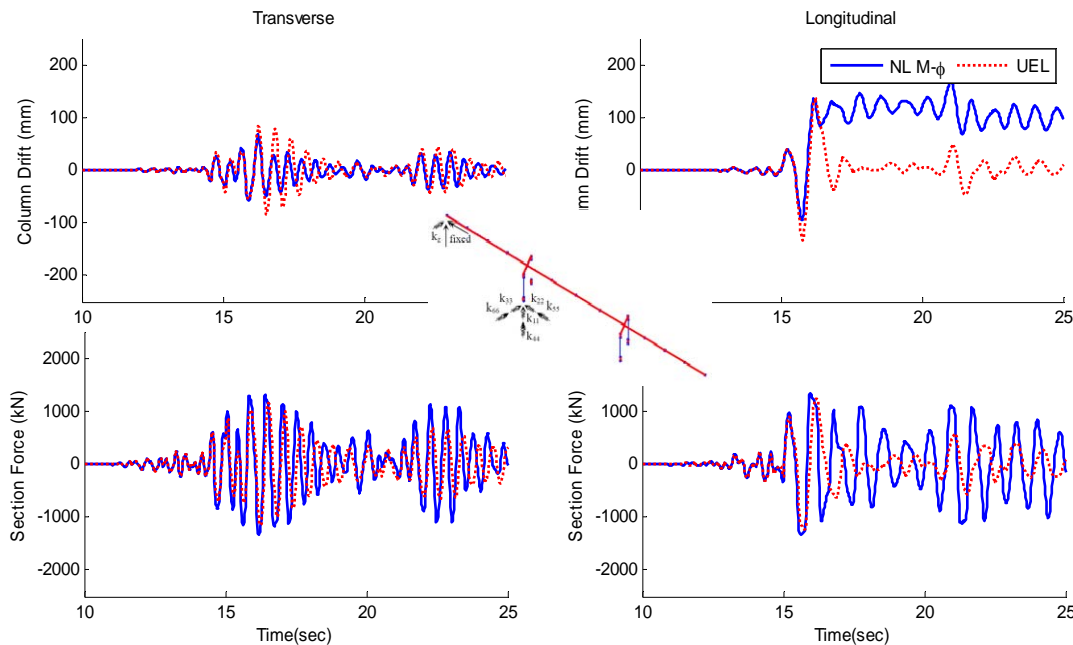
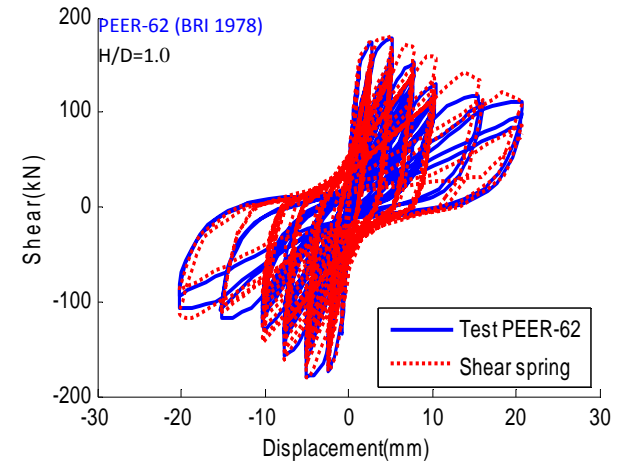
□ Dimensionless formulation of peak responses

$$\frac{u_{drift}^{\max} \omega_p^2}{a_p} = \phi \left(\frac{\omega_s}{\omega_p}, \xi_s, \frac{m_f}{m_s}, \frac{k_f}{k_s}, \frac{c_f \omega_s}{k_f}, \frac{I_t}{m_s h_s^2}, \frac{k_\theta}{k_f h_s^2}, \frac{c_\theta \omega_s}{k_\theta}, \frac{u_{sy} \omega_p^2}{a_p}, \epsilon_s \right)$$

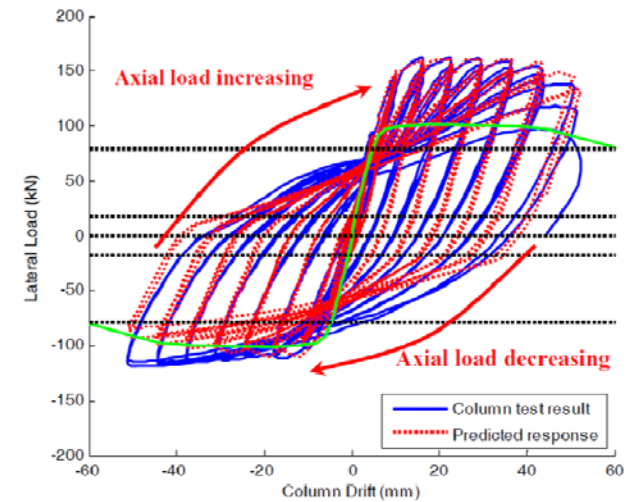
Bridge Responses Under Combined Actions



Shear-Flexure Interaction Hysteretic Model for Bridge Columns



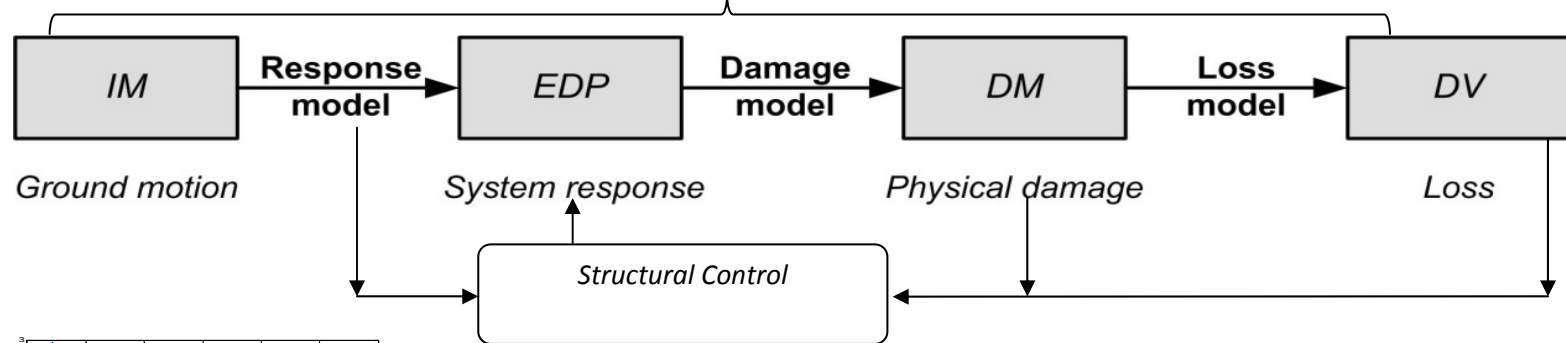
Seismic Response Assessment with Shear-Flexure Interaction



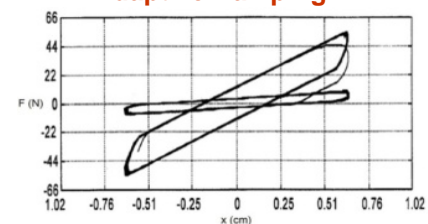
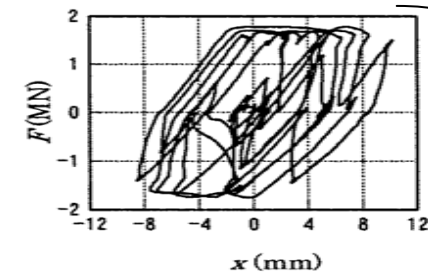
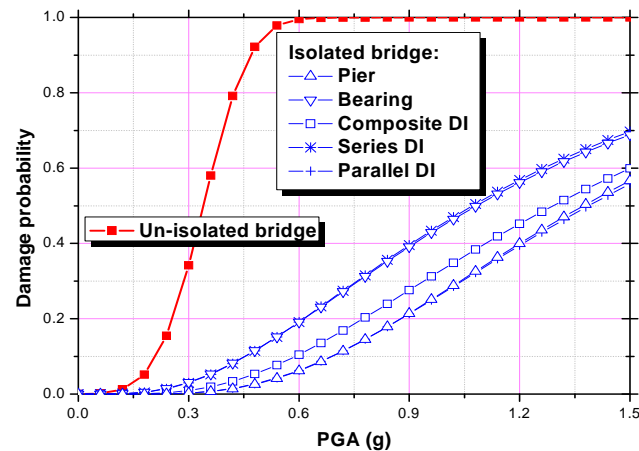
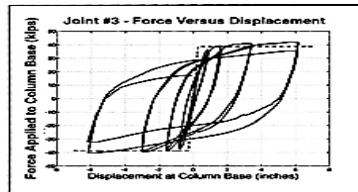
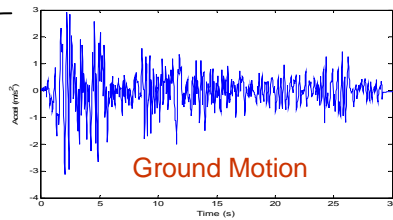
Axial-Shear-Flexure Interaction Model

Performance-Based Implementation of Protective Devices

PBEE Framework



Uncertainties & Variability



Optimal Design of ASD Devices

Presentation Outline

- ❑ Introduction
- ❑ Modeling Soil-Structure Interaction Effects
 - Macro-spring and P-y model for embankment and pile foundation
 - Static and dynamic procedure for lateral spreading
- ❑ Modeling Axial-Shear-Flexure Interaction of RC Columns for Seismic Response Assessment of Bridges
 - Axial-shear-flexure interaction
 - Inelastic displacement demand
- ❑ Fragility Functions of Bridges Under Seismic Shaking and Lateral Spreading
 - Effects of structural characterizations
- ❑ Optimum Design of Seismic Isolation for Bridges Using Fragility Function Method
 - PBEE framework

Earthquake Damages



57 deaths, 1500 injured, 1000s homeless, >\$15B cost

1994 Northridge Earthquake, Los Angeles, CA

Bridge Responses Under Seismic Shaking

□ Damage mechanisms

- Excessive strength demand
- Excessive displacement demand



1995 Kobe

□ Observed damages

- Flexure and shear failure of columns
- Unseating and pounding of decks
- Foundation movement and failure



1999
Chi-Chi



1994
Northridge



2010
Chile

Liquefaction and Lateral Spreading

□ Liquefaction

- Liquefaction occurs when the strength and stiffness of a soil are reduced due to excessive pore water pressure accumulated during seismic events.
- Liquefaction leads to:
 - Loss of bearing capacity due to reduced strength
 - Lateral spreading due to cyclic mobility

□ Lateral spreading

- Large lateral displacement of soil associated with the sloping ground and the non-liquefied crust layer with underlying liquefaction layer.
- Lateral spreading leads to large displacement and force demand on bridge foundations



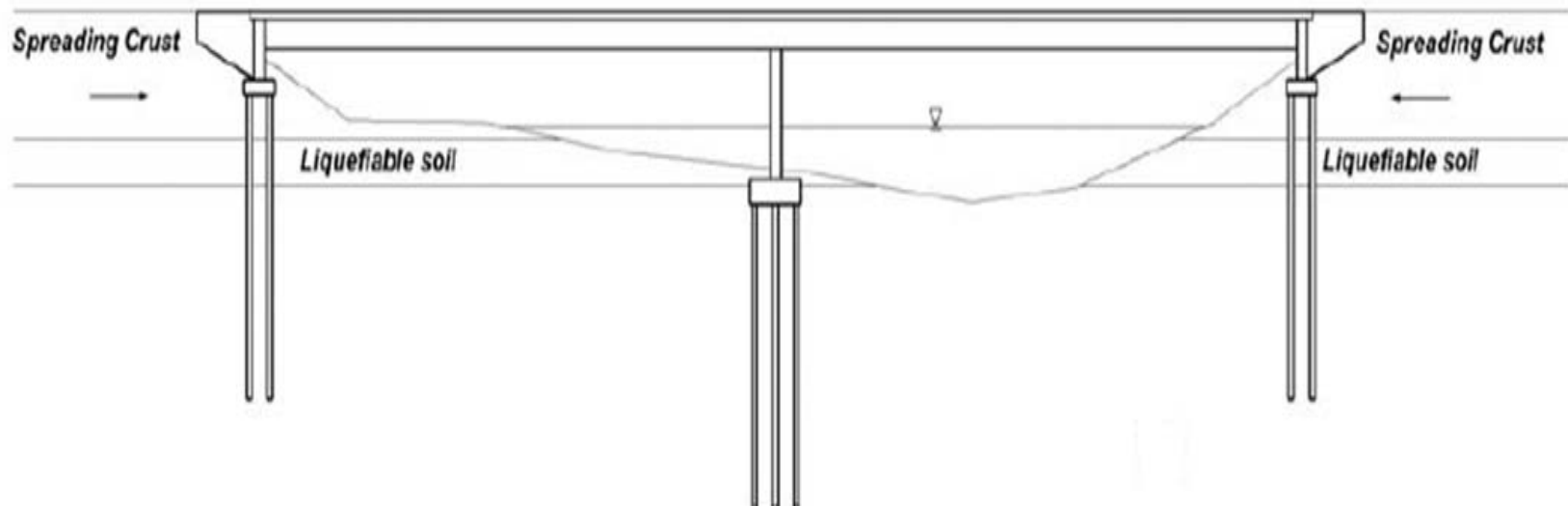
1964 Alaska



1964 Niigata

Bridge Responses Under Lateral Spreading

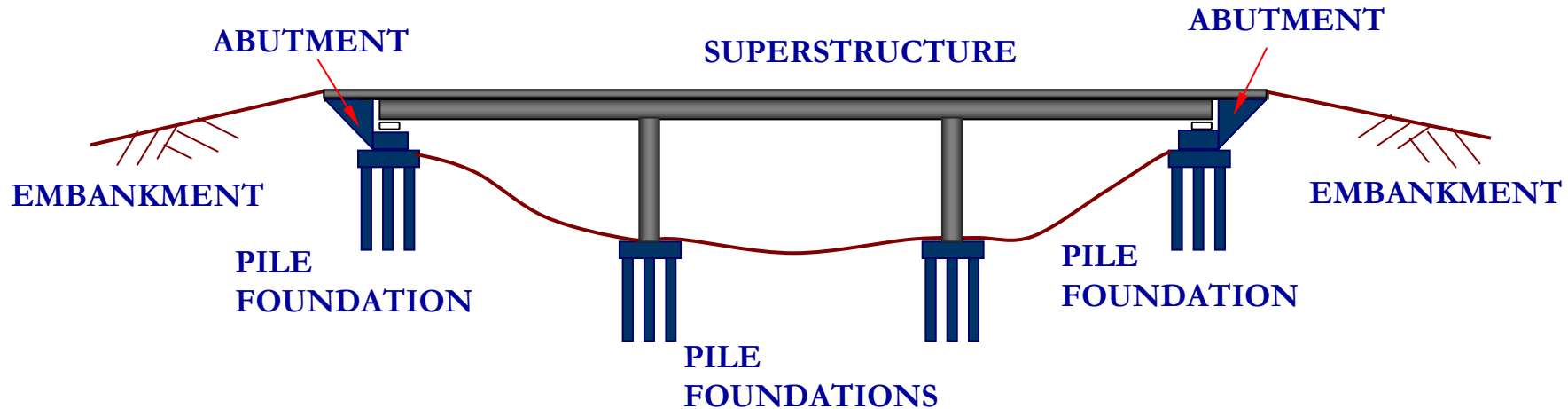
- Lateral spreading typically along the longitudinal direction toward river bank



- Dependent on the structural configurations and foundation details, bridges can perform catastrophically or reasonably well
- 3D global behavior may be necessary due to skewed geometry, multi-directional shaking and inertial effects

Major Challenges for Response Assessment of Bridges

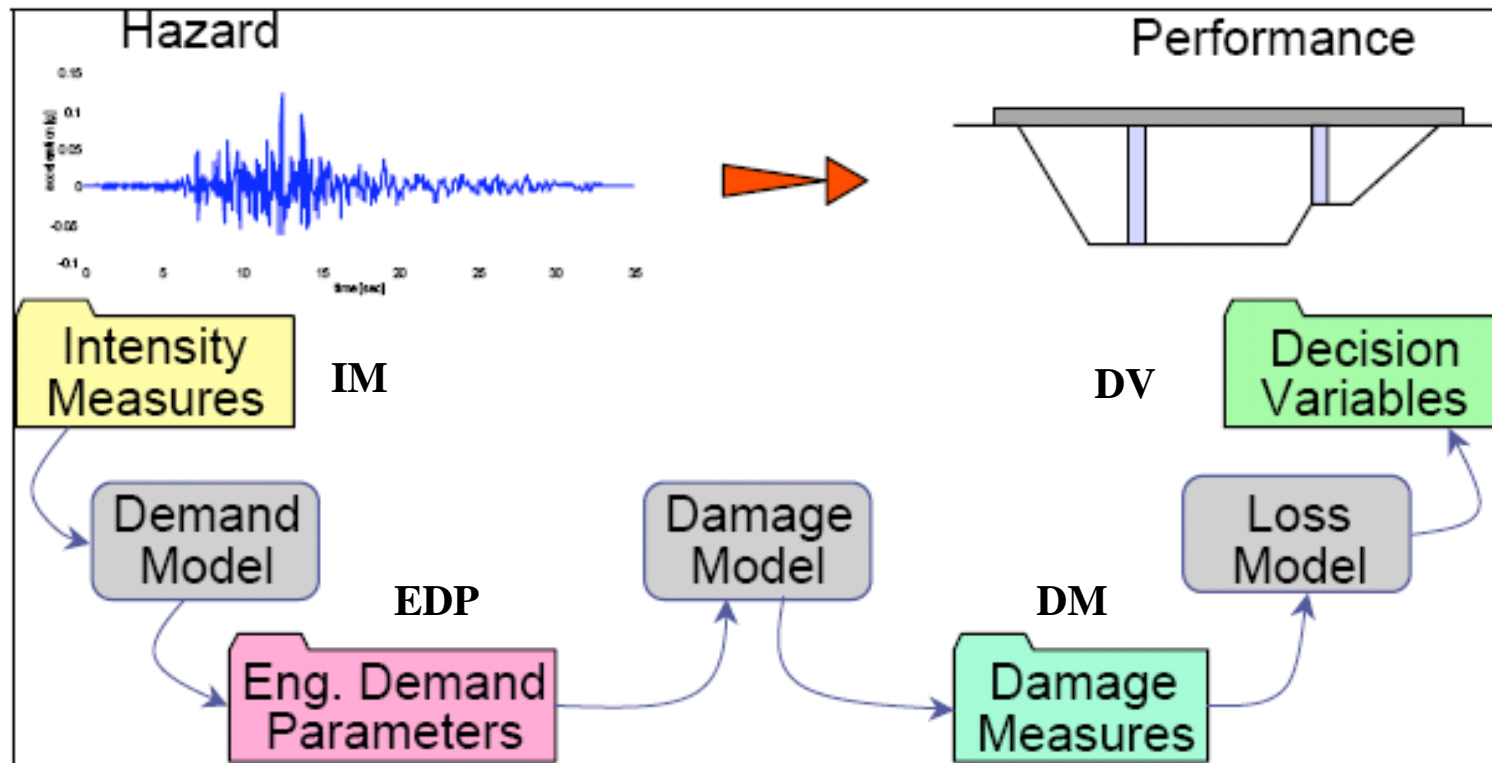
❑ Complex Soil-Foundation-Structure Interaction Effects



- ❑ Nonlinear behavior of structural components (e.g. strength deterioration, stiffness softening and pinching)
- ❑ Variability in structural characterization (e.g. type, connection, vintage etc.) and foundation characteristics
- ❑ Uncertainties in ground motions, material properties and geological profiles

Probabilistic Seismic Response Assessment of Bridges

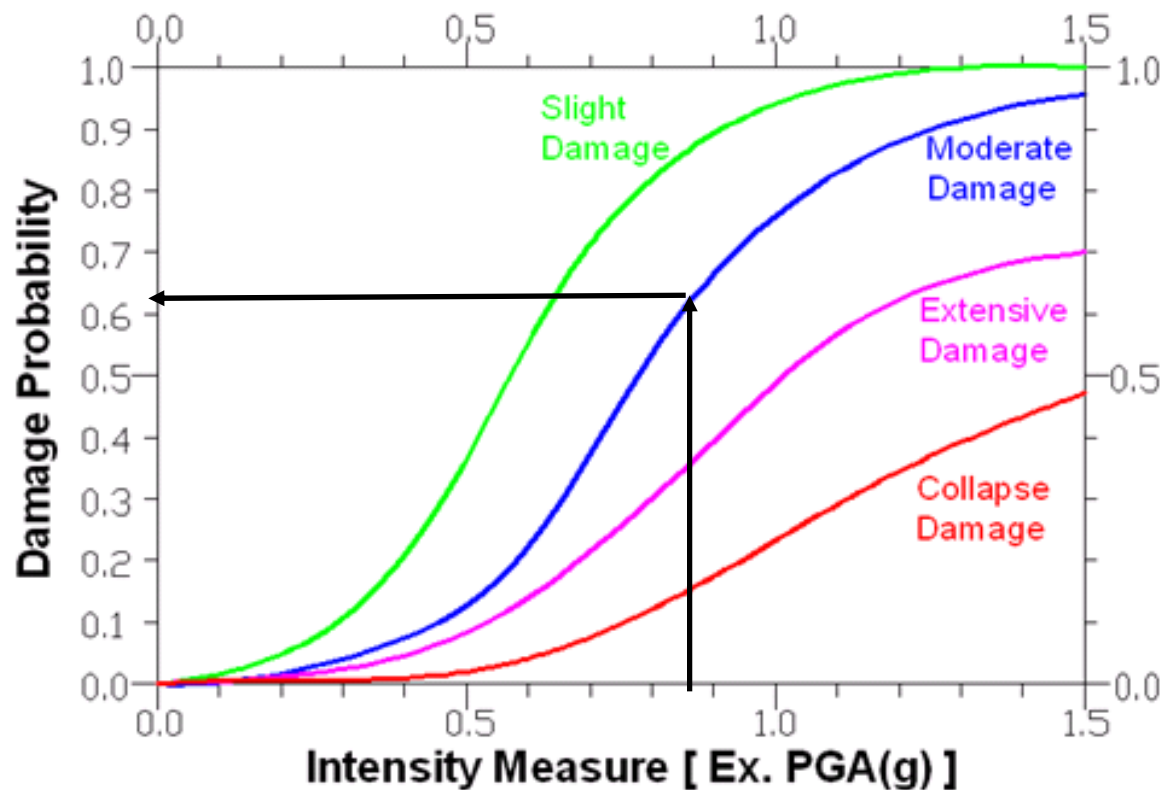
□ Performance-Based Earthquake Engineering (PBEE) Framework



(Mackie and Stojadinović, 2003)

Fragility Function Method

- Fragility function defines the conditional probability of attaining or exceeding certain damage level given the earthquake intensity.



Seismic Protection of Bridges



- ❑ Rapid implementation of energy dissipation devices for seismic protection of bridges
- ❑ Evaluate the efficiency of modern technologies, in particular, supplemental energy dissipation devices to mitigate the damaging effects of earthquake on highway bridges

Soil-Foundation-Structure Interaction for Seismic Response Analysis of Bridges

Contributors:

**Professor Jian Zhang
Mr. Yili Huo (Ph.D. Student)
Professor Scott Brandenberg**

The research presented here was funded by Caltrans and PEER Transportation Program

Outline

- ❑ Introduction
- ❑ Embankment and Pile Foundation
 - Kinematic Response Function
 - Dynamic Stiffness (“Spring” and “Dashpot” Constants)
 - Simple Procedure
- ❑ Seismic Analysis of Highway Bridges Under Seismic Shaking
 - Eigenvalue Analysis
 - Time History Analysis
- ❑ Seismic Analysis of Bridges Under Liquefaction Induced Lateral Spreading
 - Equivalent Static Analysis Approach
 - Global Dynamic Analysis Approach
- ❑ Conclusions

Introduction

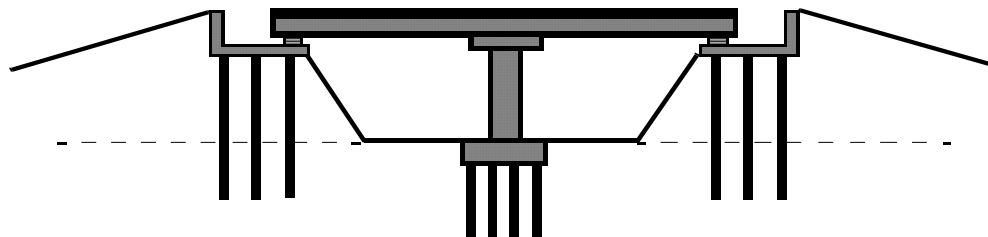
□ Motivation

- Damages experienced by highway bridges during past earthquakes due to seismic shaking and liquefaction-induced lateral spreading
- Poor understanding of the effects of soil-structure-interaction (SSI)
- Challenging numerical models for liquefaction-induced lateral spreading

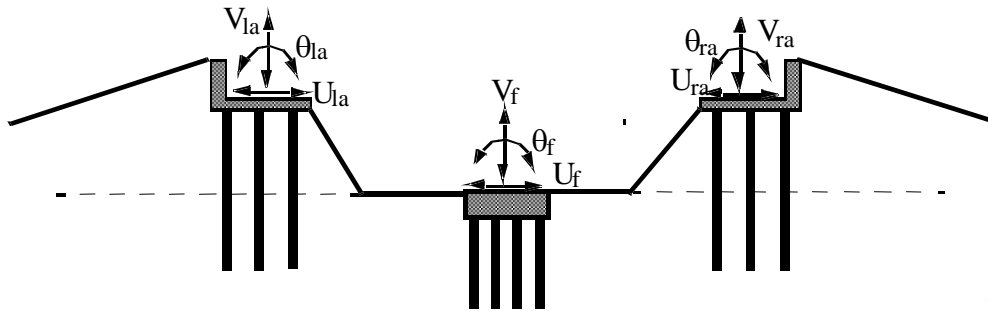
□ Objectives

- Develop and validate an analysis procedure accounting for soil-structure interaction
 - Kinematic and inertial response
 - Macro-spring and p-y models
- Develop an analysis procedure for modeling the lateral spreading and its effects on bridge responses
 - Equivalent static procedure
 - Global dynamic procedure

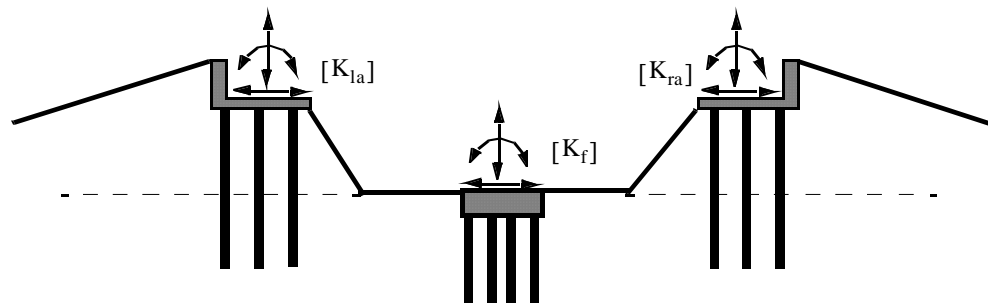
General Procedure for SSI



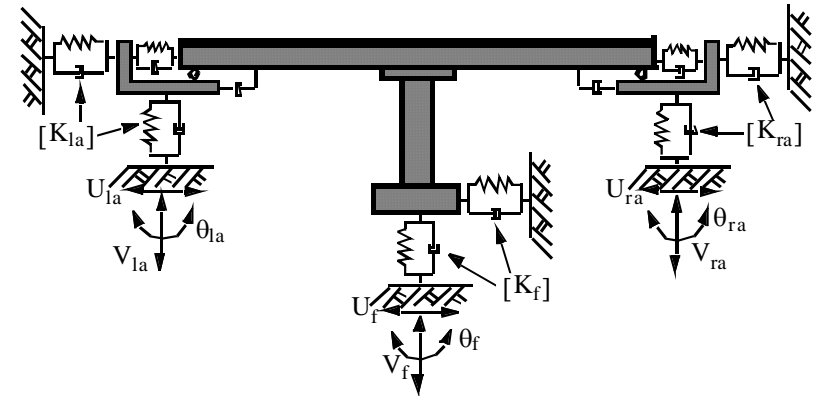
(a) Real System



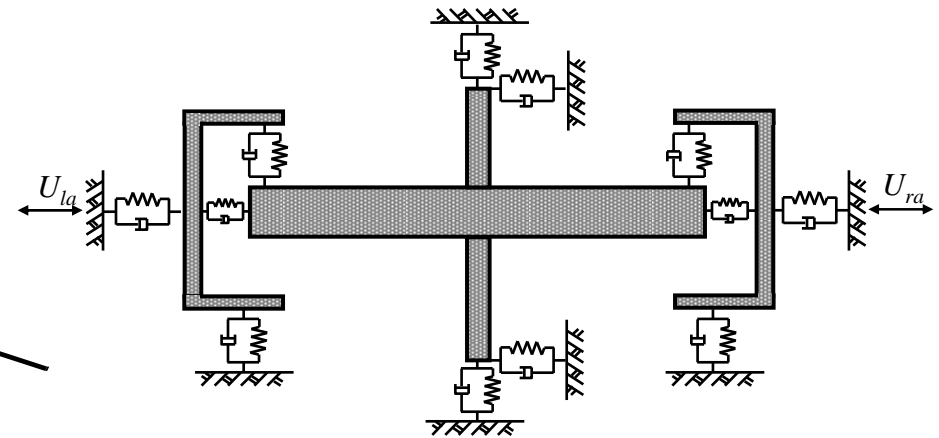
(b) Kinematic-Seismic Response



(c) Dynamic Stiffnesses of Pile Groups and Embankments



(d) Elevation View of Idealized Model



(e) Plan View of Idealized Model

Outline

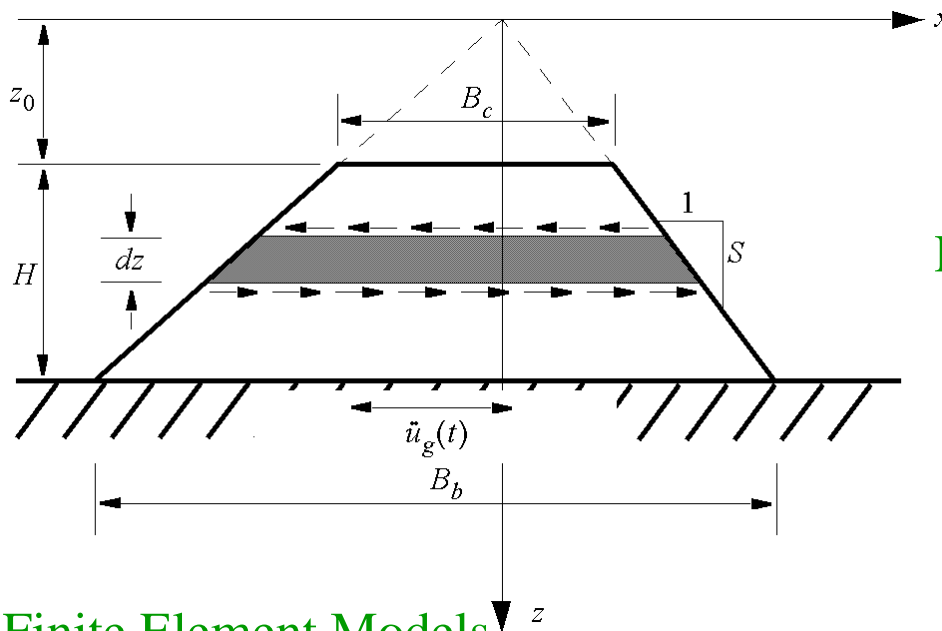
- Introduction
- **Embankment and Pile Foundation**
 - Kinematic Response Function
 - Dynamic Stiffness (“Spring” and “Dashpot” Constants)
 - Simple Procedure
- Seismic Analysis of Highway Bridges Under Seismic Shaking
 - Eigenvalue Analysis
 - Time History Analysis
- Seismic Analysis of Bridges Under Liquefaction Induced Lateral Spreading
 - Equivalent Static Analysis Approach
 - Global Dynamic Analysis Approach

Modeling of Embankment

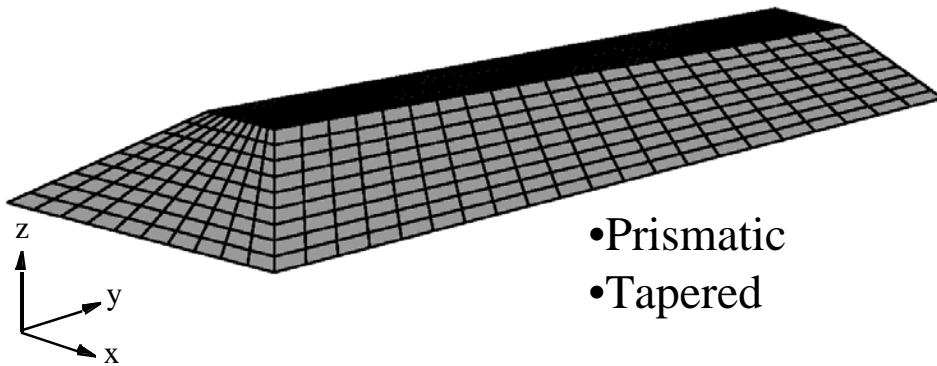
- ❑ Considerations for Response Analysis
 - Motion amplification (Kinematic Response Function)
 - Flexibility (“Spring”, Dynamic Stiffness)
 - Energy dissipation (“Dashpot”, Dynamic Stiffness)
- ❑ Validity of Equivalent Linear Analysis
 - Strain-dependent nonlinear soil behavior
 - System identification studies indicate that linear models provide good fit with measured response of bridge (Werner et al 1987)
 - Elliptical force-displacement loops even under strong earthquakes (Goel & Chopra 1997)
- ❑ Approaches
 - Shear-wedge model (1D)
 - Finite element analysis (2D/3D)

Calculation of Kinematic Response Function

Shear-Wedge Model



Finite Element Models



Analytical Solution for Shear-Wedge Model

$$|I(\omega)| = \left| 1 + \frac{u_x(z_0)}{u_{g0}} \right| = \left| \frac{c_1 J_0(kz_0) + c_2 Y_0(kz_0)}{u_{g0}} \right|$$

Wave number $k = \omega / V_s$

Hysteretic Soil Material:

$$G(\omega) = G_1 + iG_2 \text{sgn}(\omega) = G_1(1 + i\eta \text{sgn}(\omega))$$

Rayleigh Damping: (2D/3D FEM)

$$[C] = \alpha[M] + \beta[K]$$

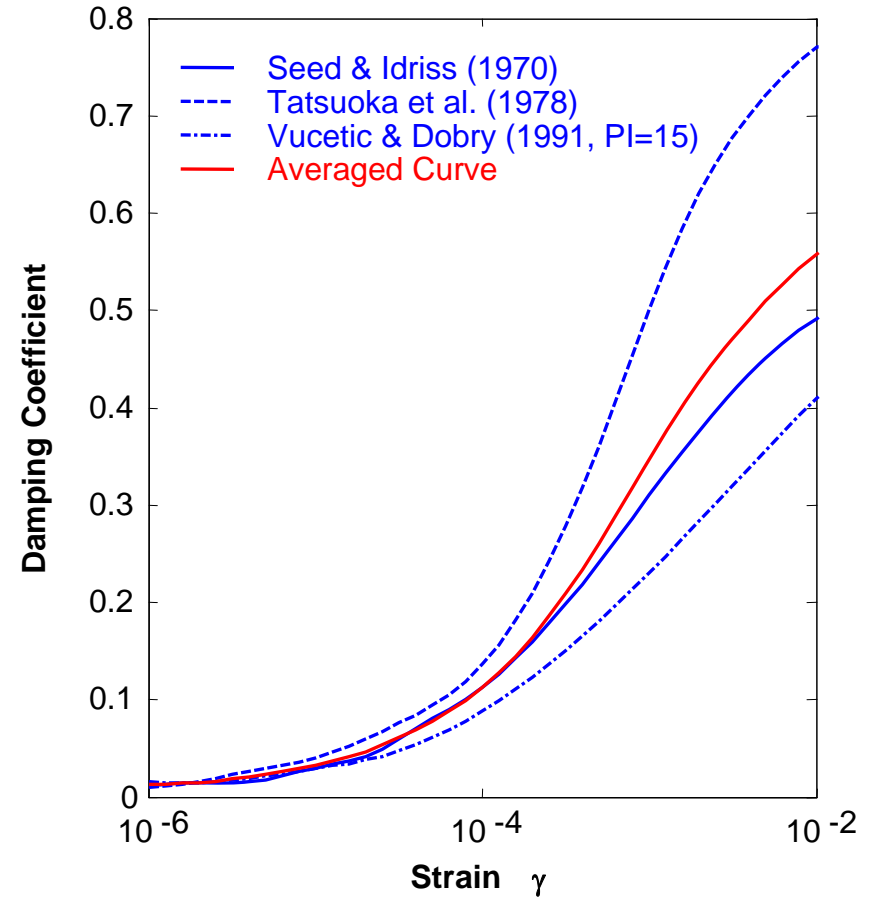
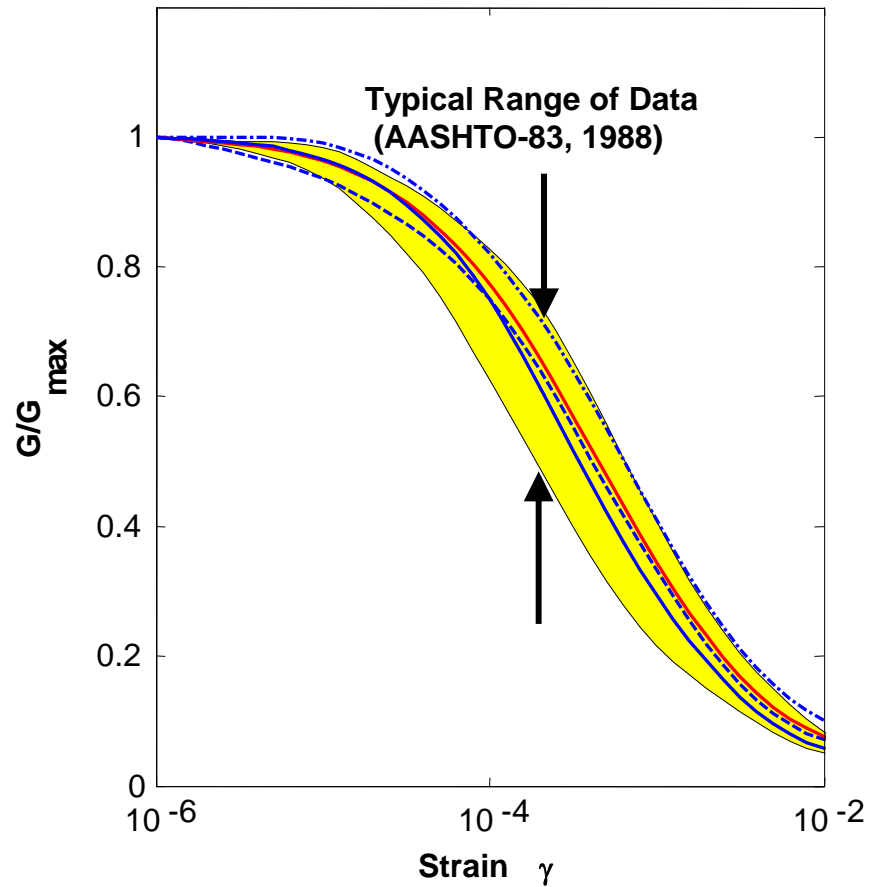
Crest Response:

$$u^c(t) = \frac{1}{2\pi} \int_{-\infty}^{\infty} I(\omega) u^b(\omega) e^{i\omega t} d\omega$$

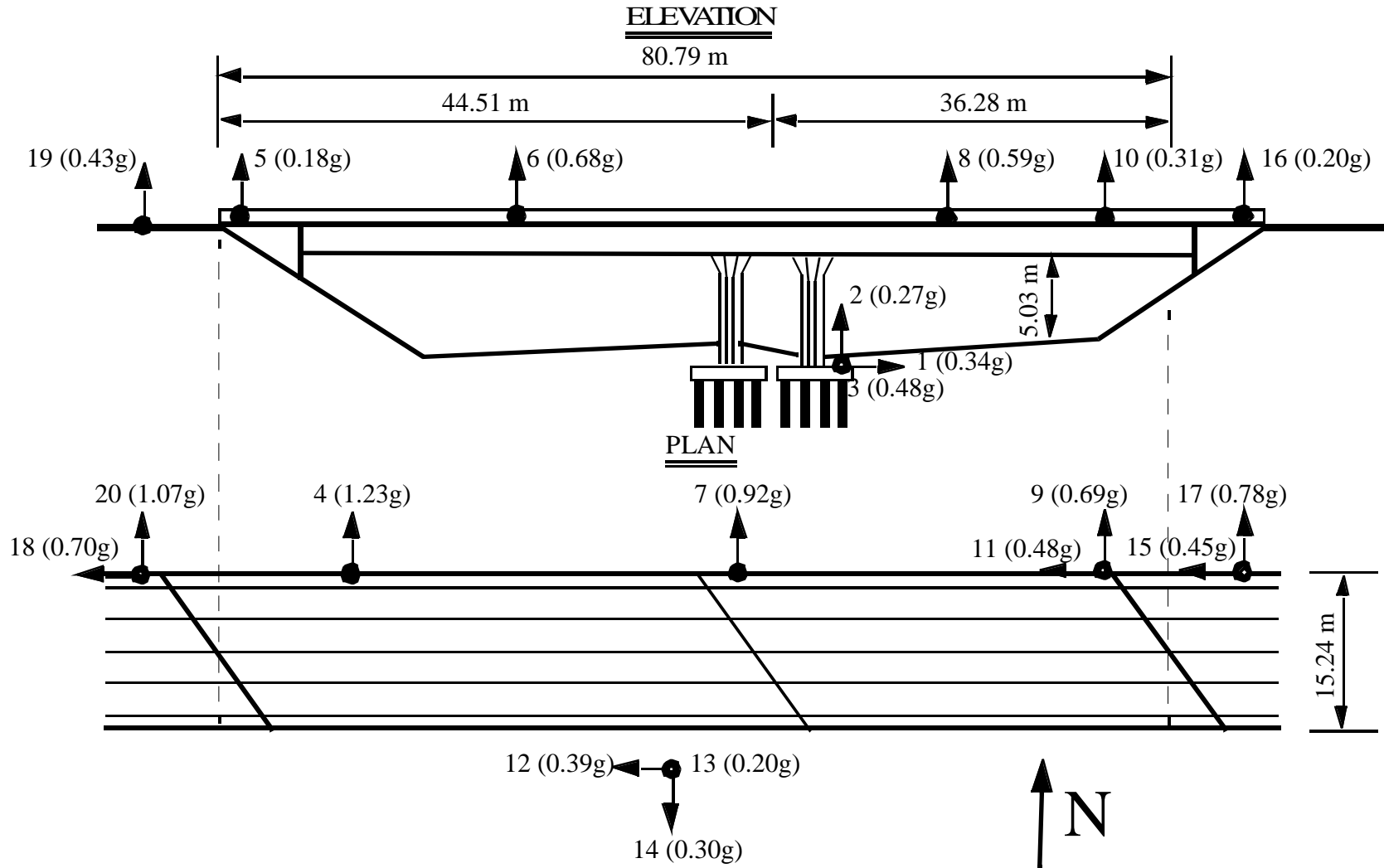
Averaged Strain $\hat{\gamma} = \frac{2}{3} \frac{u_{x, \max}^c}{H}$

Iterative Process !

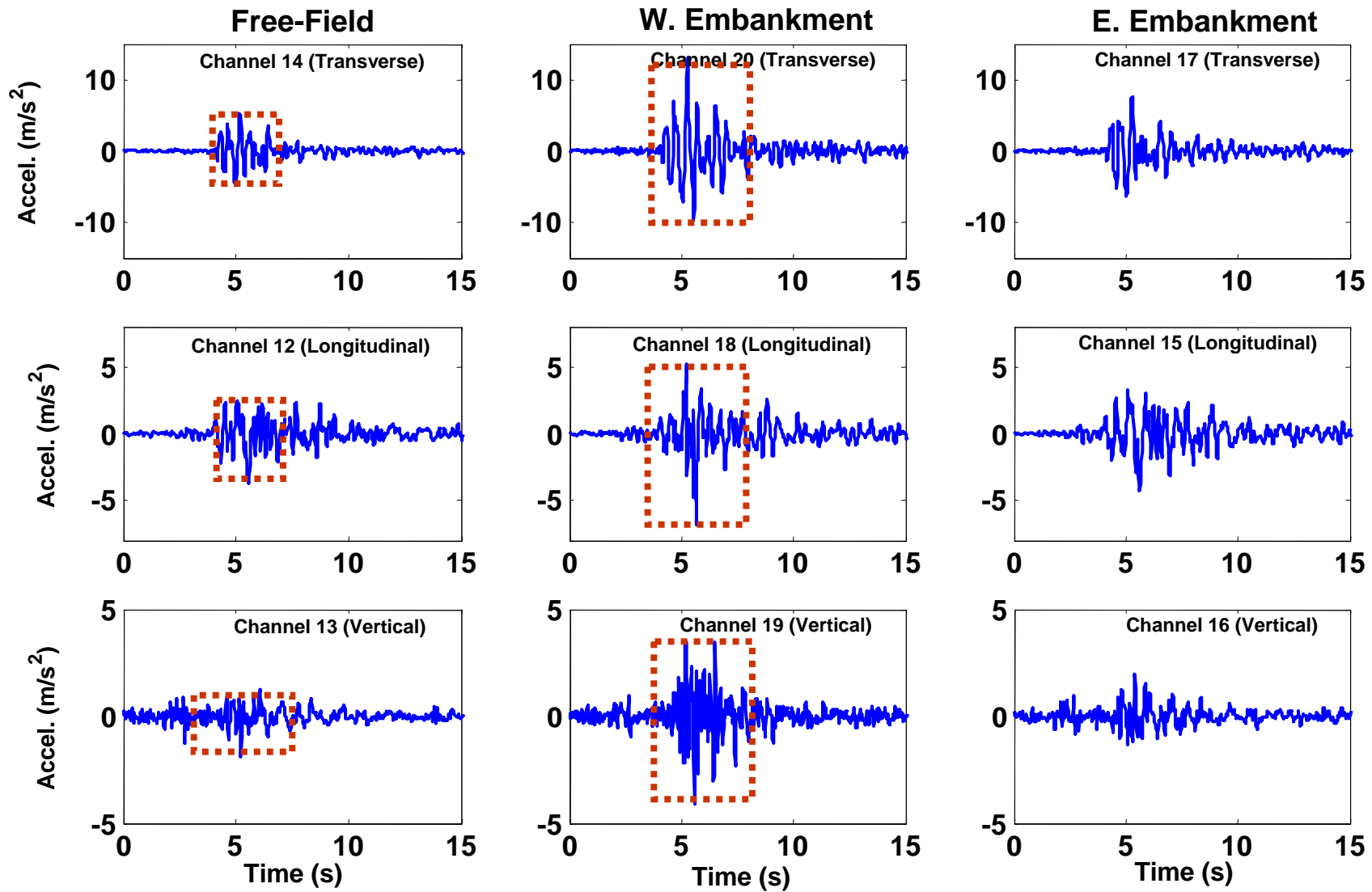
Strain-Dependent Behavior of Soil



Painter Street Bridge (PSB)

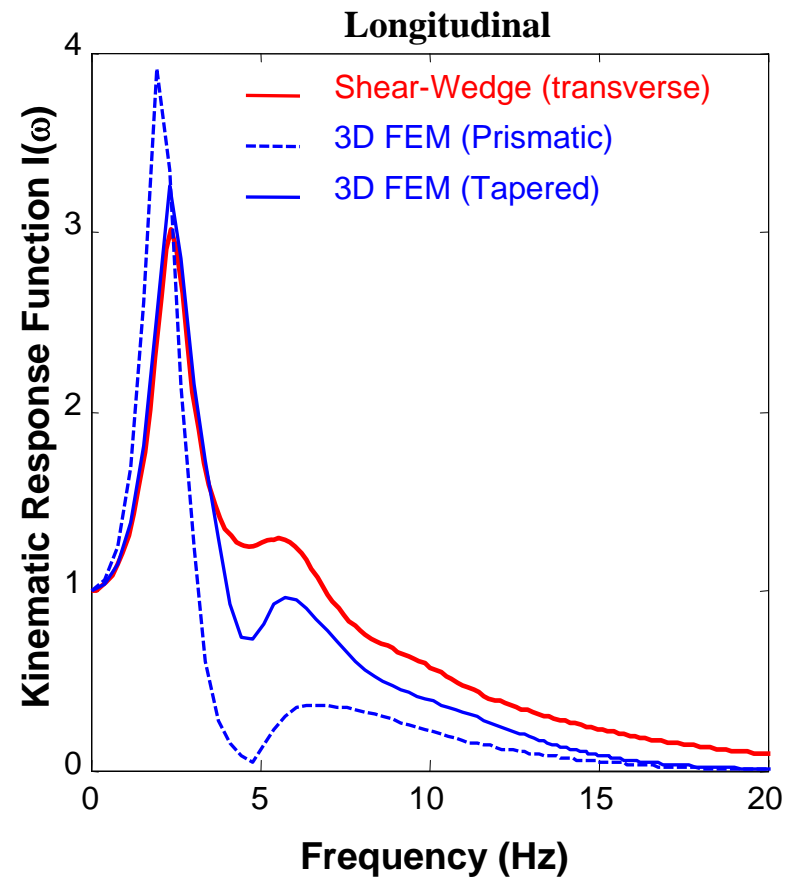
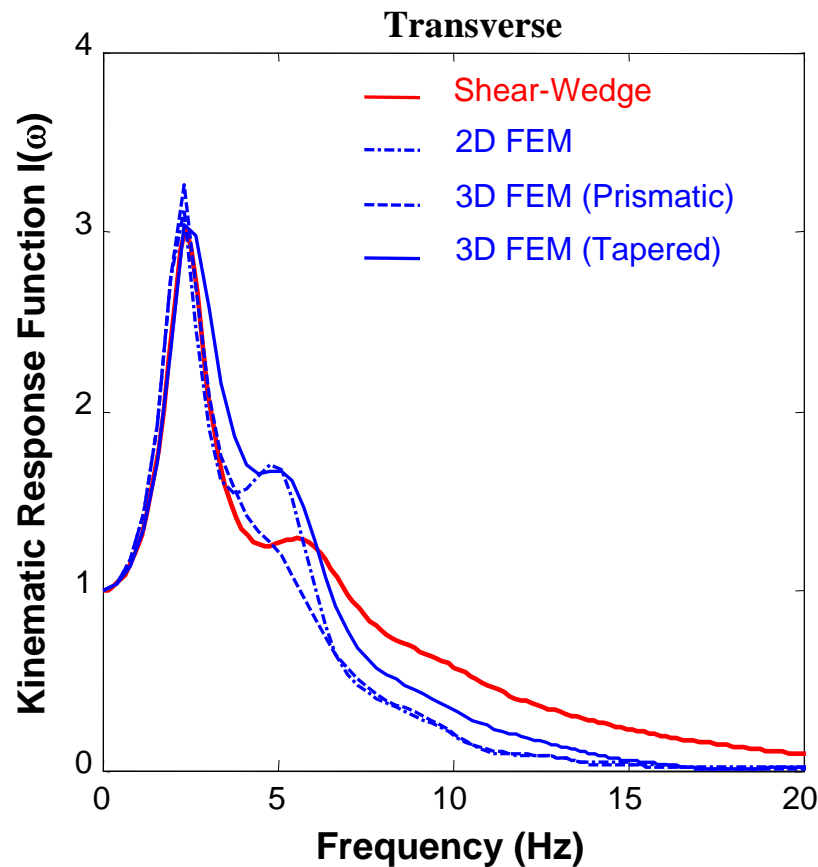


Recorded Motions (PSB, 1992 Petrolia Earthquake)



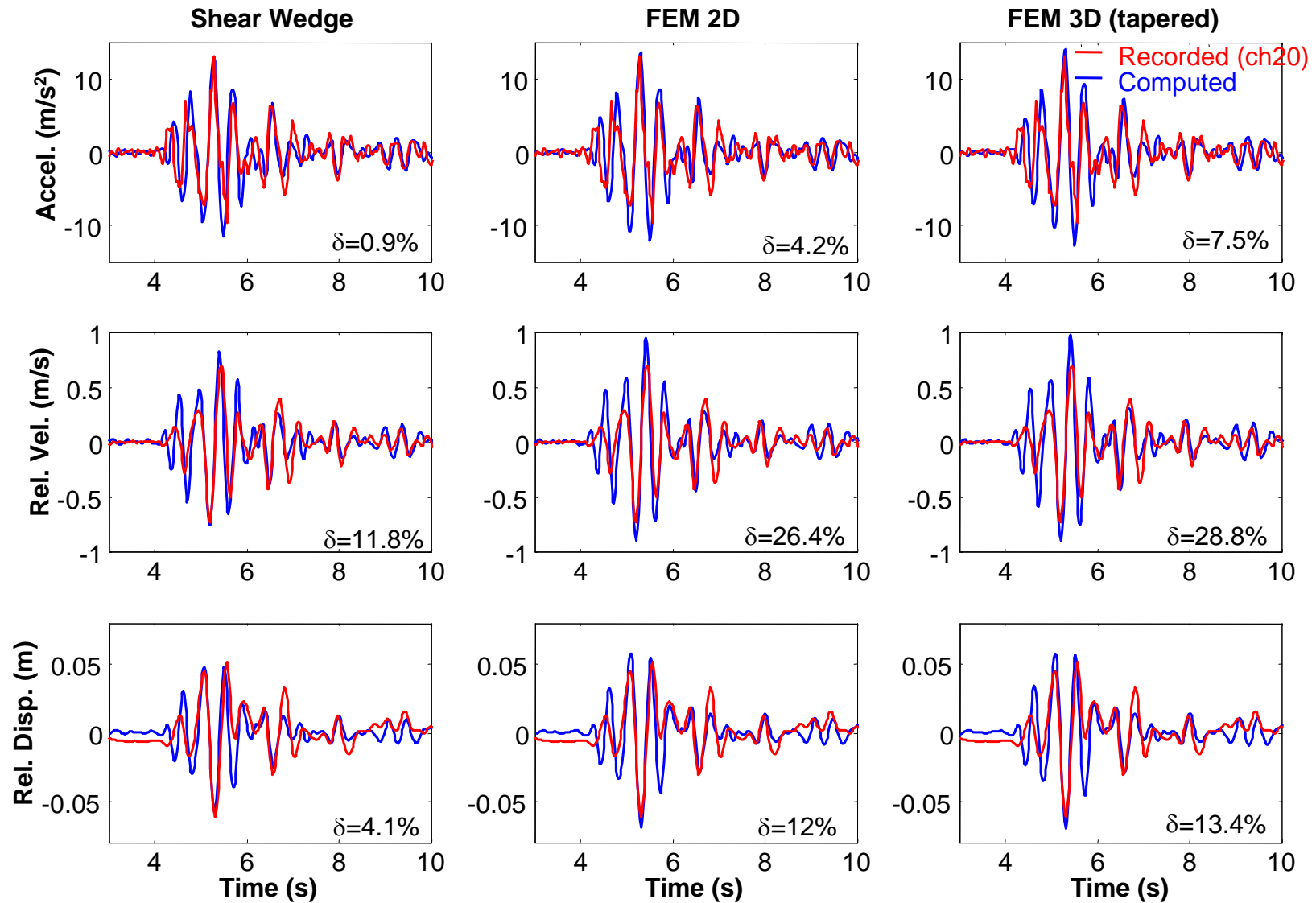
Computed Kinematic Response Functions

Painter Street Bridge ($G=8\text{MPa}$, $\eta=0.5$)

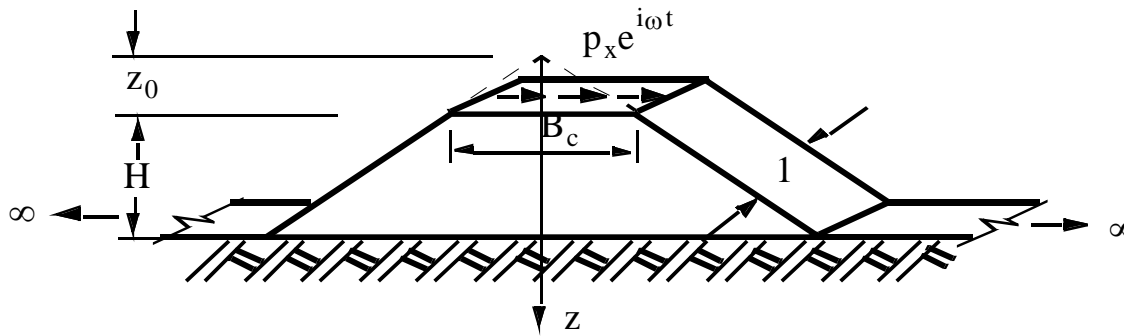


Typical Fundamental Frequency of Highway Bridges: 1.0Hz ~ 3.0Hz

Computed Crest Response (Transverse, PSB)



Dynamic Stiffness of Embankment



Rigid Support

Governing Equation:

$$\frac{\partial^2}{\partial z^2} u_x(z, t) + \frac{1}{z} \frac{\partial}{\partial z} u_x(z, t) = \frac{1}{V_s^2} \frac{\partial^2}{\partial t^2} u_x(z, t)$$

Rigid Support:

$$u_x(z, t)|_{z=z_0+H} = 0 \quad Q(z_0, t) = p_x e^{i\omega t}$$

Flexible Support:

Sommerfeld radiation condition

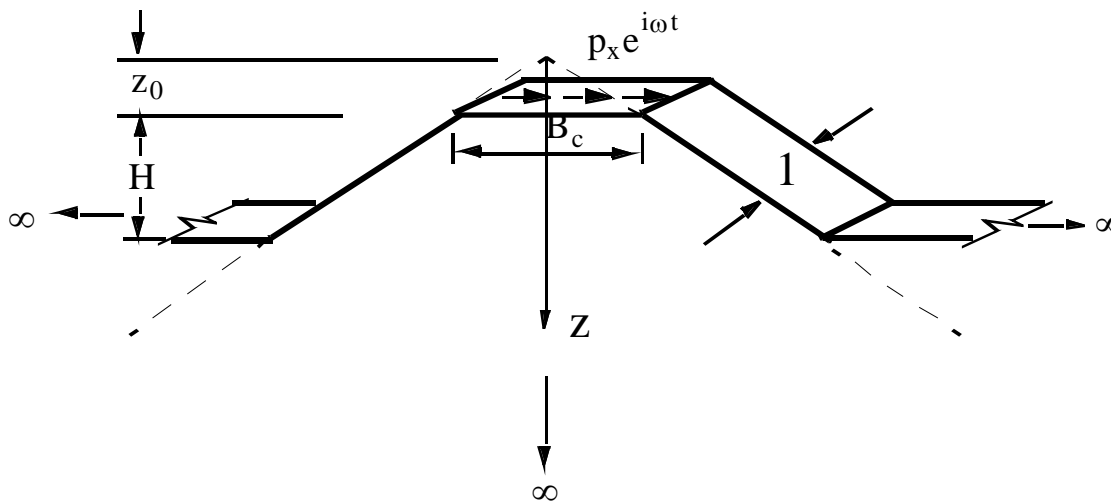
$$Q(z_0, t) = p_x e^{i\omega t}$$

Dynamic Stiffness:

$$p_x(z_0, t) = \hat{k}_x(\omega) u_x(z_0, t)$$

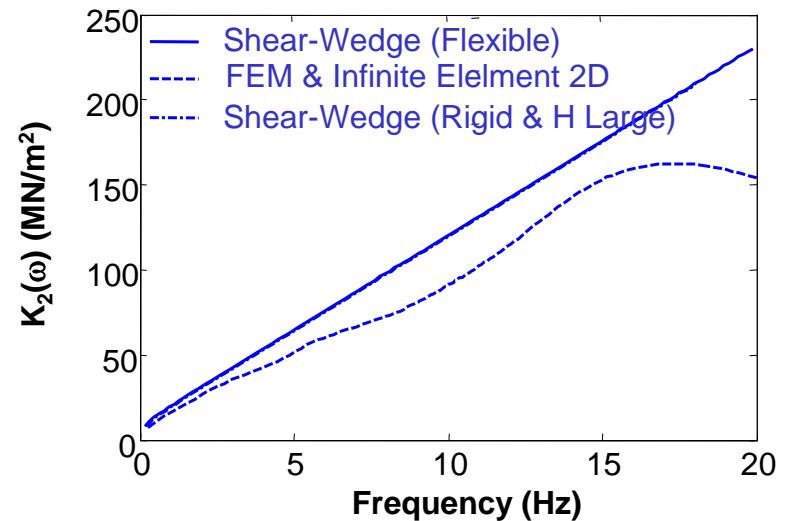
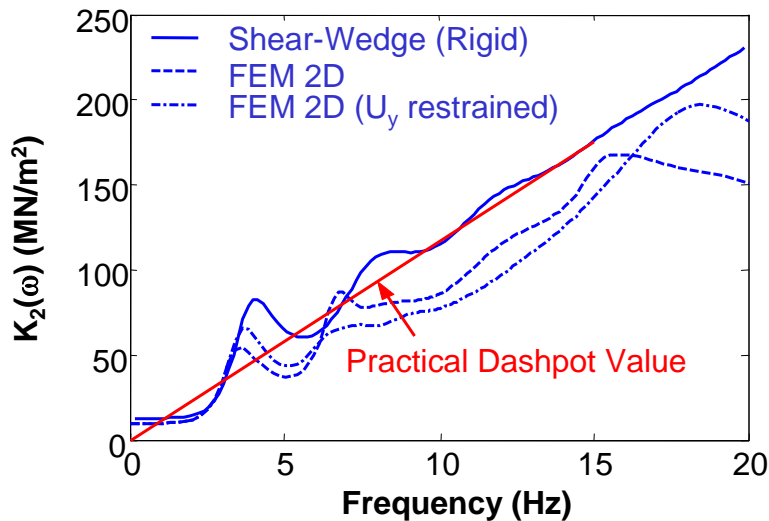
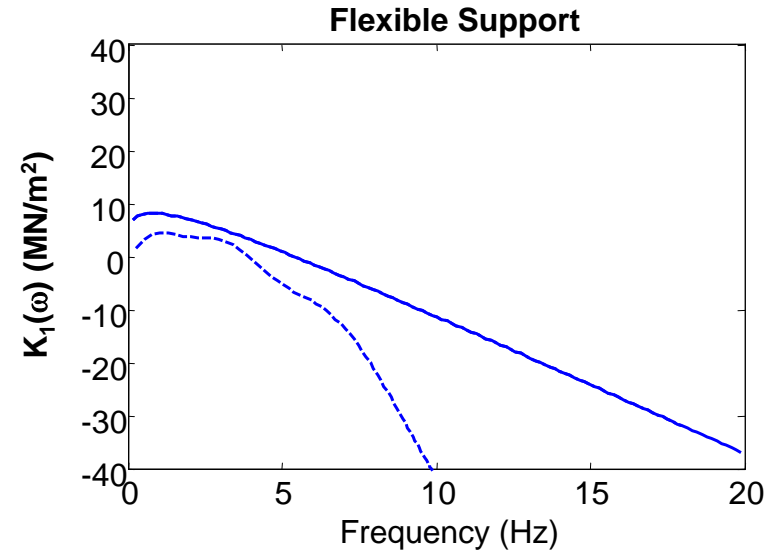
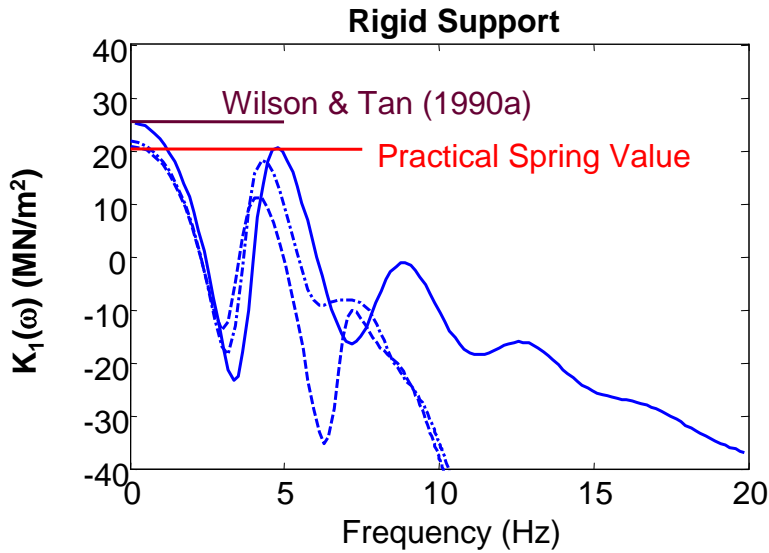
$$\hat{k}_x(0) = \frac{p_x}{u_x} = \frac{GB_c}{z_0 \ln\left(\frac{z_0+H}{z_0}\right)}$$

(Wilson & Tan 1990)

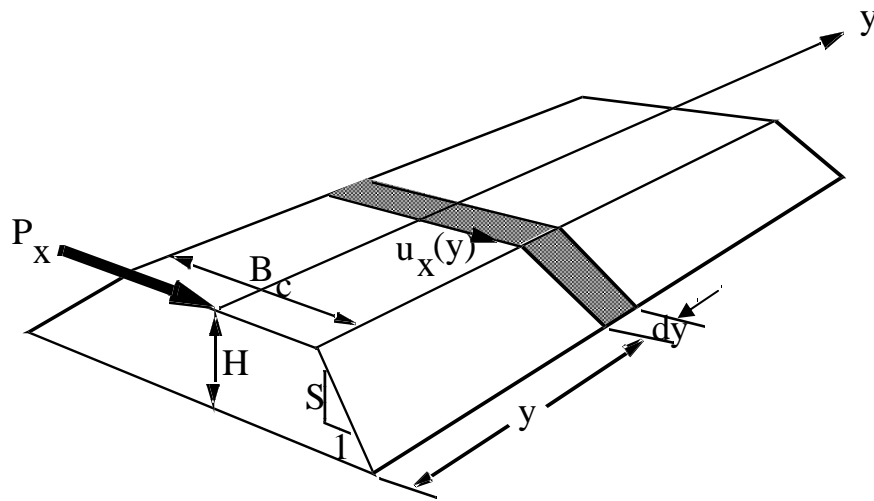


Flexible Support

Computed Dynamic Stiffness (Shear-Wedge)



Estimation of Critical Length L_c



$$\frac{d}{dy}Q(y) - \hat{k}_x u_x(y) = 0$$

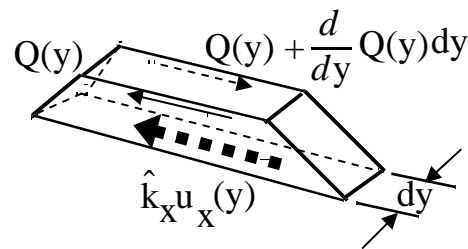
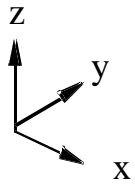
$$Q(y) = AG \frac{d}{dy} u_x(y)$$

$$\lambda = \sqrt{\frac{B_c}{z_0 A \ln(1 + H/z_0)}}$$

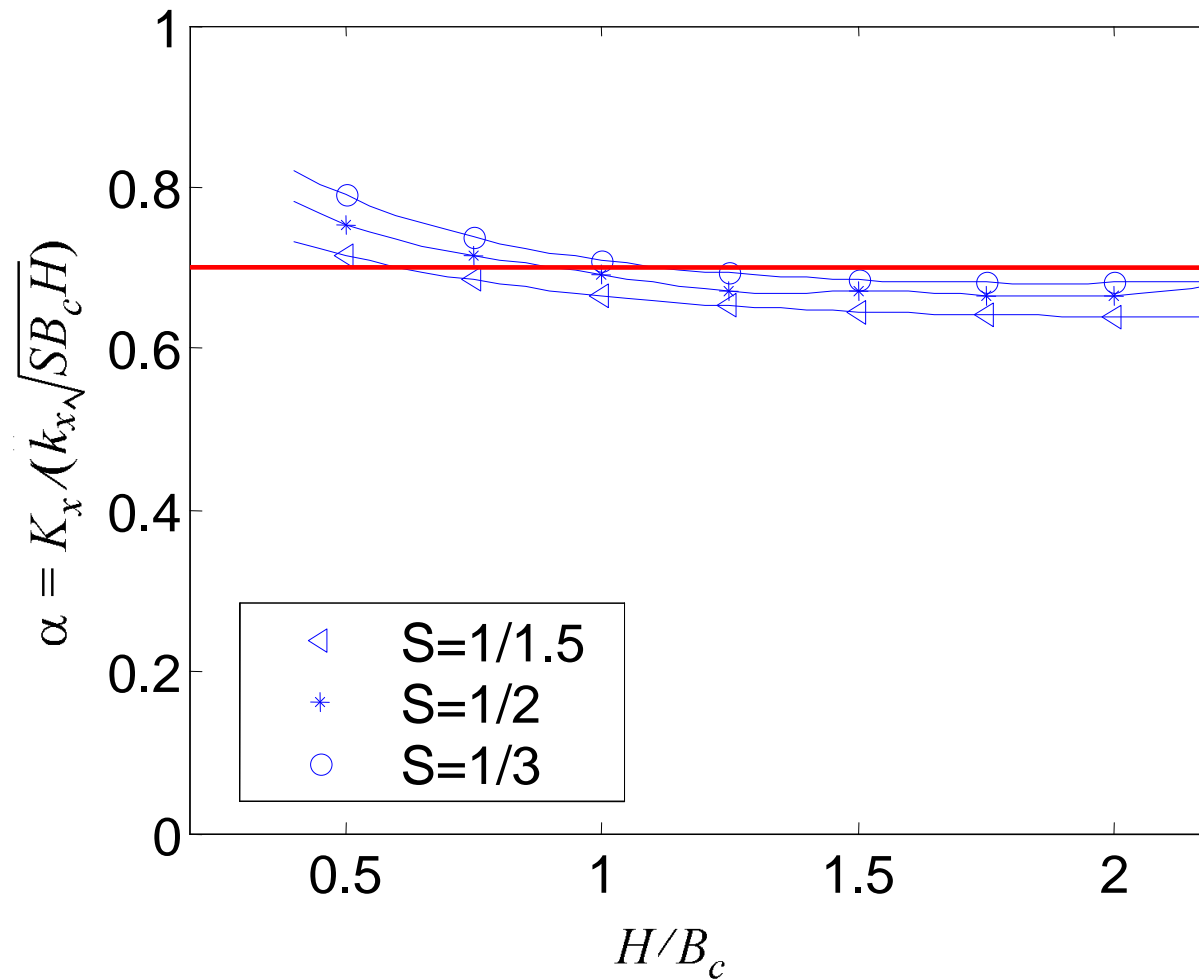
$$u_x(y) = \frac{P}{AG\lambda} e^{-\lambda y}$$

$$K_x = G \sqrt{\frac{2A}{S \ln\left(1 + \frac{2H}{SB_c}\right)}}$$

$$L_c = \frac{K_x}{\hat{k}_x} = \frac{\sqrt{2}}{2} \cdot \sqrt{AS \ln\left(1 + \frac{2H}{SB_c}\right)}$$



Critical Length L_c

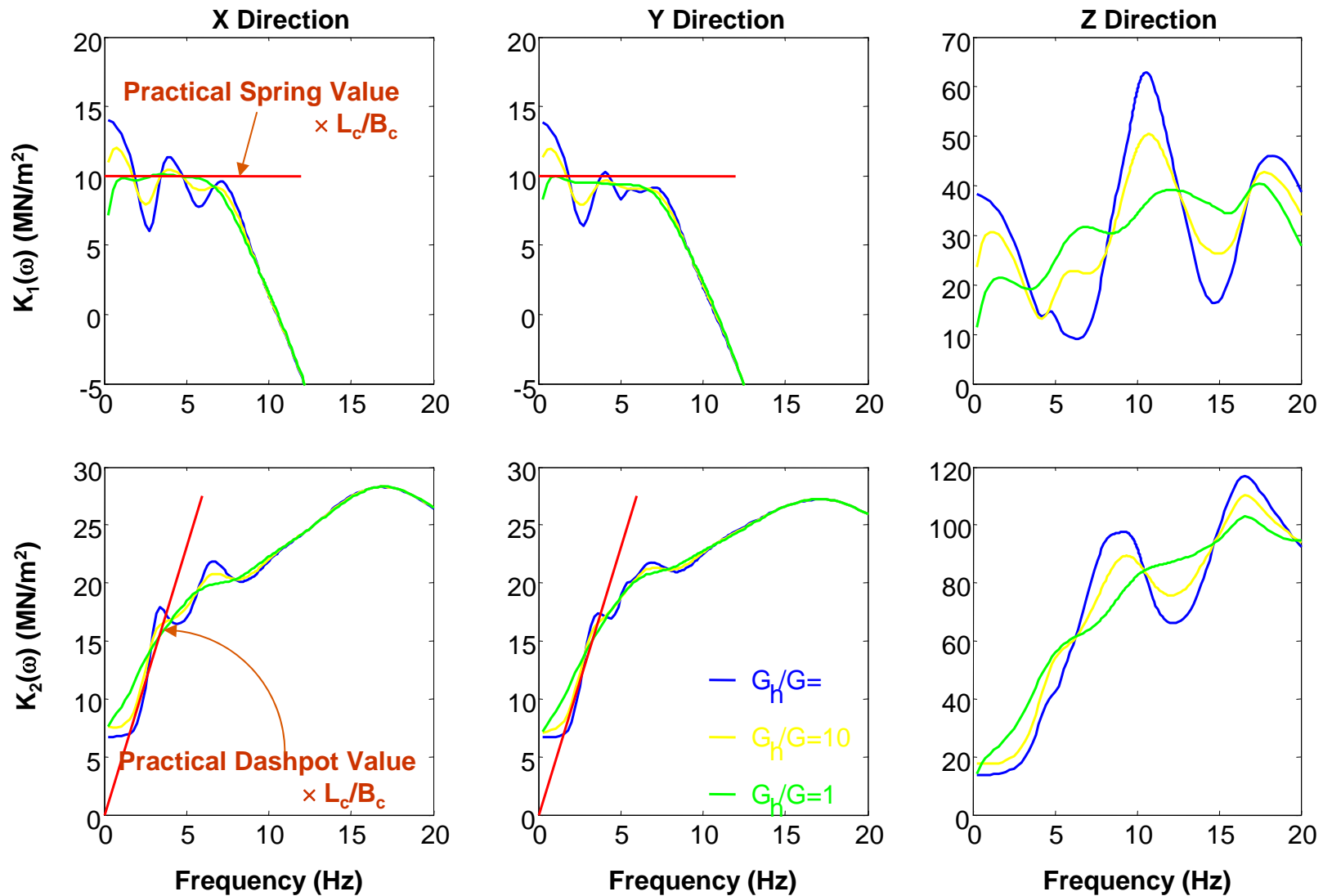


$$L_c = \frac{K_x}{\hat{k}_x} = \alpha \sqrt{SB_c H}$$

$$L_c \approx 0.7 \sqrt{SB_c H}$$

$$\mathcal{K}_x = \hat{k}_x(\omega) \cdot L_c$$

Computed Dynamic Stiffness (3D FEM)



Comparisons of Abutment Stiffness

		Meloland Road Overcrossing H = 7.92m, B _c = 10.36m, S = 1/2, L _c = 4.5m, ρ = 1.6Mg/m ³ , G _{max} = 19MPa, G = 2MPa, η = 0.52			Painter Street Bridge H = 9.6m, B _c = 15.24m, S = 1/2, L _c = 6.0m, ρ = 1.6Mg/m ³ , G _{max} = 58MPa, G = 8MPa, η = 0.50		
Stiffnesses (MN/m ²)		K _x /B _c	K _y /B _c	K _z /B _c	K _x /B _c	K _y /B _c	K _z /B _c
1	Douglas et al. 1991	8.8	8.8	25.4	/	/	/
2	McCallen & Romstad 1994	/	/	/	56.0	53.0	/
3	Werner1994	10.3	/	/	/	/	/
4	Goel & Chopra 1997	/	/	/	9.6~14.0	9.6~46.9	/
5	Price and Eberhard 1998	/	/	/	4.7	/	/
6	Caltrans: Method A	58.6	57.5	/	53.2	57.5	/
7	Caltrans: Method B	7.4	/	/	6.9	/	/
8	Wilson 1988	12.1	12.1	16.1	24.6	24.9	52.5
9	Wilson & Tan 1990a	3.3	/	9.2	13.2	/	37
10	Siddharthan et al 1997	10~48	0.3~1.5	12~54	27~126	0.7~3.4	21.6~101.3
11	FEM 3D	2~3	2~3.1	7.5	9~14	9~13.8	38.2
12	Proposed Procedure	2	2	/	10	10	/

Modeling of Pile Foundation

□ Input Motion at Pile Caps

- For motions that are not rich in high frequencies, the scattered field generated from the difference between pile and soil rigidities is weak
- Support Motion \approx Free-Field Motion

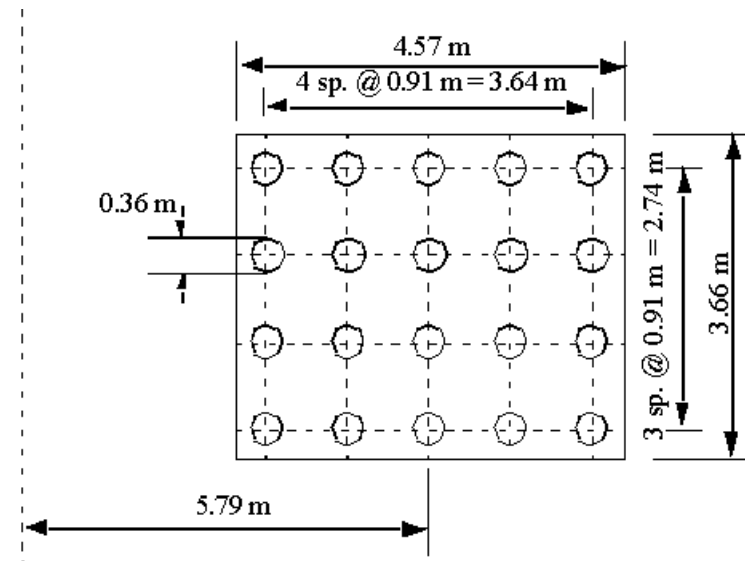
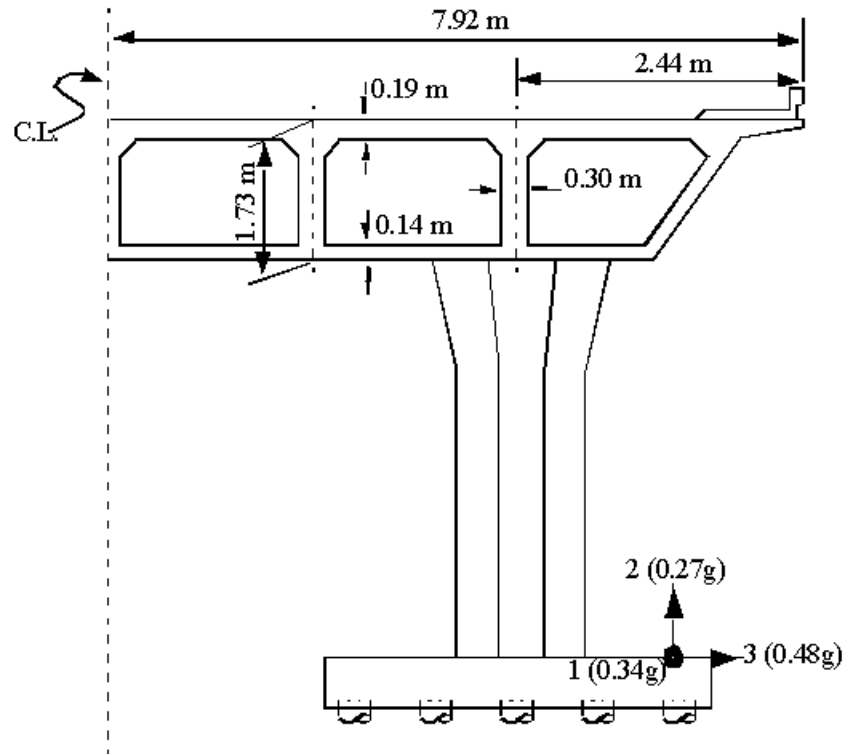
□ Dynamic Stiffnesses

- Single pile-soil system is represented with a dynamic Winkler model with frequency dependent spring and dashpot coefficients
- The group stiffness is obtained using superposition principle, i.e. single pile stiffness in conjunction of dynamic interaction factors

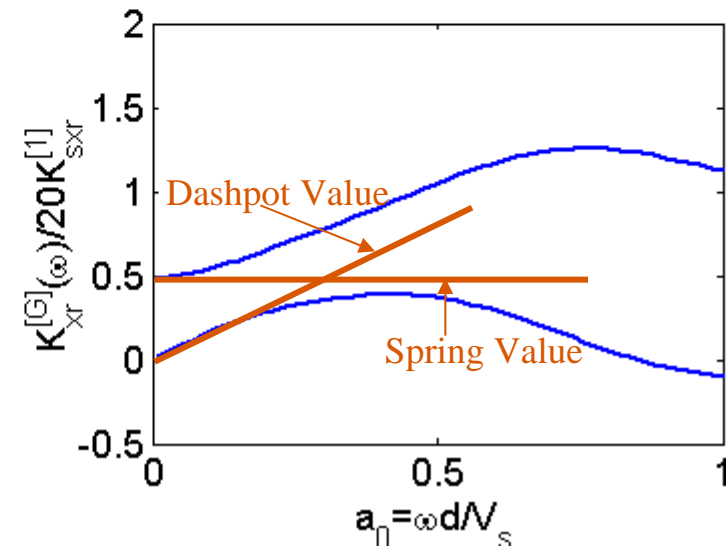
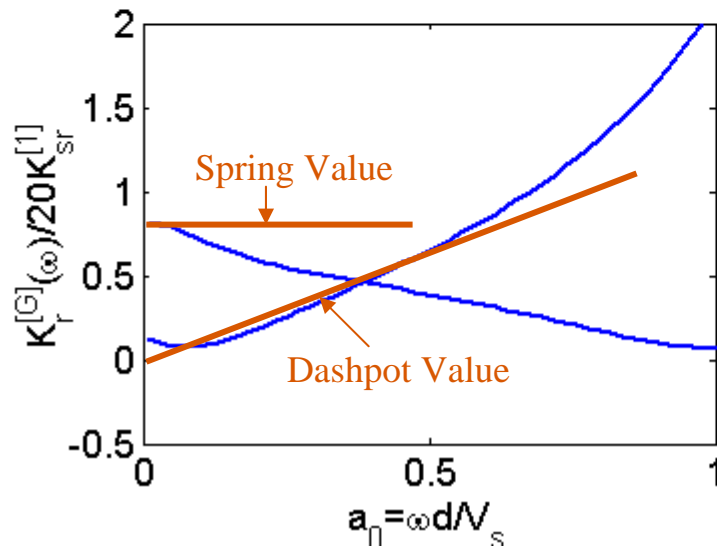
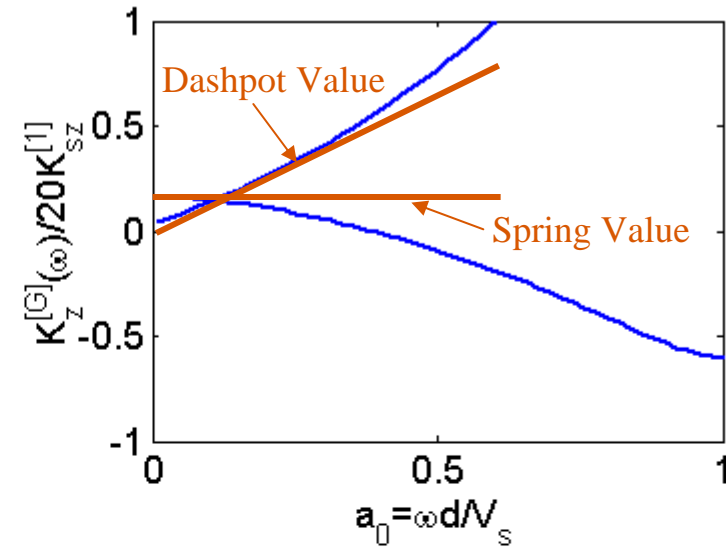
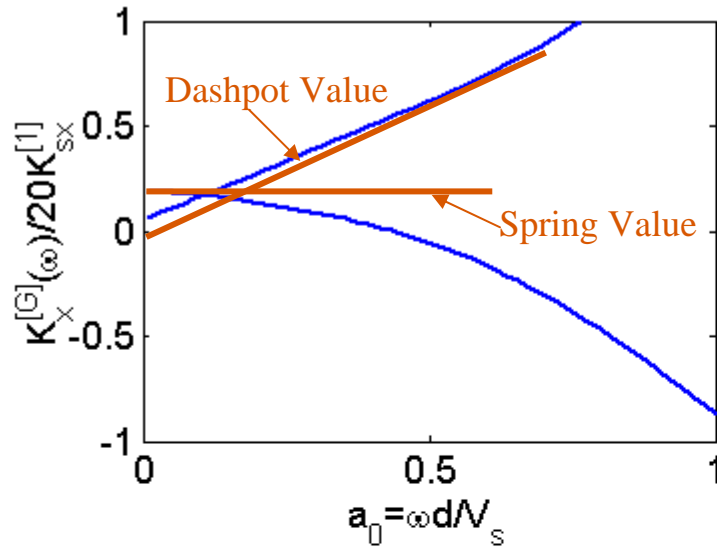
□ Equivalent Flexural-Shear Beam

- To include the cross-rocking term of pile group stiffness
- By matching stiffnesses of equivalent beam and that of pile group, one can solve for beam length L , cross-section area A , moment inertia I and shear modulus G

Pile Group @ Center Bent (PSB)



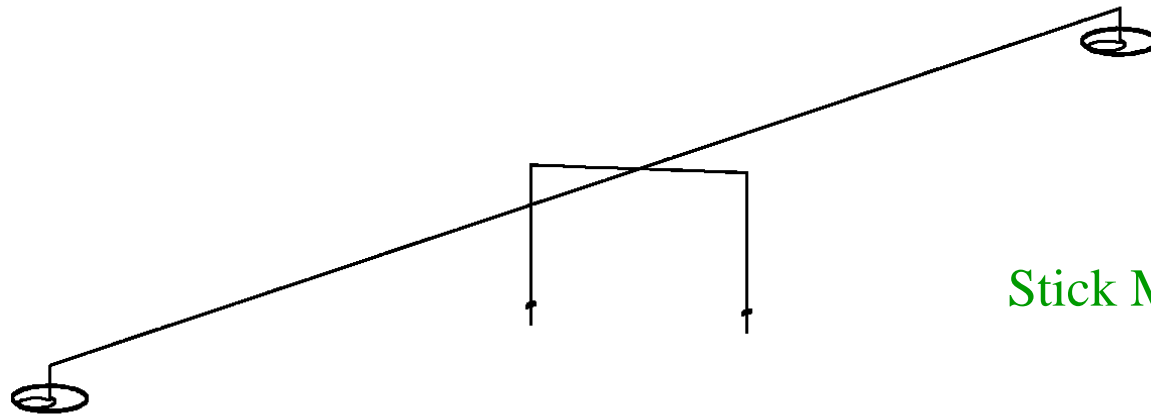
Dynamic Stiffnesses of Pile Group (PSB)



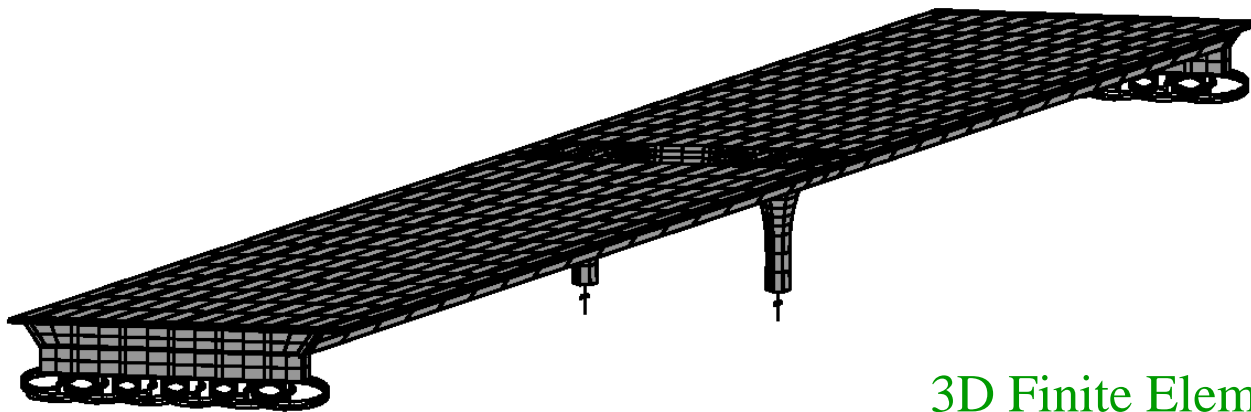
Outline

- Introduction
- Embankment and Pile Foundation
 - Kinematic Response Function
 - Dynamic Stiffness (“Spring” and “Dashpot” Constants)
 - Simple Procedure
- **Seismic Analysis of Highway Bridges Under Seismic Shaking**
 - Eigenvalue Analysis
 - Time History Analysis
- Seismic Analysis of Bridges Under Liquefaction Induced Lateral Spreading
 - Equivalent Static Analysis Approach
 - Global Dynamic Analysis Approach

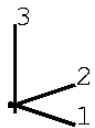
Numerical Models (PSB)



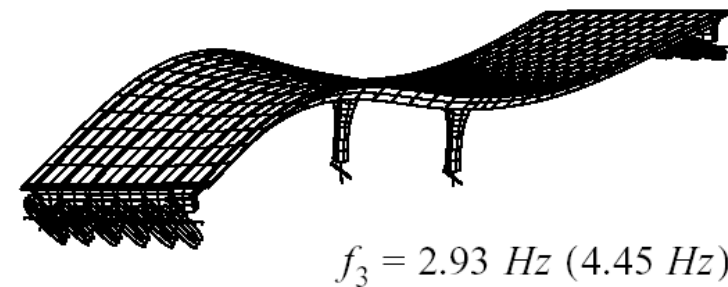
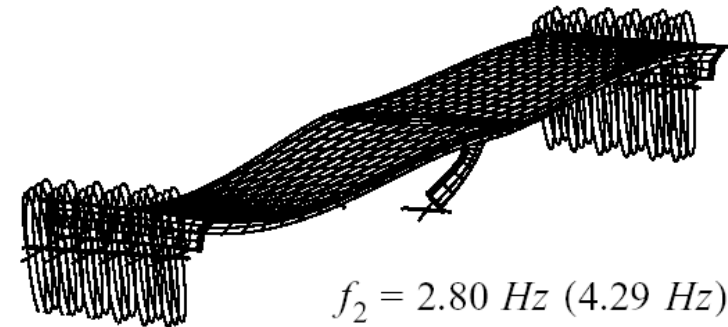
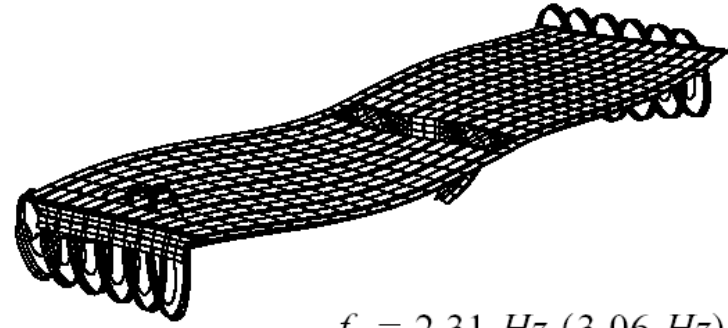
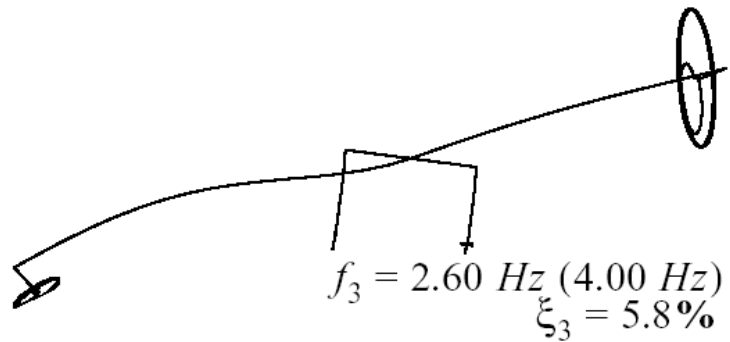
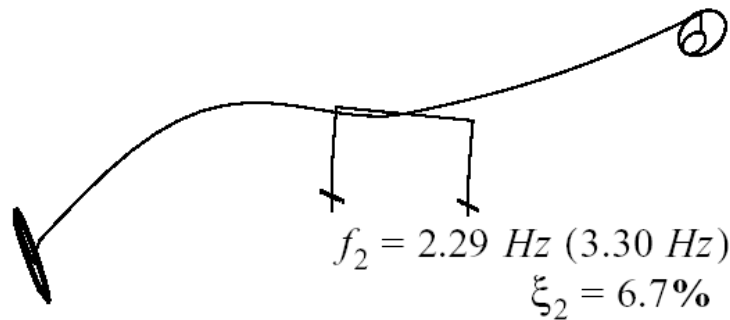
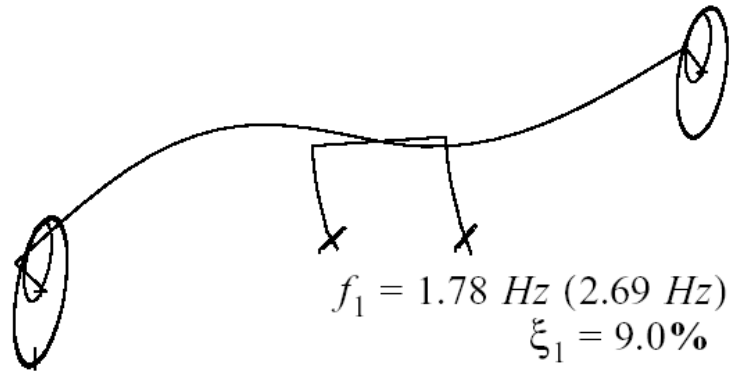
Stick Model



3D Finite Element Model



Natural Frequencies and Modes (PSB)



Complex Eigenvalue Analysis

Equation of Motion: $[M]\{\ddot{u}\} + [C]\{\dot{u}\} + [K]\{u\} = 0$

Damping Matrix: $[C] = \alpha[M] + \beta[K] + [c_{ij}]$ (Nonclassical)

Dashpots of embankments & pile foundations

Response Vector: $\{u\} = \{\phi\}e^{i\Omega t}$



$$(-\Omega^2[M] + i\Omega[C] + [K])\{\phi\} = 0$$

Complex Eigenvalues: $\Omega_j = \pm\sqrt{\omega_j^2 - \xi_j^2\omega_j^2} + i\xi_j\omega_j$

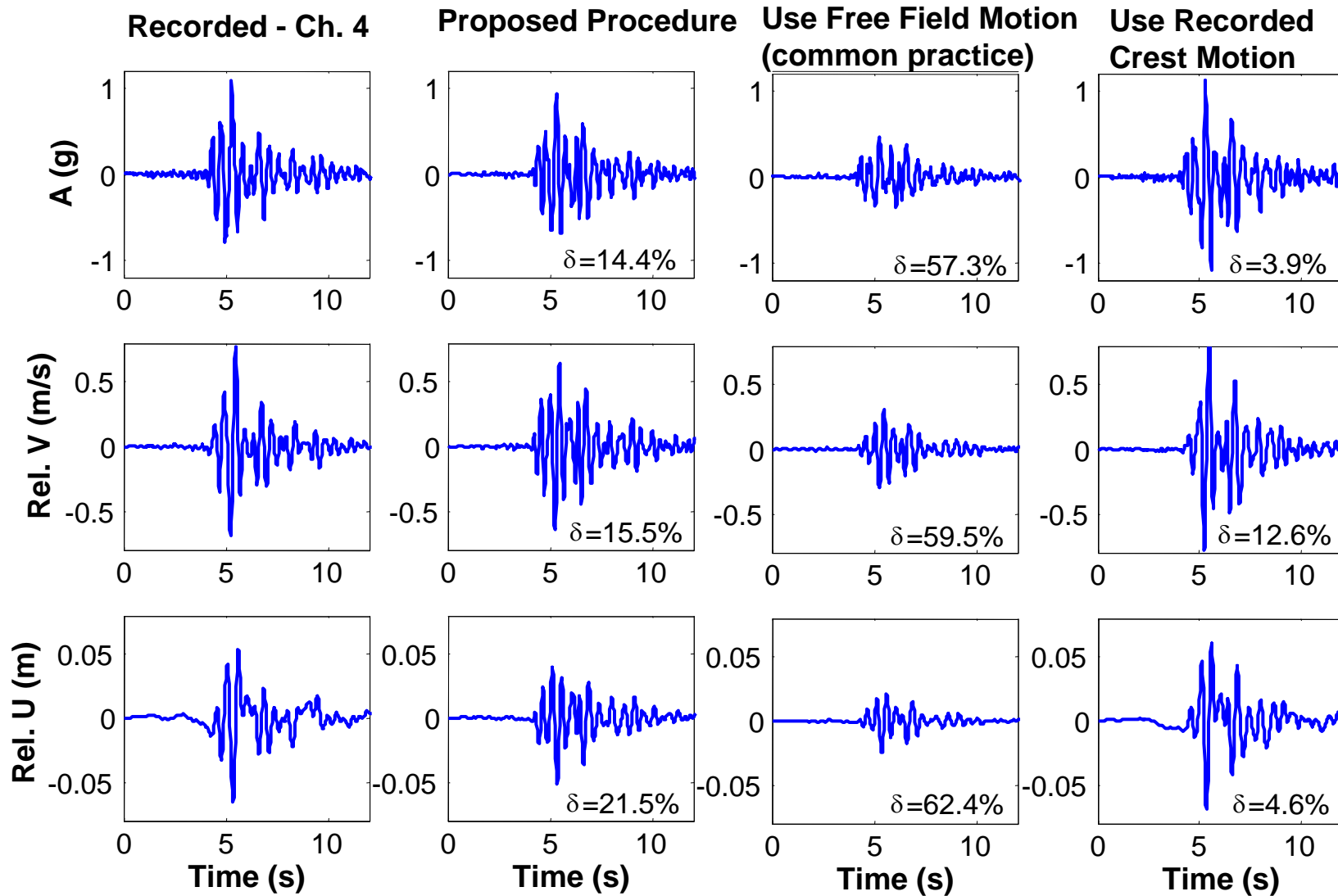
Modal Frequencies: $\omega_j = \sqrt{\Omega_{jR}^2 + \Omega_{jI}^2}$

Modal Damping Ratios: $\xi_j = \frac{\Omega_{jI}}{\omega_j}$

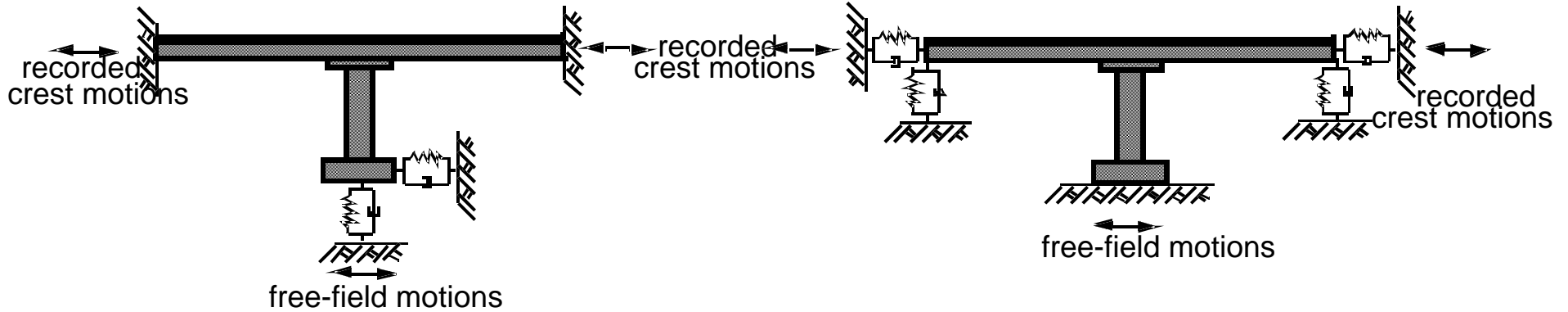
Modal Frequencies & Damping Ratios (PSB)

Modes	Eigenvalues (rad/s)				1		2		3		4	
	Model A	Model B	Model C	Model D	ω_j	ξ_j	ω_j	ξ_j	ω_j	ξ_j	ω_j	ξ_j
1 st transverse /antisymmetric vertical	14.514	11.162	11.364 (11.587)	11.490+1.040i (11.730+1.116i)	11.5 (11.8)	9.0 (9.5)	20.7	20	11.0~ 17.9	5.6~ 8.5	10.3	16.6
antisymmetric vertical /tor-sion about vertical axis	17.593	14.409	14.578 (14.751)	14.683+0.984i (14.863+1.006i)	14.7 (14.9)	6.7 (6.8)	16.9	3				
torsion about vertical axis/ symmetric vertical	18.410	16.366	16.365 (16.366)	16.527+0.962i (16.524+0.972i)	16.6 (16.6)	5.8 (5.9)	25.1	3				
symmetric vertical/longitudi-nal	23.562	20.691	20.808 (20.994)	21.075+1.761i (21.370+1.809i)	21.1 (21.4)	8.3 (8.4)	32.9	5				
longitudinal	26.641	21.545	20.938 (21.265)	20.176+10.383i (20.394+10.395i)	22.7 (22.9)	45.8 (45.4)	29.6	30				
2nd transverse/torsion about longitudinal axis	32.233	31.156	22.052 (22.532)	23.754+4.096i (24.236+4.302i)	24.1 (24.6)	17.0 (17.5)	41.5	5				
A: Undamped original 3D FEM model B: Undamped original stick model (618 d.o.f) C: Undamped reduced stick model with 174 d.o.f and (138 d.o.f) respectively D: Damped reduced stick model with 174 d.o.f and (138 d.o.f) respectively					1: This study 2: McCallen and Romstad 1994 3: Goel 1997 4. Price and Eberhard 1998							

Time History Analysis (Ch. 4)

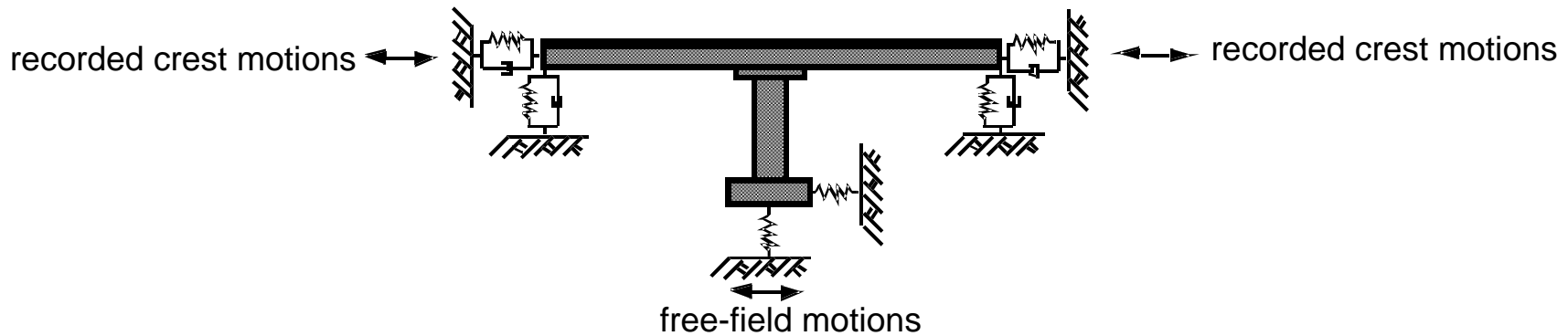


Effects of Support Idealizations



(a) Monolithic embankments and viscoelastic foundation at the center bent

(b) Viscoelastic embankments and monolithic support at the center bent



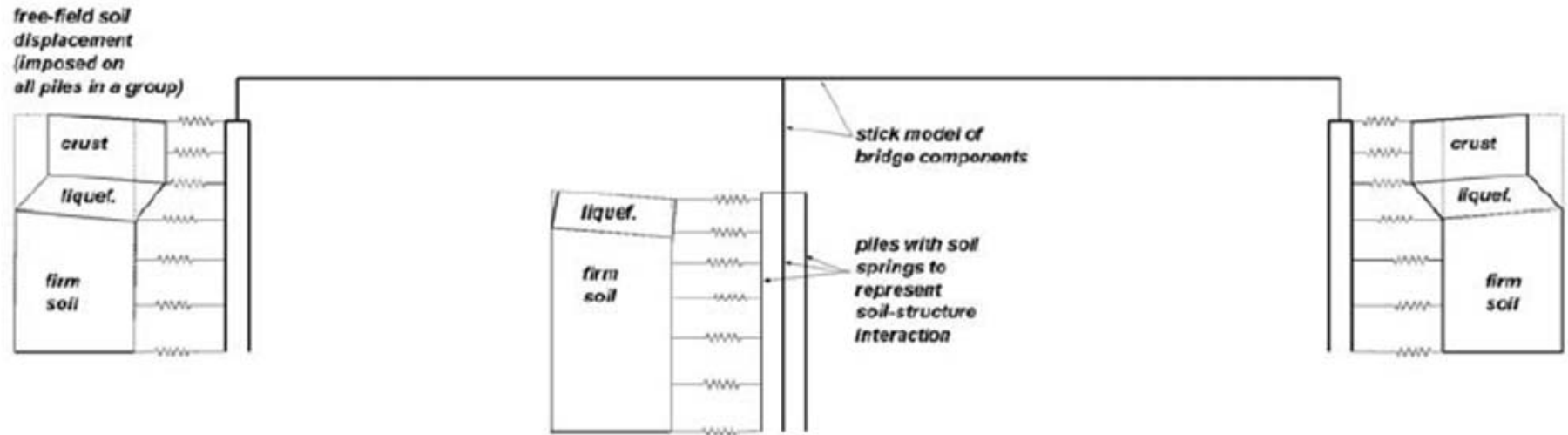
(c) Viscoelastic embankments and elastic support at the center bent

Outline

- ❑ Introduction
- ❑ Embankment and Pile Foundation
 - Kinematic Response Function
 - Dynamic Stiffness (“Spring” and “Dashpot” Constants)
 - Simple Procedure
- ❑ Seismic Analysis of Highway Bridges Under Seismic Shaking
 - Eigenvalue Analysis
 - Time History Analysis
- ❑ **Seismic Analysis of Bridges Under Liquefaction Induced Lateral Spreading**
 - Equivalent Static Analysis Approach
 - Global Dynamic Analysis Approach

Static Procedure to Simulate Bridge Under Lateral Spreading

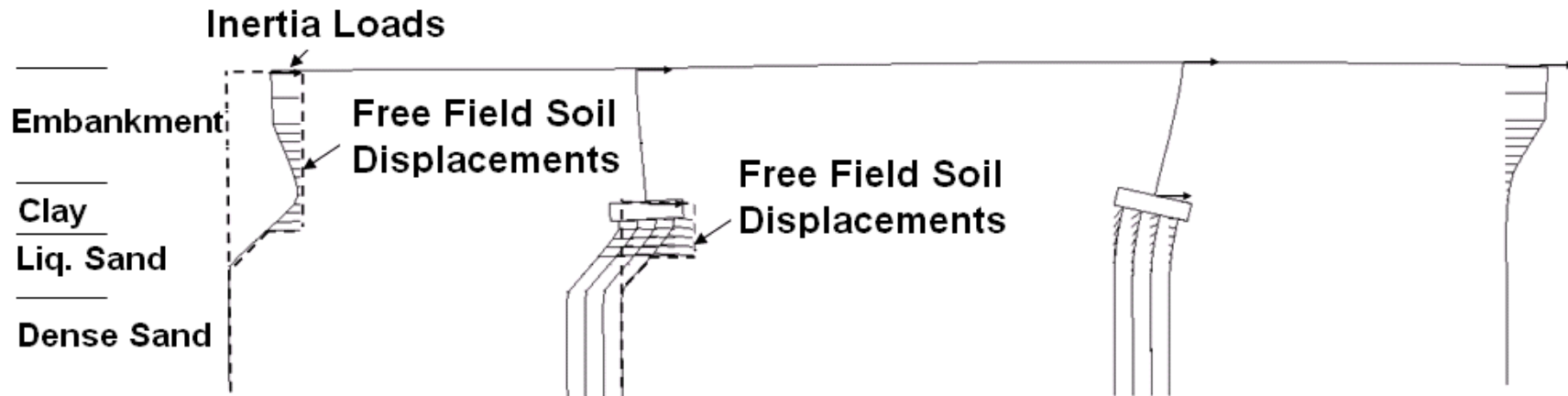
- Equivalent static procedure: apply static displacement loading profile in longitudinal direction



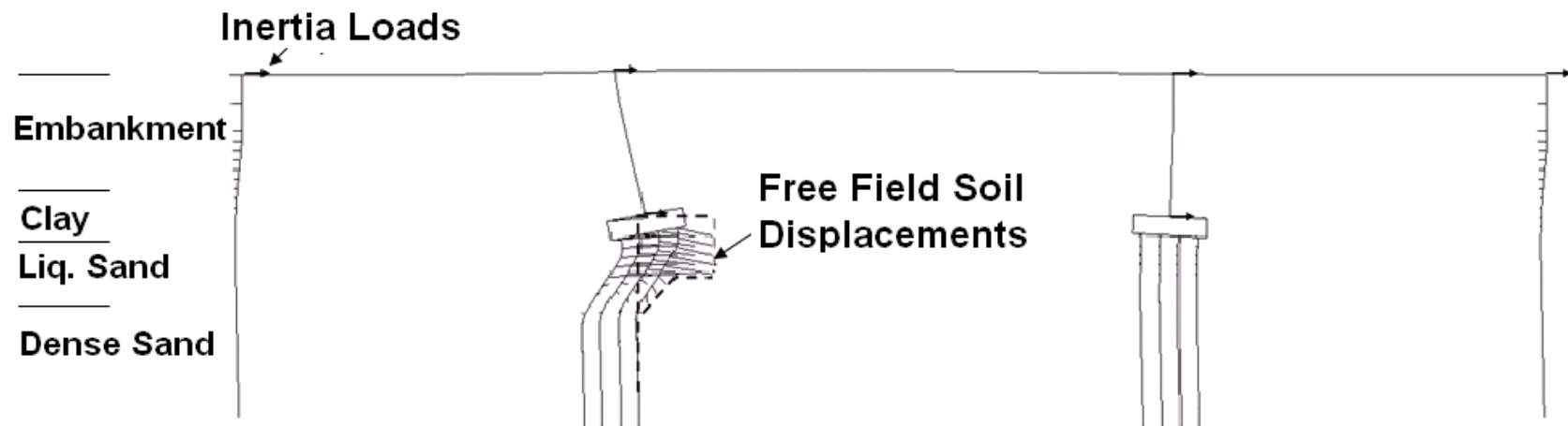
- P-y spring springs are weaker and softer in non-liquefied crust layer due to the flow of liquefied layer
 - Passive pressure change from log-spiral to Rankine type
 - Soil can flow around strong foundations
 - Crust layer can exert large forces to pile cap

Responses of Bridges Using Static Procedure

□ Case No. 1

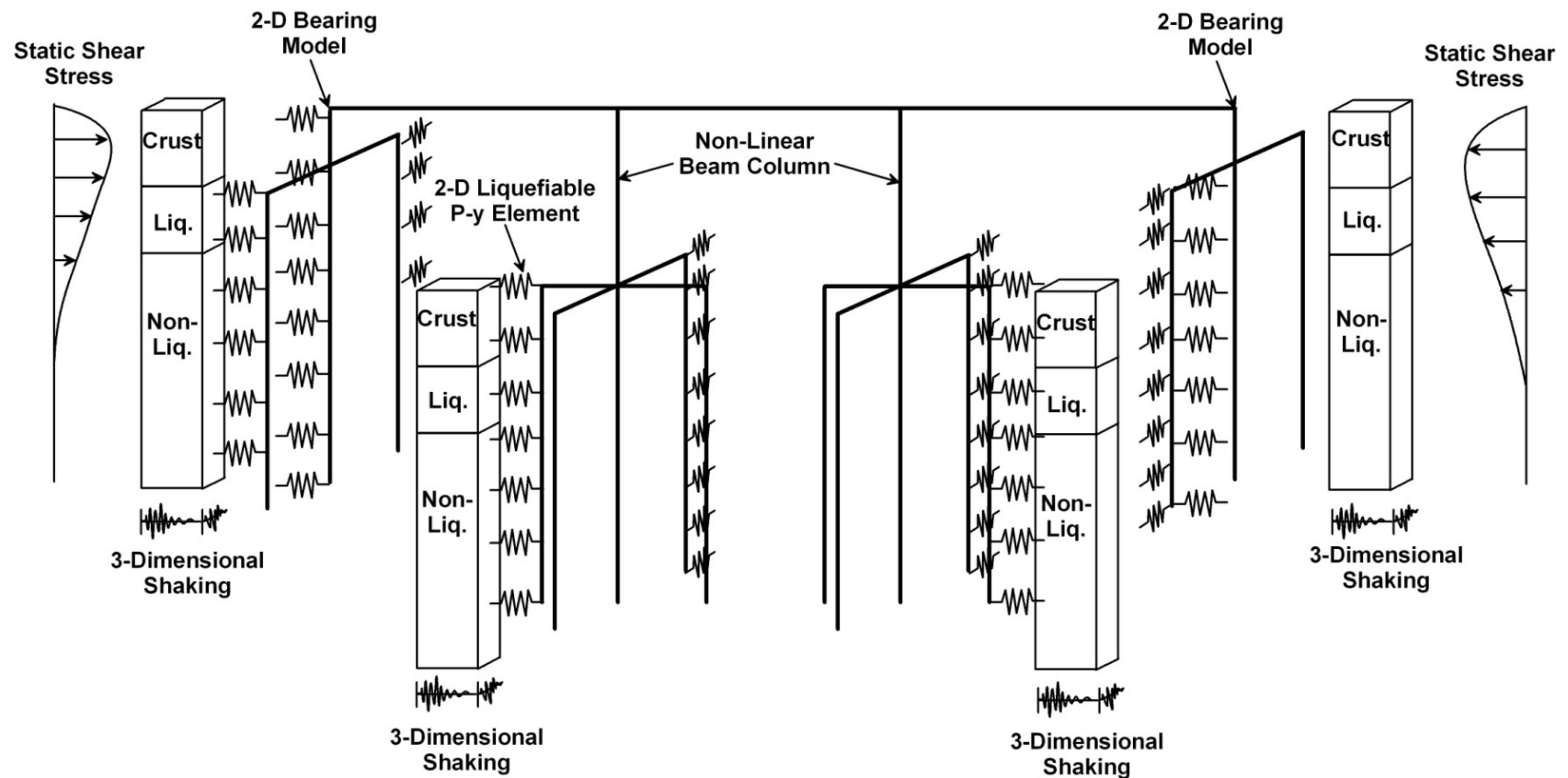


□ Case No. 2

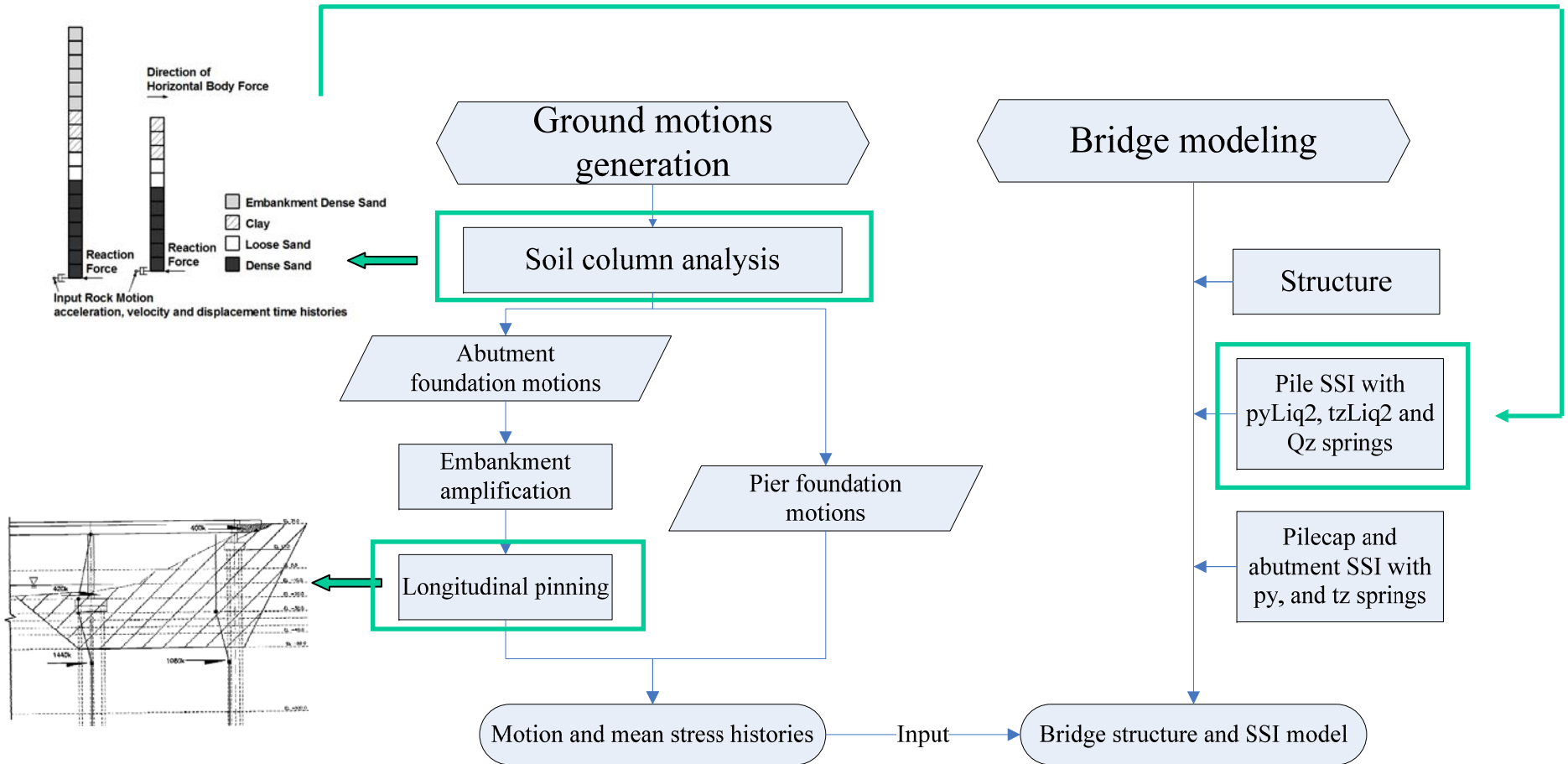


Dynamic Procedure for Lateral Spreading

- The global dynamic analysis procedure can capture both transverse and longitudinal coupled responses, the ground motion dependencies and inertial effects etc.

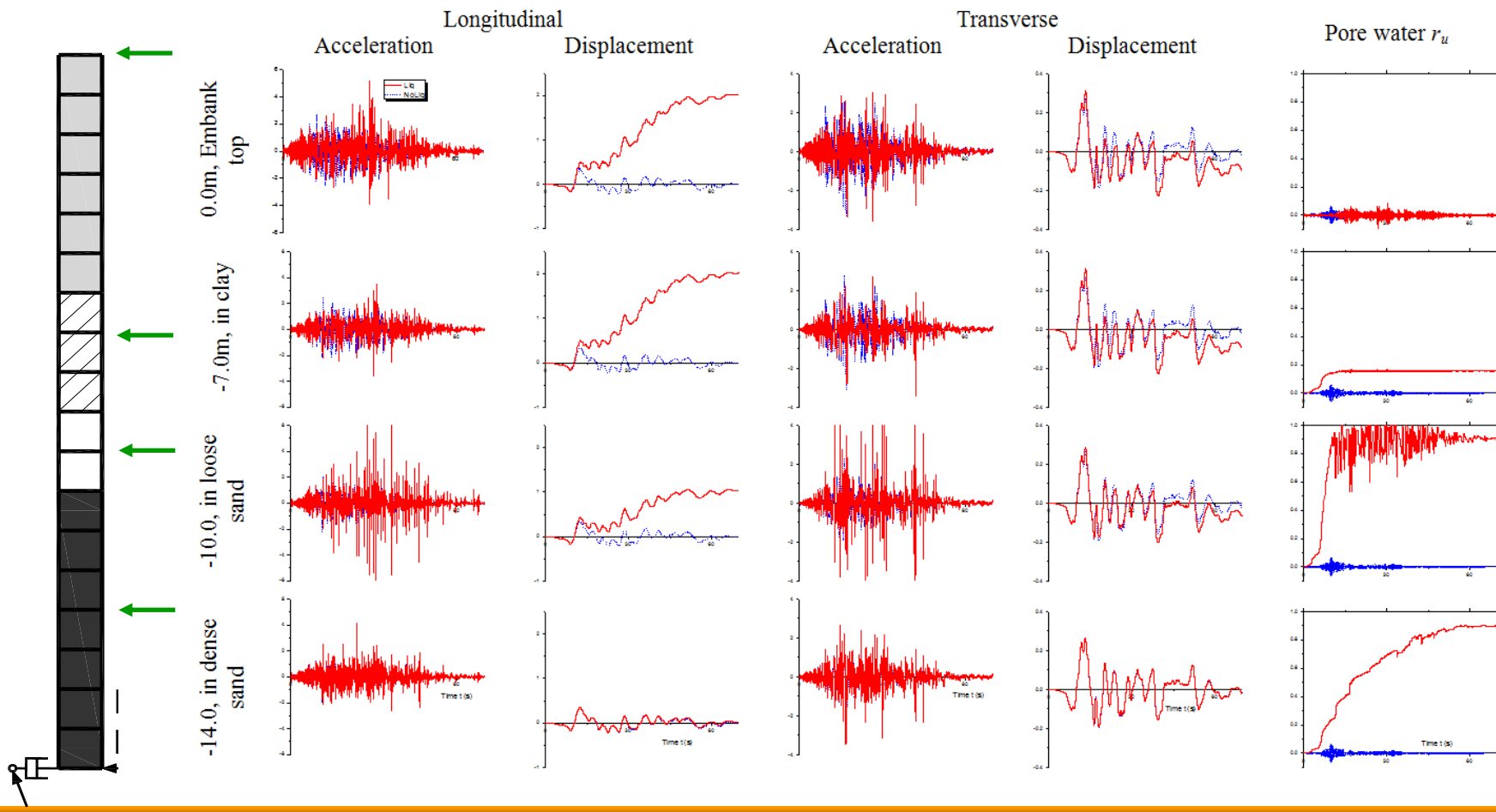


Detailed Steps of Dynamic Procedure



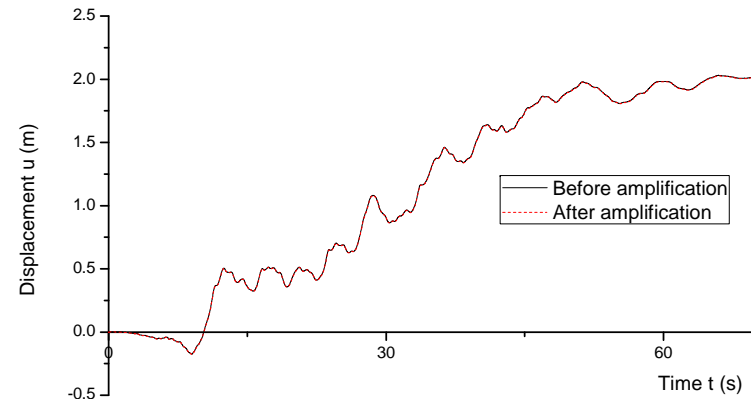
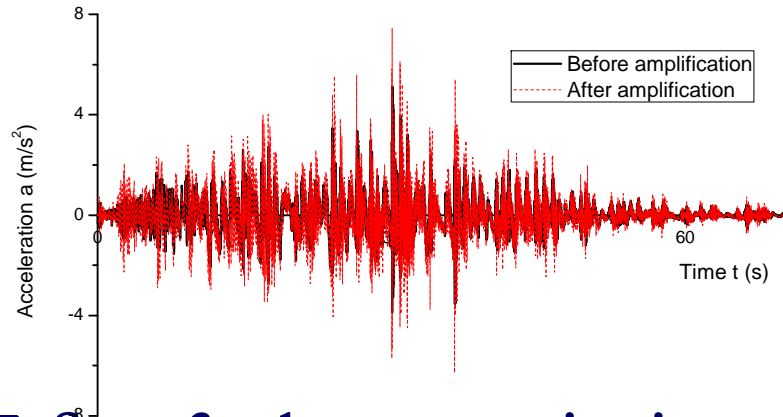
Generation of Depth Varying Ground Motions

- 40 rock motions (Baker et al., 2011)
- Step 1: nonlinear site responses

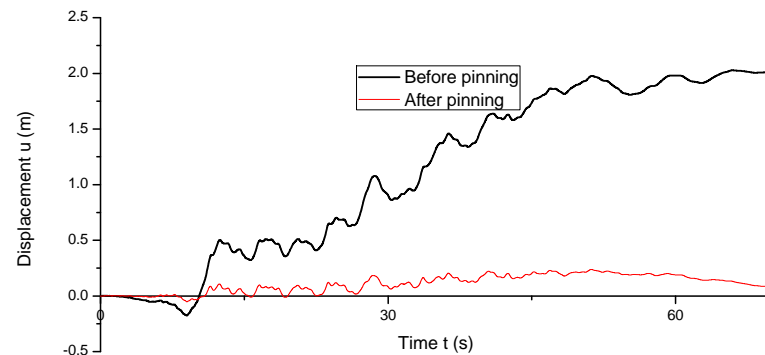
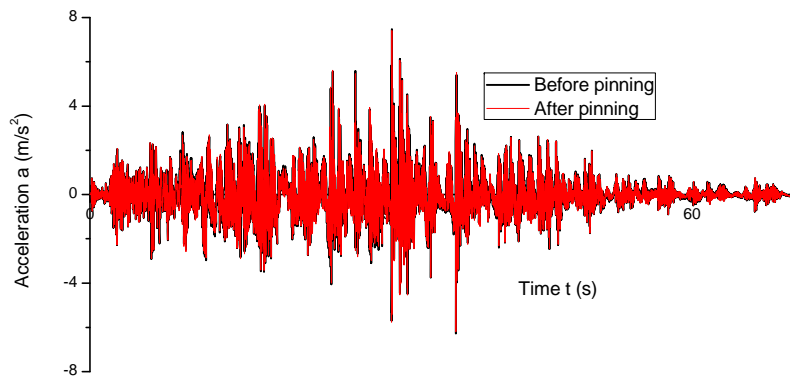


Generation of Depth Varying Ground Motions

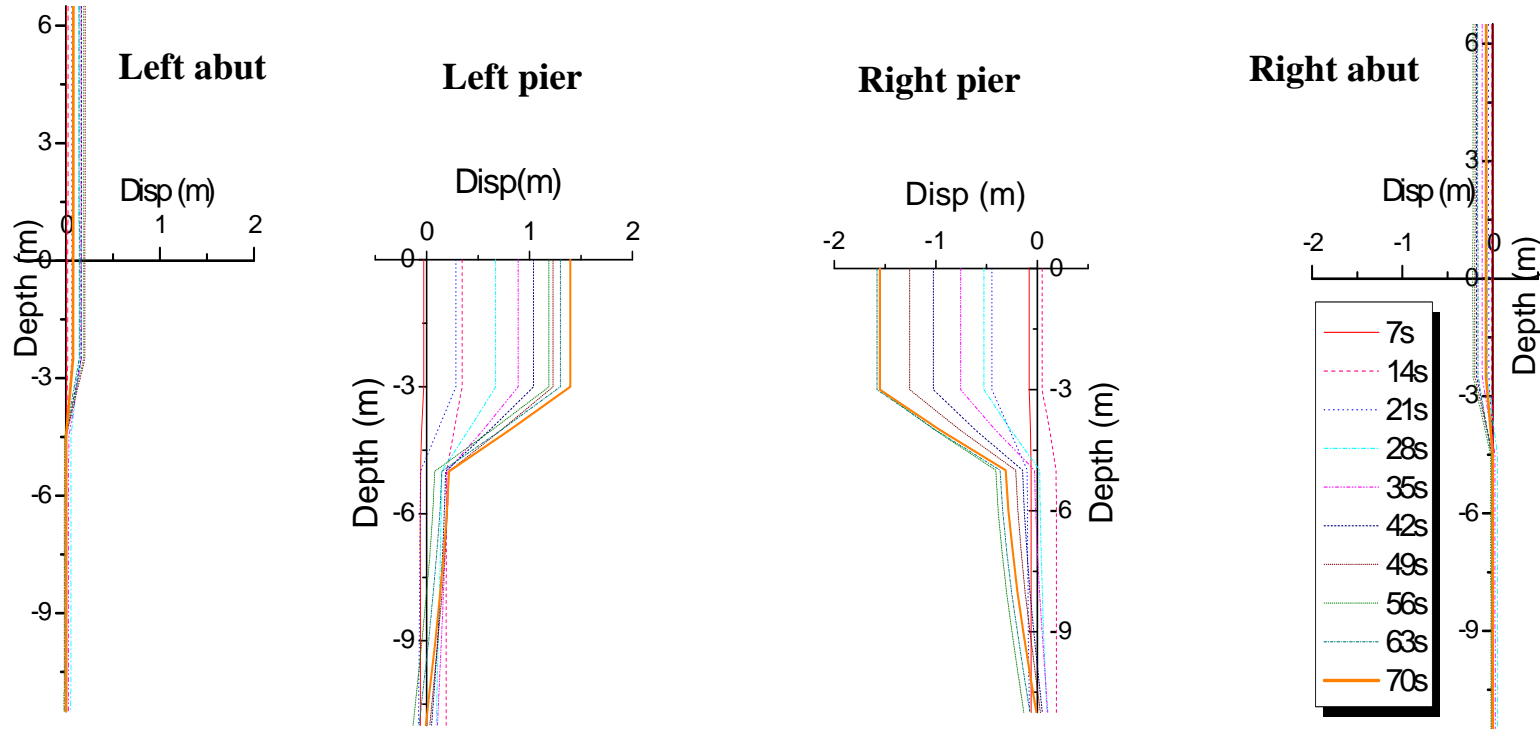
□ Step 2: embankment amplification



□ Step 3: abutment pinning effect

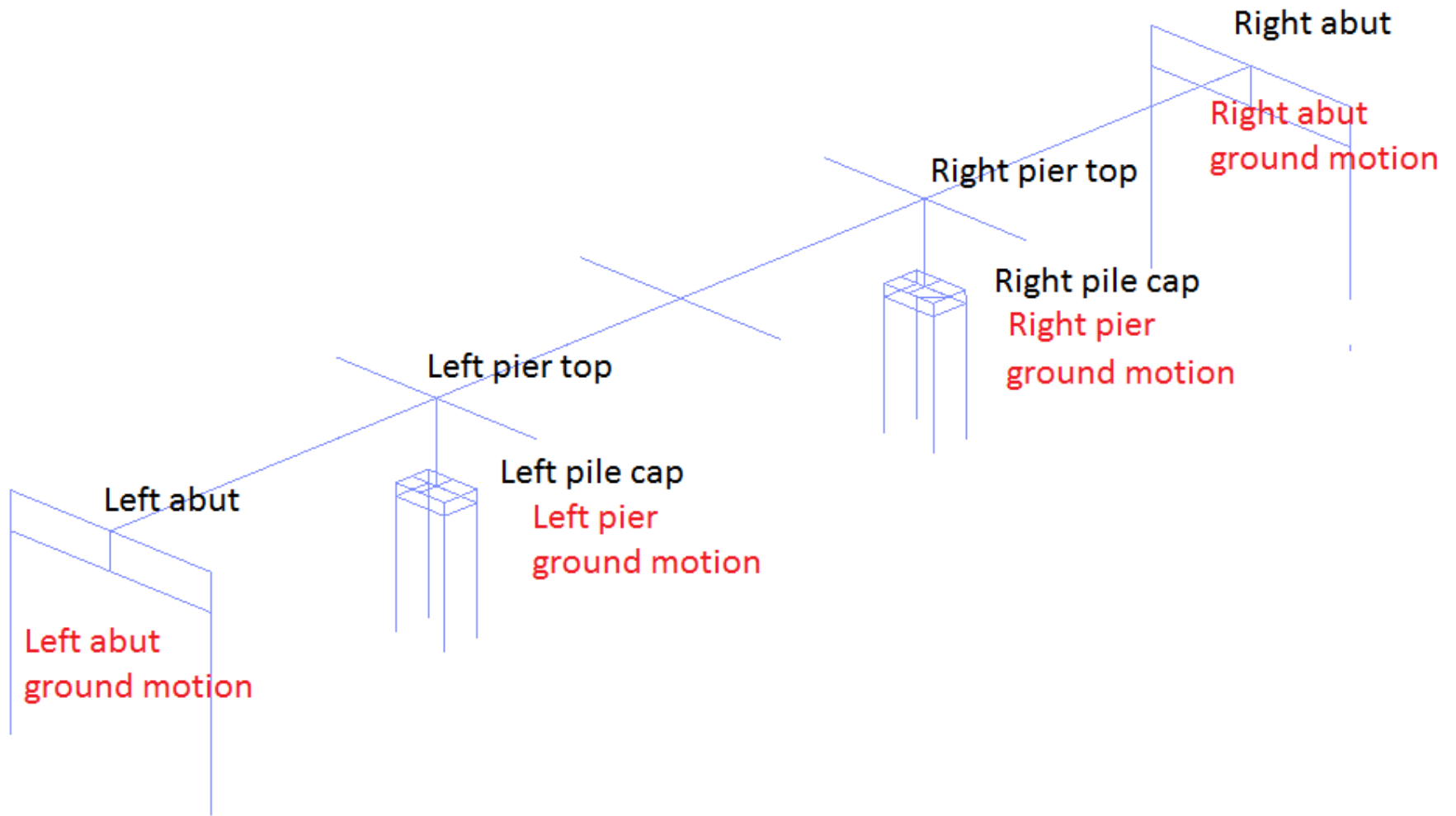


Displacement Loading Profile

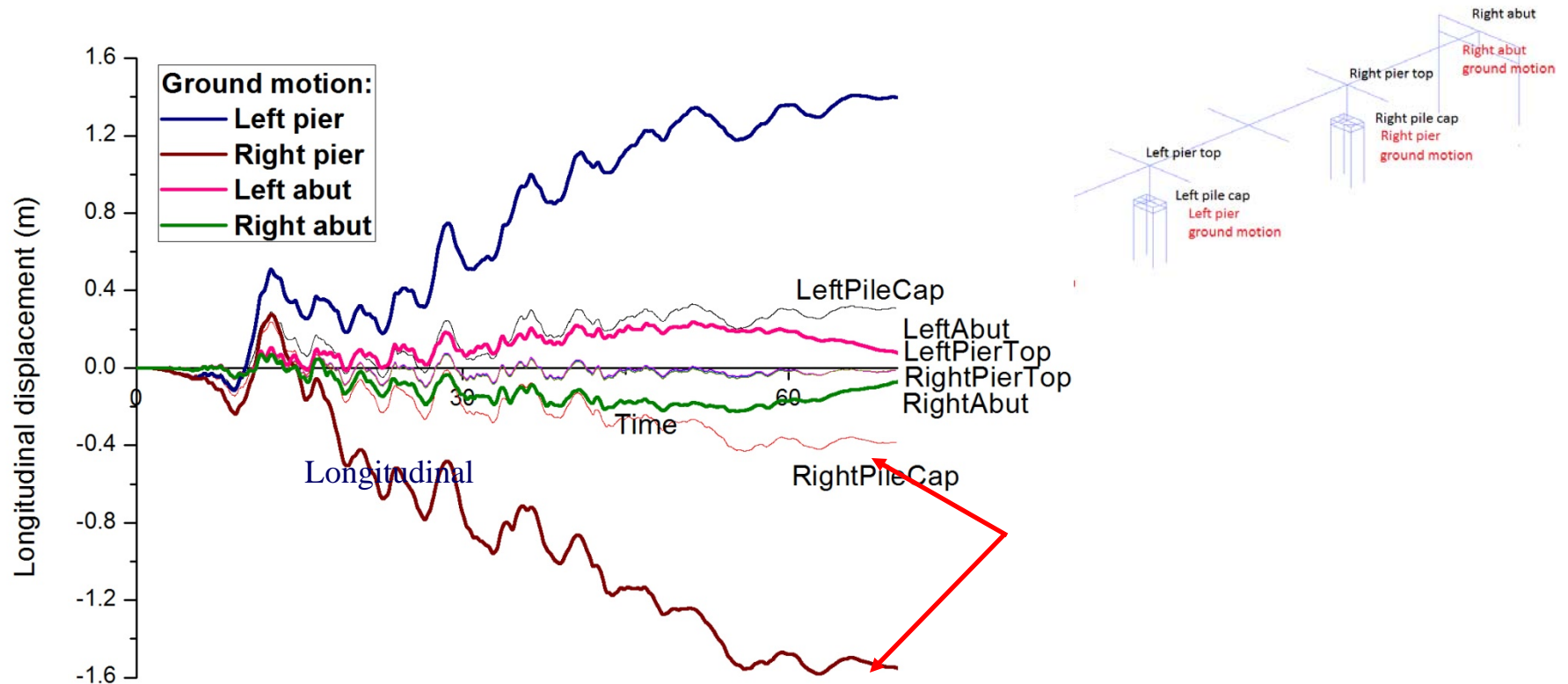


- ❑ Larger displacement at pier foundation than abutment (reduced by pinning effects).
- ❑ Small displacement in layers beneath the liquefied layer.

Finite Element Model of Bridges in OpenSees

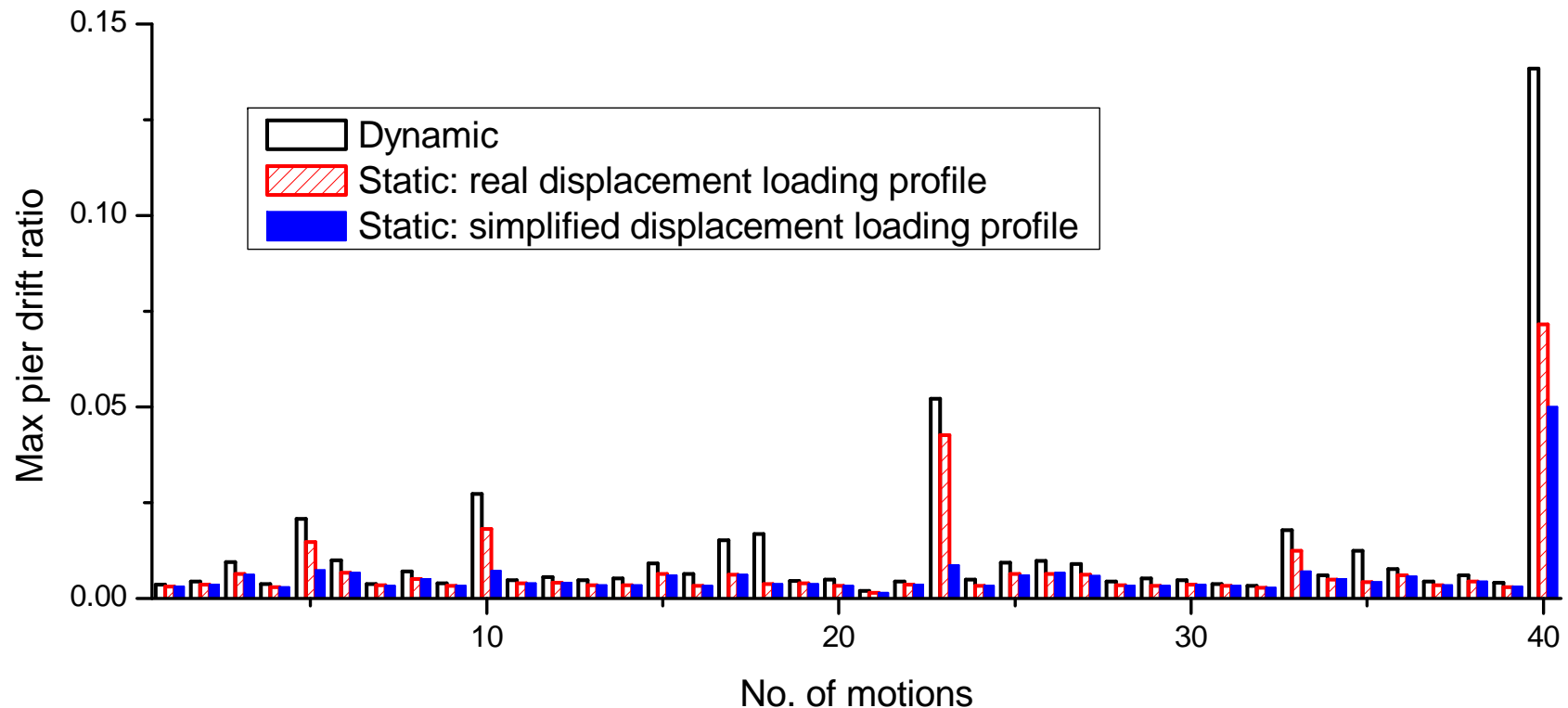


Displacement at Various Locations of Bridges



- ❑ Extensive lateral spreading displacement ($\sim 1.5\text{m}$).
- ❑ Pier column experiences large deformation ($\sim 0.4\text{m}$ drift).
- ❑ Soil flows around pile cap.

Pier Drift Ratio: Dynamic vs. Static Procedure



- ❑ Static loading mechanism dominates the responses of bridges and a “realistic” displacement profile can improve the prediction of static procedure

Modeling Axial-Shear-Flexure Interaction of RC Columns for Seismic Response Assessment of Bridges

Contributors:

Dr. Shi-Yu Xu

Professor Jian Zhang

The research presented here was funded by National Science Foundation through the Network for Earthquake Engineering Simulation Research Program (0530737).

Outline

- **Introduction**
 - Motivation & Objectives
 - Significance of Axial-Shear-Flexure Interaction
- **Shear-Flexure Interaction Hysteretic Model Under Constant Axial Load**
 - Generation of Primary Curves Considering Shear-Flexure Interaction
 - Improved Reloading/Unloading Hysteretic Rules
- **Inelastic Displacement Demand Model for Bridge Columns**
 - Modeling of Columns & Consideration of Ground Motions
 - Dimensional Analysis
- **Seismic Response Simulation of Bridges**
 - Site Specific Ground Motions
 - Soil-Structural Interaction
 - Nonlinear Behavior of Columns
- **Axial-Shear-Flexure Interaction Hysteretic Model Under Variable Axial Load**
 - Generation of Primary Curve Family
 - Stress Level Index & Two-stage Loading Approach
- **Conclusion**

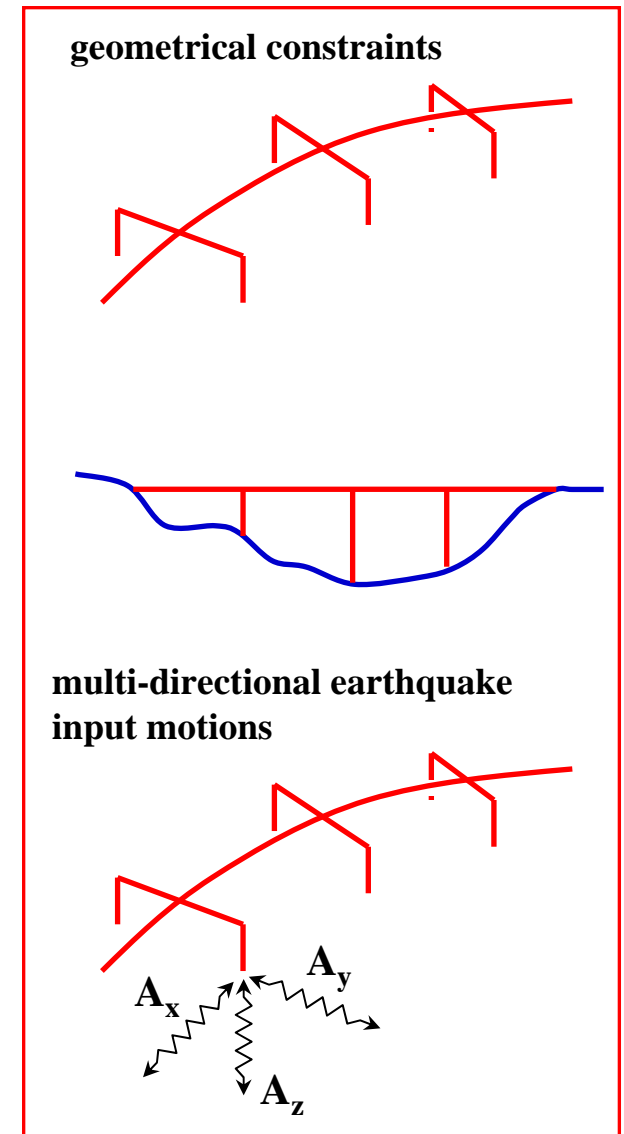
Introduction

Motivation

- ◆ Bridge columns are subjected to *combined actions* of axial, shear and flexure forces.
- ◆ Bridges performance can be improved if *accurate prediction* of seismic demand on columns can be achieved.

Objectives

- ◆ **An efficient analytical scheme** considering *axial-shear-flexural interaction* in columns
- ◆ **An systematic procedure** producing accurate seismic response assessment of *bridge system*
 - Site specific ground motion
 - Soil-structure interaction
 - Nonlinear behavior of columns (strength deterioration, stiffness degrading, & pinching behavior)



Significance of Axial-Shear-Flexural Interaction

- Significance of Non-linear Shear-Flexural Interaction (Ozcebe and Saatcioglu 1989; Saatcioglu and Ozcebe 1989)
 - *Shear displacement* can be significant -- even if a RC member is not governed by shear failure (as is the case in most of RC columns).
 - RC members with higher shear strength than flexural strength do not guarantee an elastic behavior in shear deformation (*Inelastic* shear behavior).
 - *Strength and ductility* of columns -- strongly depend on the combined effects of applied loads, as evidenced in field observation as well as laboratory tests.

- Coupling of Axial-Shear-Flexural Responses (ElMandooh and Ghobarah 2003)
 - Dynamic variation of axial force -- will cause significant change in the lateral *hysteretic* moment-curvature relationship and consequently the overall structural behavior in RC columns.

Analytical Models for RC Columns

□ Plastic Hinge Type Models

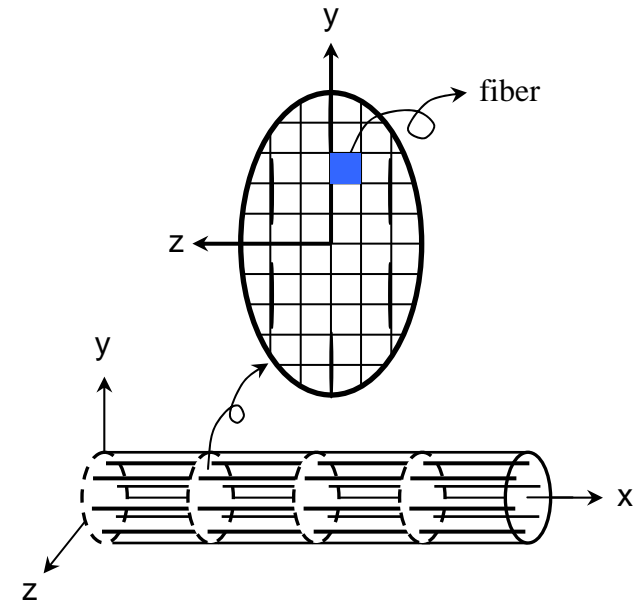
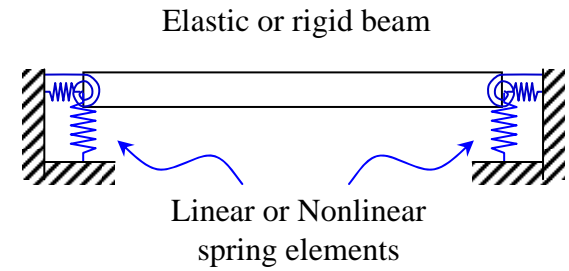
- Using equivalent springs to simulate shear and flexural responses of columns at the element level
- Empirical and approximate
- Difficult to couple together the axial, shear, and flexural responses

□ Fiber Section Formulation

- Controlling the element responses directly at the material level
- Coupling the axial-flexural interaction
- Rotation of principal axes in concrete due to the existence of shear stress is not considered

□ Timoshenko Beam-Column Element

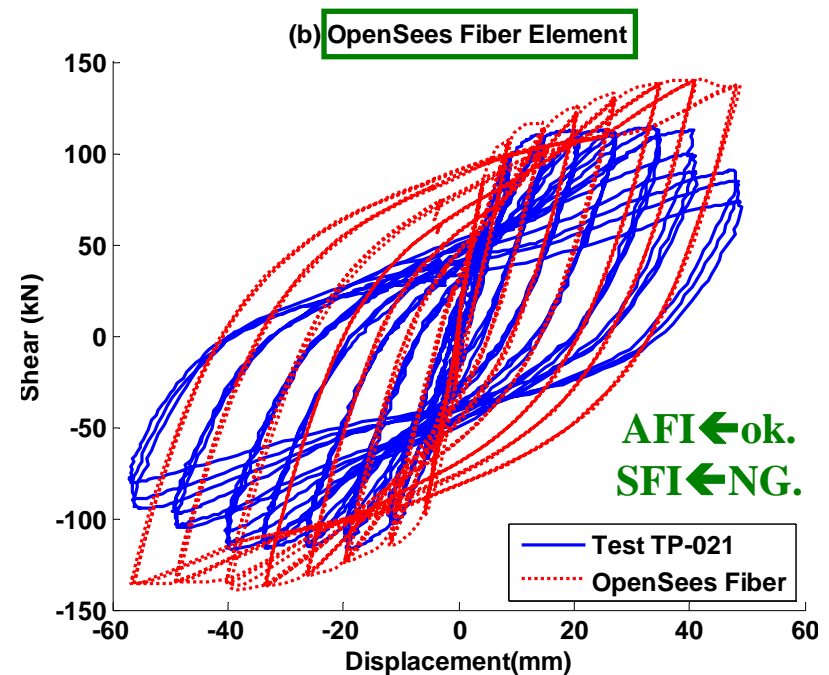
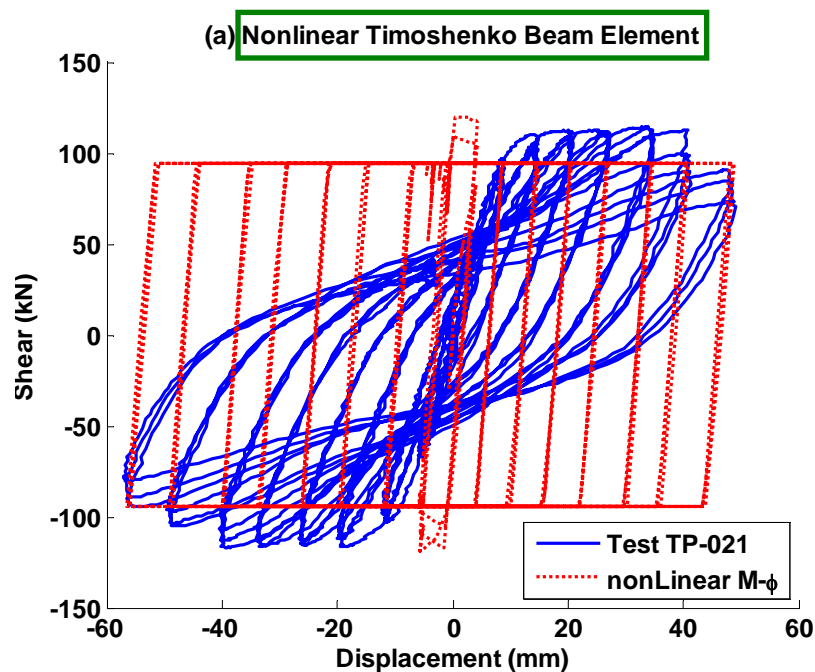
- Assuming uniform material



Deficiencies of Current Numerical Models

□ Deficiencies of Current Models

- Non-linearity in shear deformation is not accounted for.
- Material damage (strength deterioration and pinching) due to cyclic loading is not considered.
- Axial-Shear-Flexural interaction is not captured.



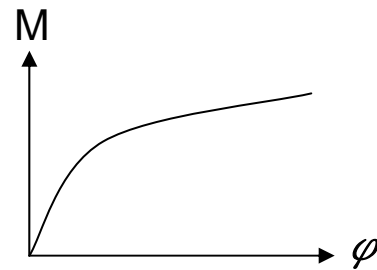
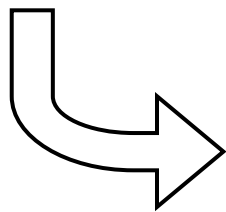
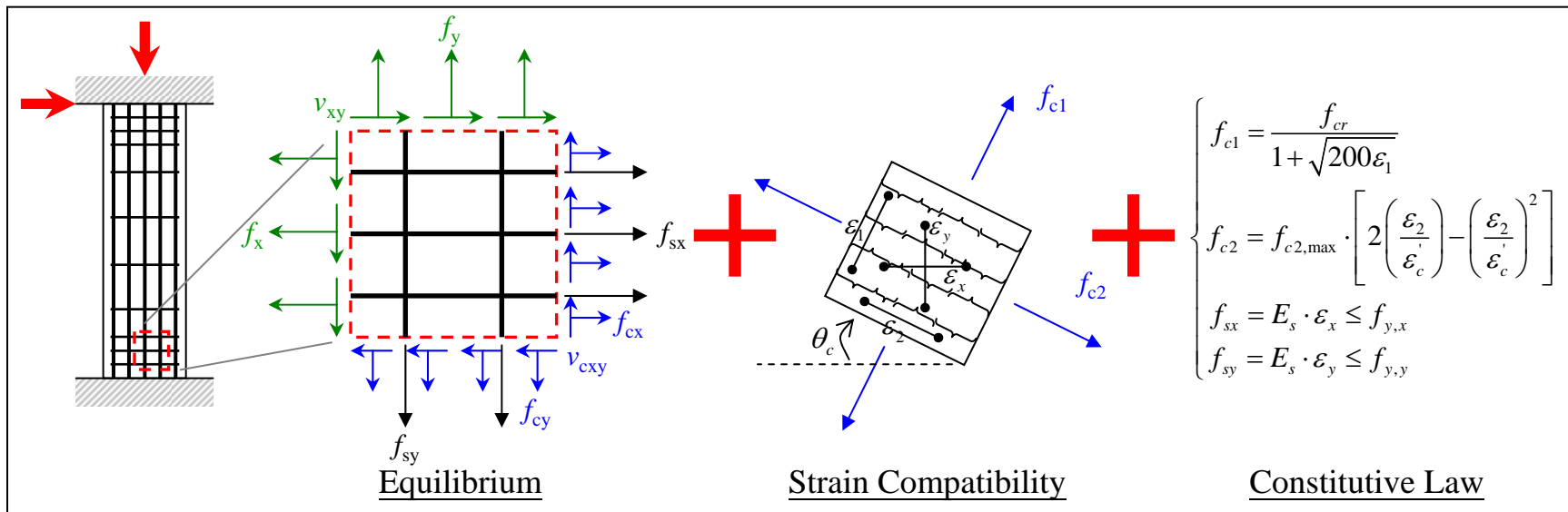
Outline

- **Introduction**
 - Motivation & Objectives
 - Significance of Axial-Shear-Flexure Interaction
- **Shear-Flexure Interaction Hysteretic Model Under Constant Axial Load**
 - Generation of Primary Curves Considering Shear-Flexure Interaction
 - Improved Reloading/Unloading Hysteretic Rules
- **Inelastic Displacement Demand Model for Bridge Columns**
 - Modeling of Columns & Consideration of Ground Motions
 - Dimensional Analysis
- **Seismic Response Simulation of Bridges**
 - Site Specific Ground Motions
 - Soil-Structural Interaction
 - Nonlinear Behavior of Columns
- **Axial-Shear-Flexure Interaction Hysteretic Model Under Variable Axial Load**
 - Generation of Primary Curve Family
 - Stress Level Index & Two-stage Loading Approach
- **Conclusion**

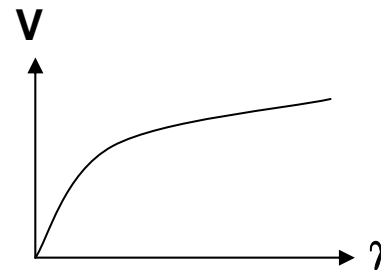
Axial-Shear-Flexure Interaction at Material Level

MCFT II

Modified Compression Field Theory
(Vecchio and Collins 1986)

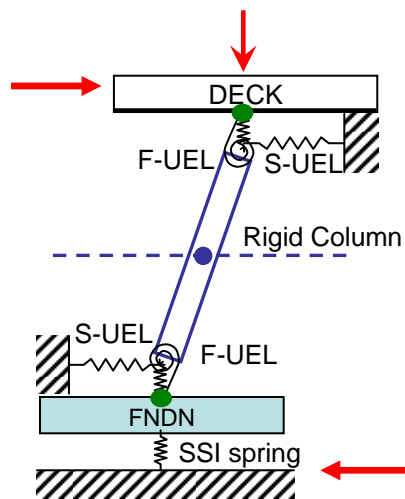
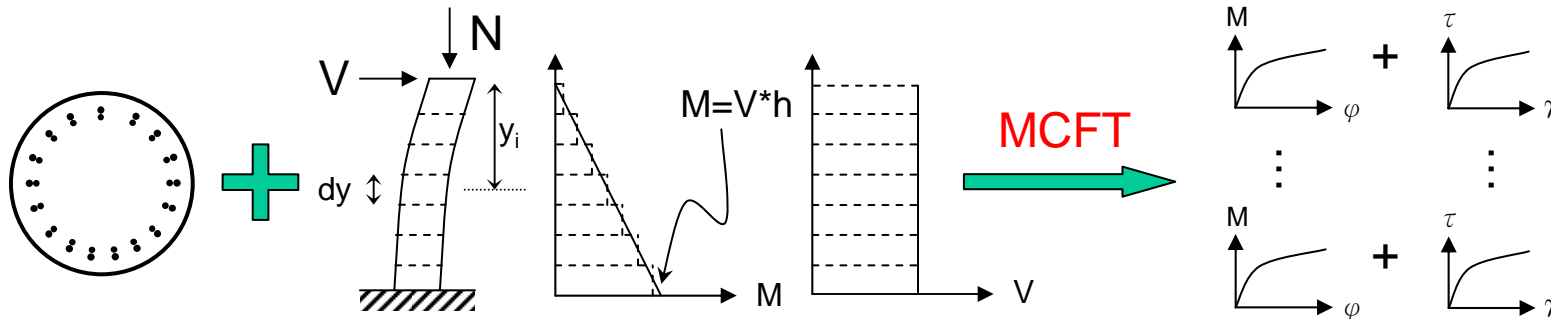


+



Derivation of Flexural and Shear Primary Curves

- Discretize RC member into small pieces. For each piece of RC element, estimate M- ϕ and τ - γ relationship by **Modified Compression Field Theory** (MCFT, Vecchio and Collins 1986).

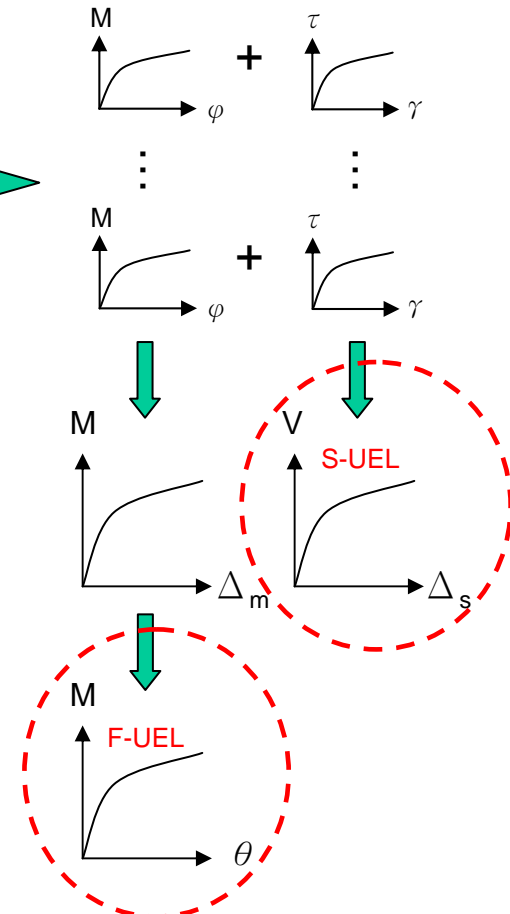


- Integrate curvature and shear strain to get tip displacement.

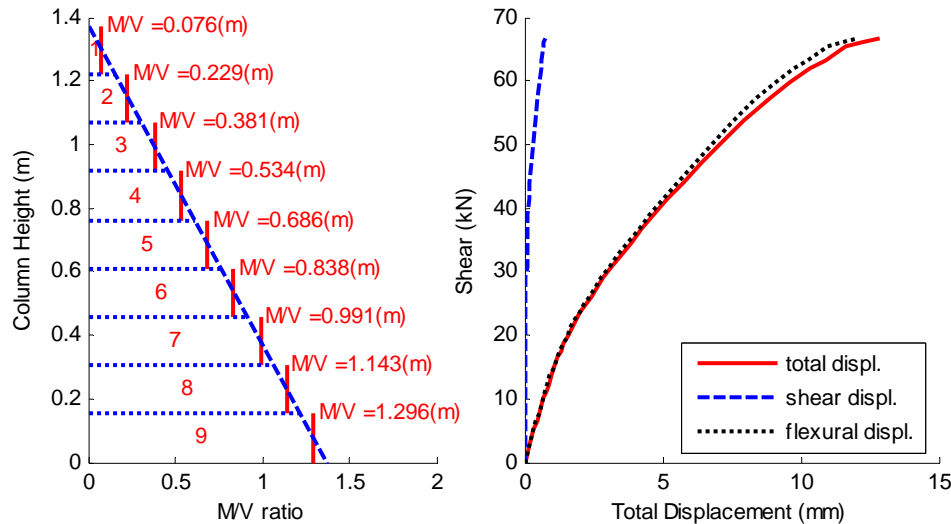
$$\delta = \sum \{ \underbrace{\phi_i * dy * y_i}_{\text{Flexural deformation}} + \underbrace{\gamma_i * dy}_{\text{Shear deformation}} \}$$

$$= h * \theta + \Delta_s$$

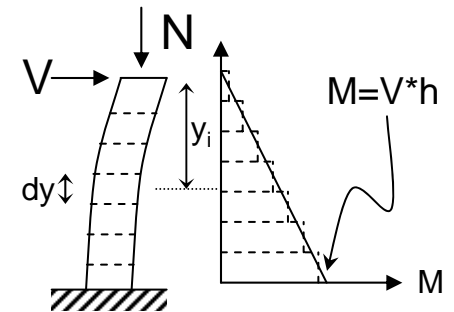
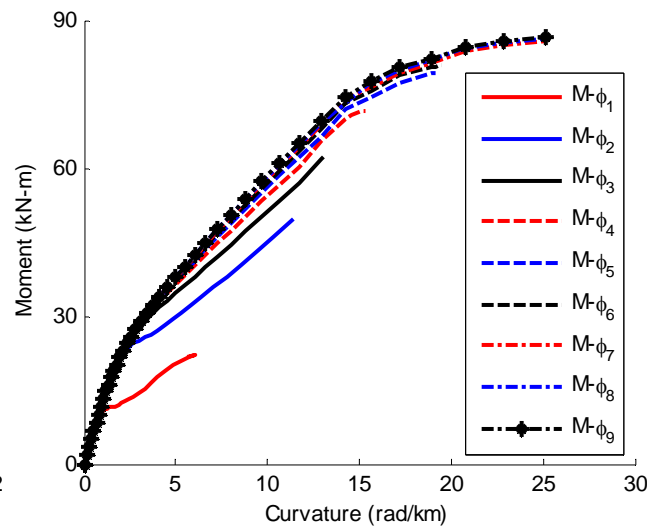
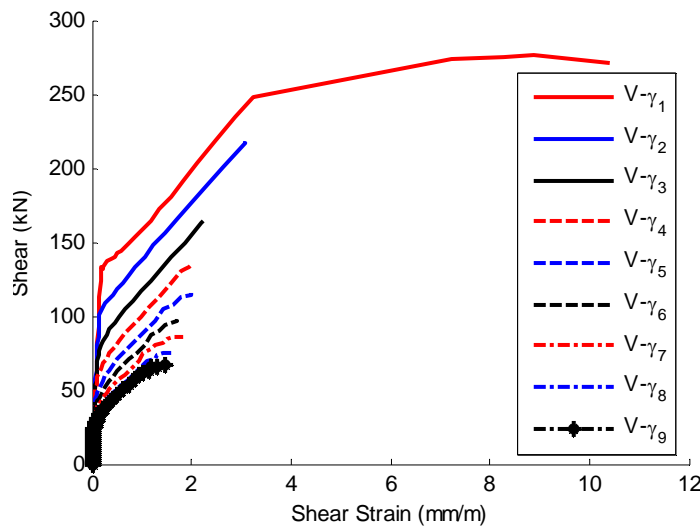
- Input the V- Δ_s and M- θ curve to Shear-UEL & Flexural-UEL.



Shear-Flexure Interaction (SFI) under Constant Axial Load



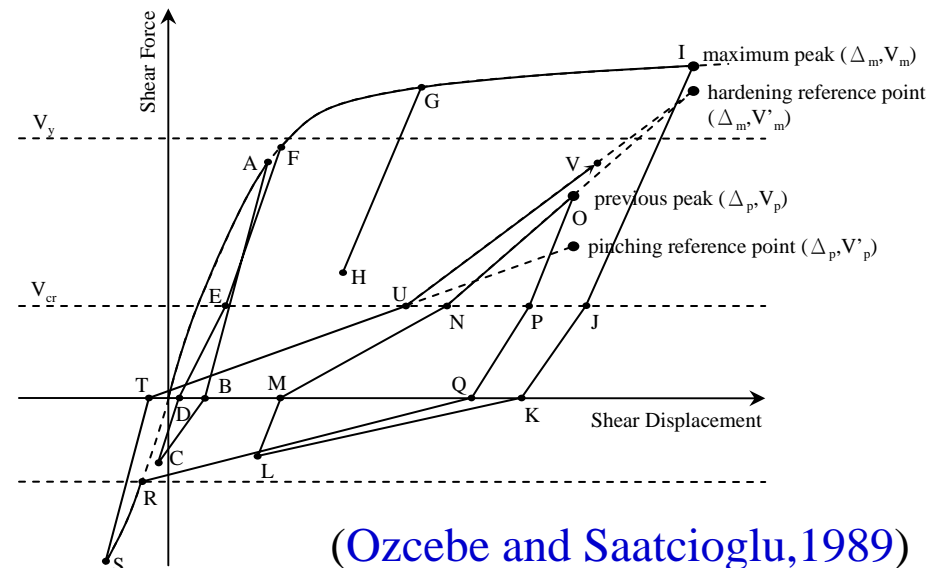
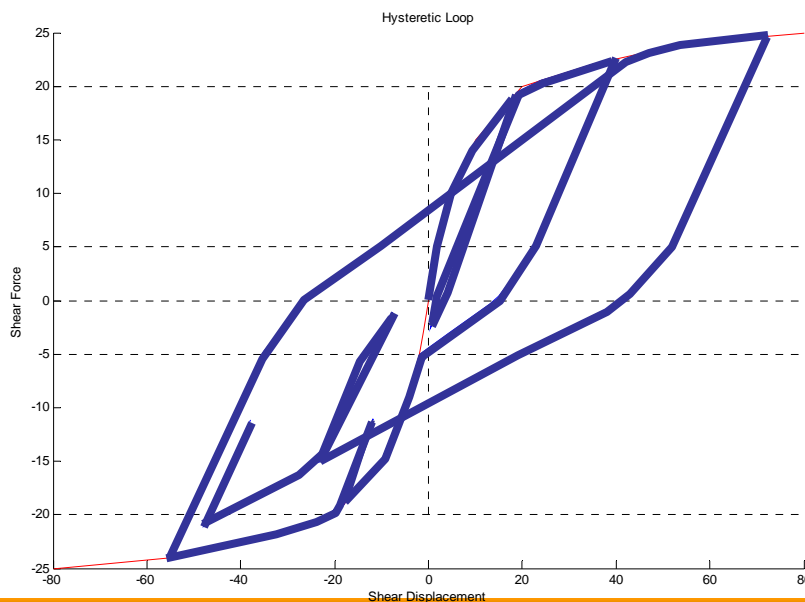
- Sections with different M/V ratio (level of shear-flexural interaction) demonstrate different mechanical properties and behaviors
- Section with higher M/V ratio:
 - Larger moment capacity
 - Smaller shear capacity
- Maximum moment capacity is bounded by pure bending case



Improved Hysteretic Rules for Shear & Flexural Springs

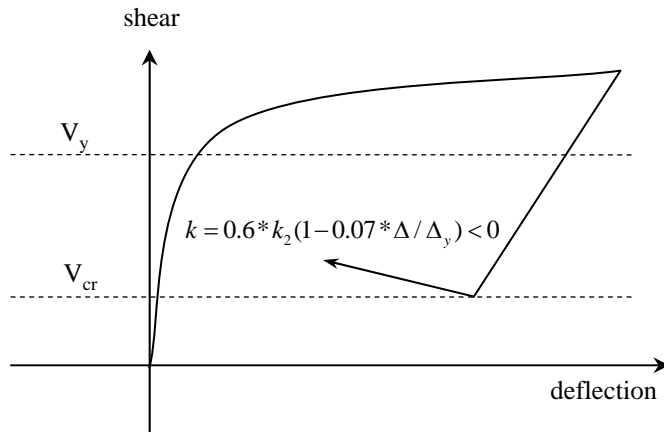
□ Unloading & reloading stiffness depend on: (Xu and Zhang 2011)

- Primary curve (K_{elastic} , Crack, & Yield) ← Structural characteristics
 - Cracked? Yielded? ← Damage in the column
 - Shear force level
 - Max ductility experienced
 - Loading cycles at max ductility level
 - Axial load ratio
- ← Past loading history
- ← Varying during earthquake !!

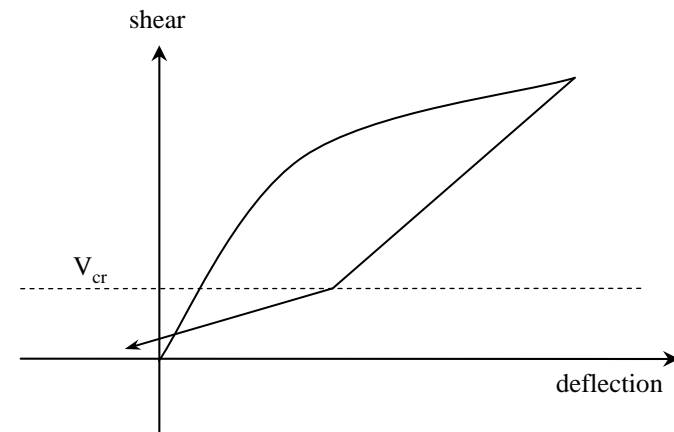


(Ozcebe and Saatcioglu, 1989)

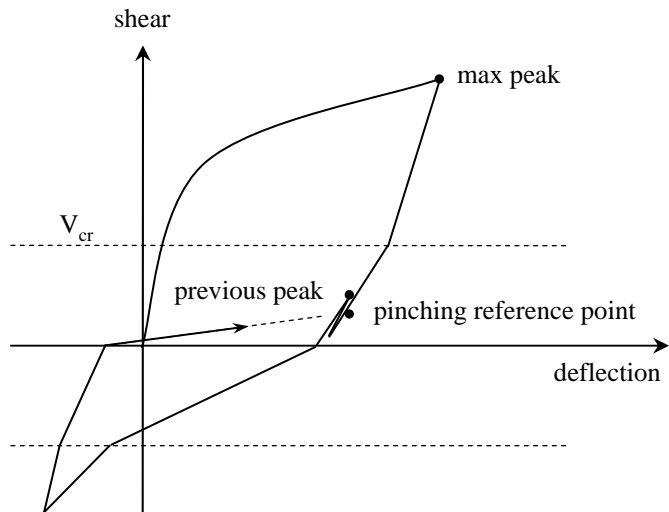
Defects of Ozcebe & Saatcioglu's Model



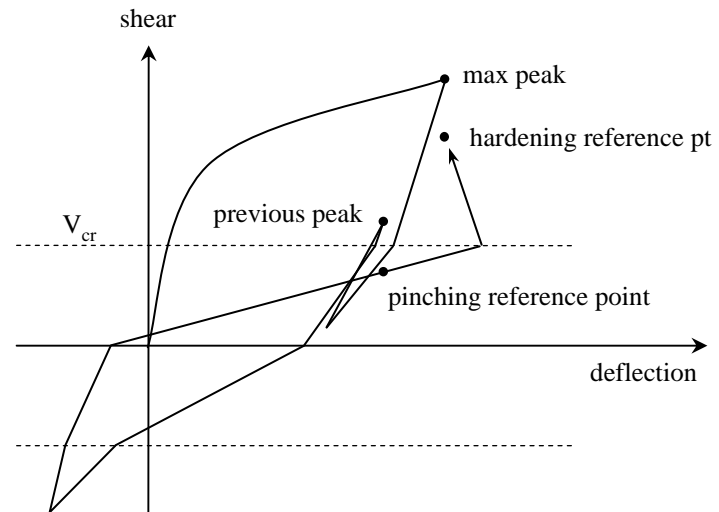
(a) negative unloading stiffness at large ductility level



(b) negative residual in a positive unloading branch



(c) nearly-zero pinching stiffness



(d) negative hardening stiffness

Proposed Flexural Hysteretic Model

- Using the same numerical framework as the shear hysteretic model to expedite the programming procedure
- Unloading stiffness above and below crack load is given by:

$$k_{uld1} = k_2 * 1.2 * e^{-0.125 * (\theta / \theta_y)^{0.25}} * (1 - 0.016 * \theta / \theta_y)^{3.5}$$

$$k_{uld2} = 0.70 * k_2 * 1.2 * e^{-0.125 * (\theta / \theta_y)^{0.35}} * (1 - 0.020 * \theta / \theta_y)^{4.5}$$

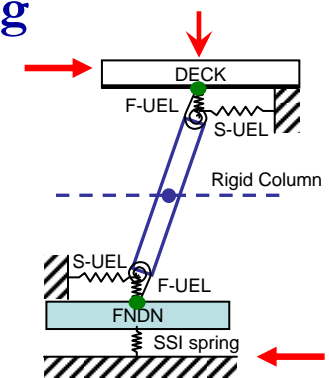
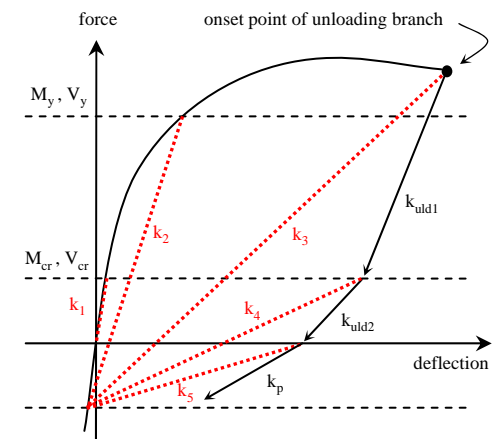
- Reloading stiffness from 0 to M_{cr} is replaced by:

$$k_p = 0.56 * k_2 * 1.2 * e^{-0.125 * (\theta / \theta_y)^{0.35}} * (1 - 0.020 * \theta / \theta_y)^{4.5}$$

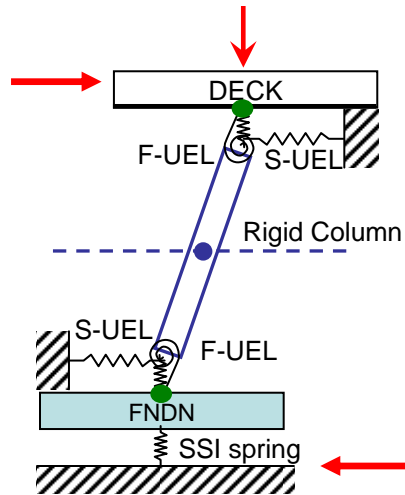
Apply minimum stiffness k_5 to prevent extremely soft reloading stiffness at small ductility level

- Reloading reference point is controlled by:

$$M'_m = M_m * e^{[-0.002 * \sqrt{\theta_m / \theta_y} * n - 0.010 * \sqrt{n} * (\theta_m / \theta_y)]}$$

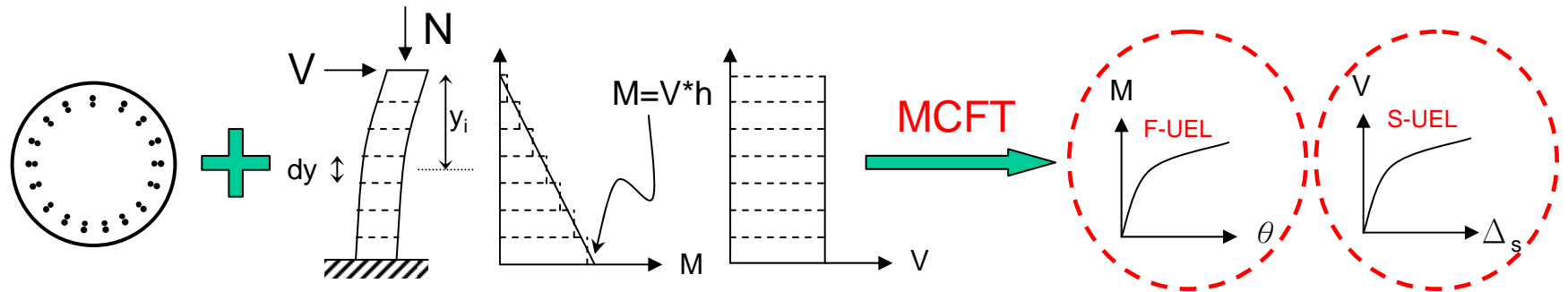


Shear-Flexure Interaction (SFI) Model



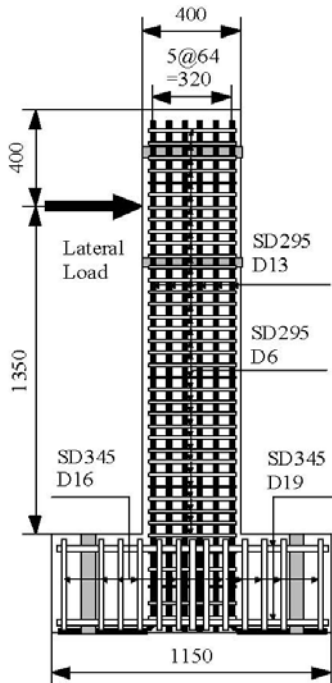
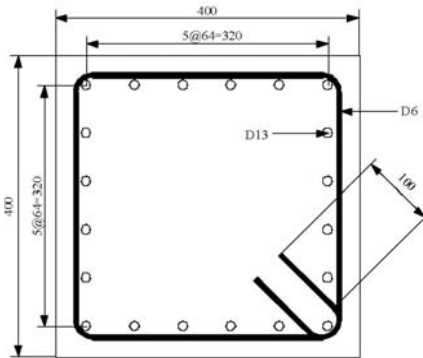
Shear-Flexure Interaction (SFI) is captured in this model at

- (1) Section/material level when deriving the backbone curves for the rotational and shear springs using **MCFT**;
- (2) Element level when the balance between shear force and moment is enforced by the **local equilibrium**.

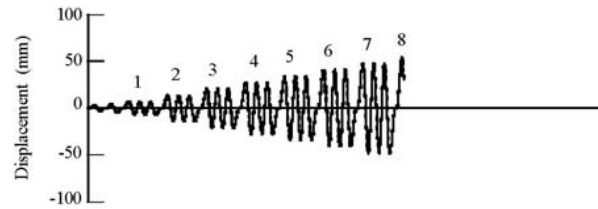


$$M = V * h$$

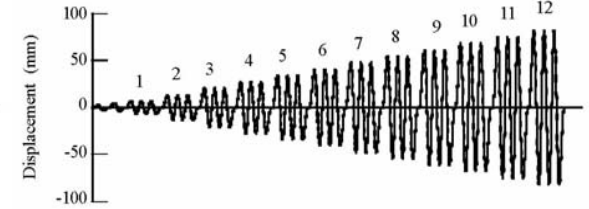
Cyclic Test: Experimental Program – TP031 & TP032



TP-031



TP-032

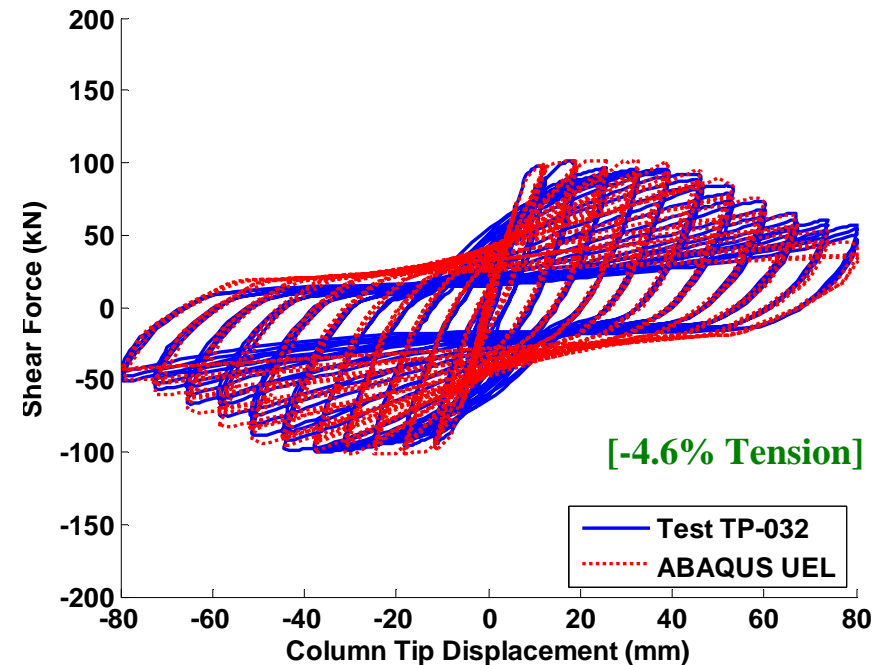
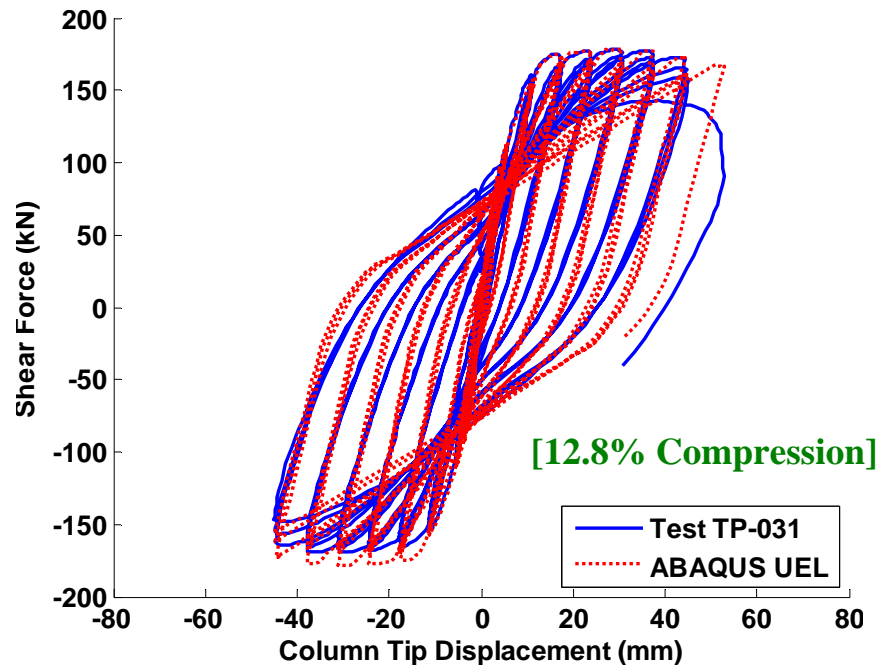


A measure of the level of Shear-Flexure Interaction

	TP-31	TP-32	TP-33	TP-34
ID in the Reference	CC	CT	V1	V2
Section	Square			
Section Size (mm)	400 × 400			
Effective Height h (mm)	1350			
Effective Depth d (mm)	360			
Aspect Ratio	3.75 $\equiv \frac{\text{Height}}{\text{Diameter}}$			
Longitudinal Reinforcement Ratio (%)	1.58			
Volumetric Ratio of Tie Reinforcement ρ_s (%)	0.79			
Cylinder Strength of Concrete σ_{c0} (MPa)	22.9	23.0	22.9	23.0
Longitudinal Reinforcement	SD295A D13 (Yield Strength=374MPa)			
Tie Reinforcement	SD295A D6 (Yield Strength=363MPa)			
Axial Force (kN) (at the Bottom)	470 (3.0MPa) (Constant)	-170 (-1.0MPa) (Constant)	-10~310 (0~2.0MPa) (Varying)	-170~420 (-1.0~2.7MPa) (Varying)

compression tension

Column Responses: Compression vs Tension

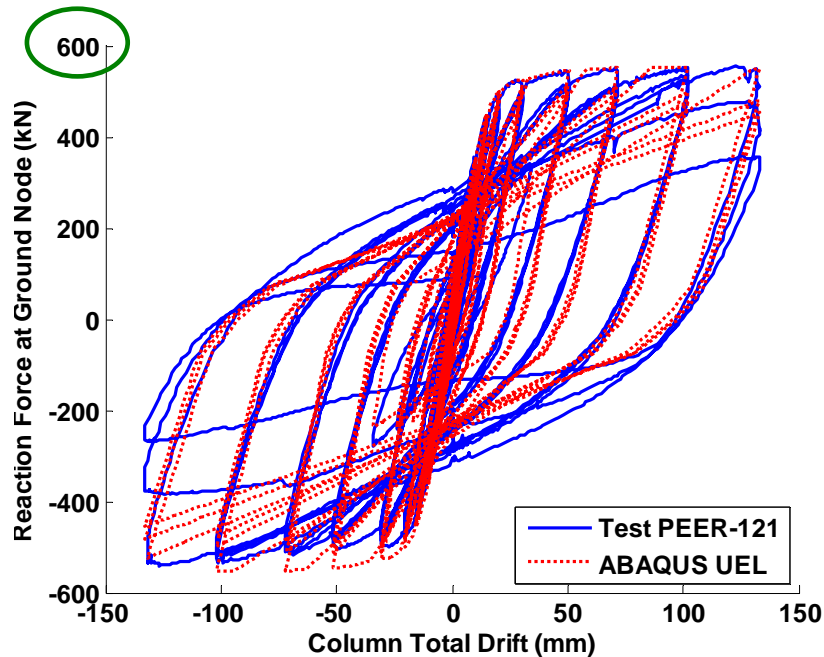


- ❑ Developed SFI-UEL works fine with columns under **either compressive or tensile axial force**.
- ❑ **Variation in axial force DOES HAVE significant effect on the lateral hysteretic response of RC columns !**

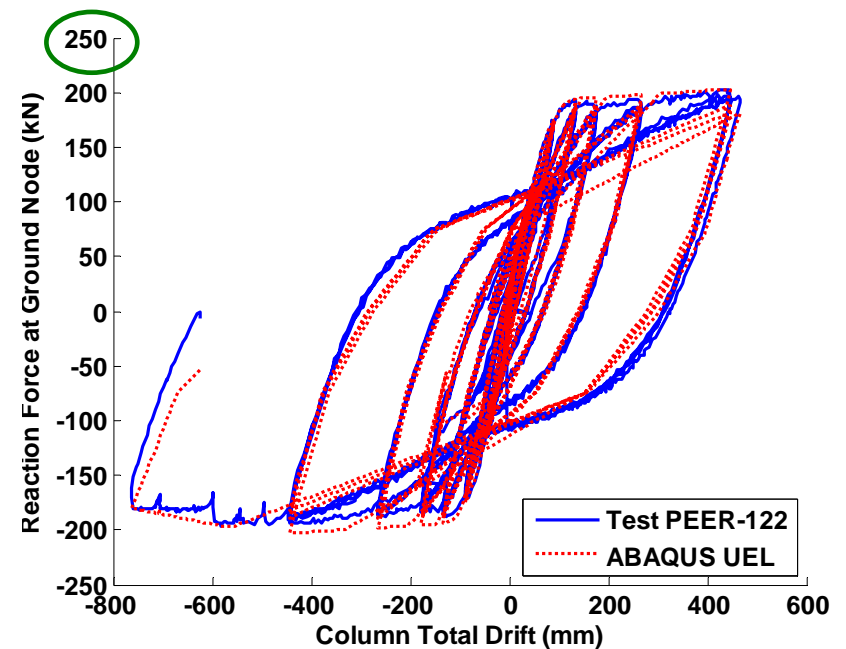
Column Responses: Shear vs Flexural Dominant

Column Index	Column Size (mm)	Column Height (mm)	Number of Steel Rebars	Longitud. Steel Diameter (mm)	Transverse Steel Diameter (mm)	Longitud. Reinforce. Ratio	Transverse Reinforce. Ratio	f_y (MPa)	f_c' (MPa)	Axial Load (kN)	Axial Load Ratio
PEER-121	606.6 circ.	1828.8	28	19.05	6.4	2.73%	0.89%	441	34.5	911.84	9.0%
PEER-122	606.6 circ.	4876.8	28	19.05	6.4	2.73%	0.89%	441	34.5	911.84	9.0%

- Developed SFI model is able to simulate the responses of either **shear-flexural dominant** or **flexural dominant** RC columns.



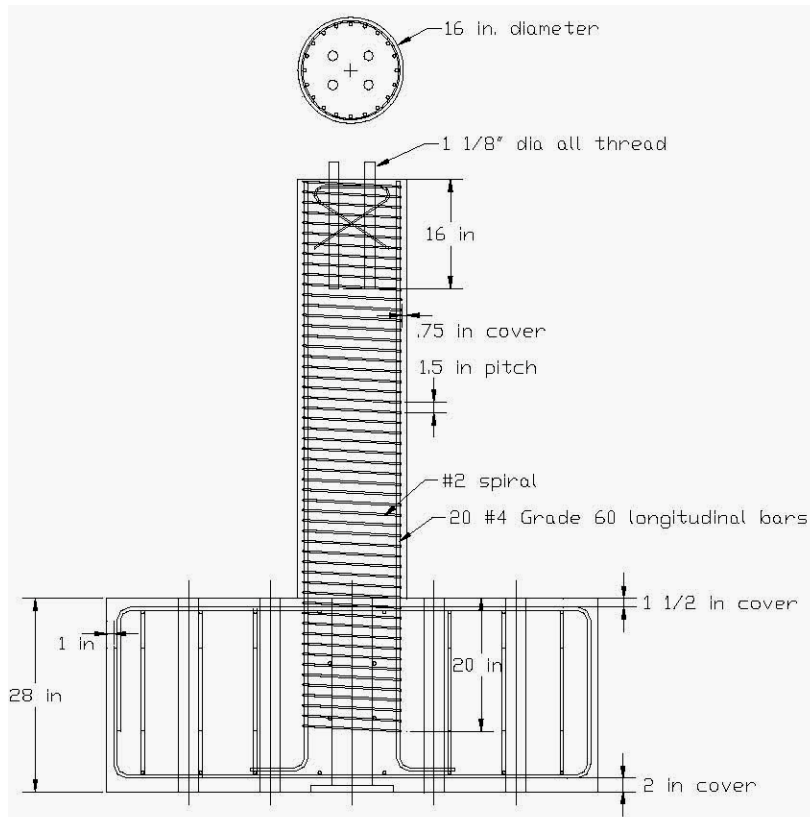
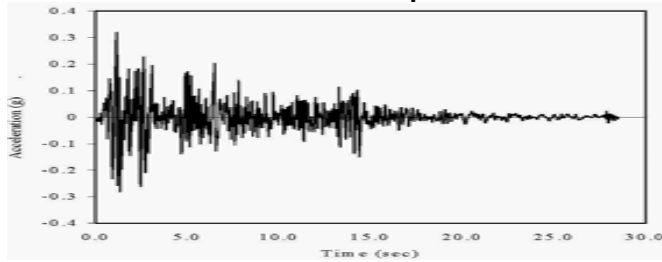
(a) PEER-121, **Aspect ratio (H/D) = 3**



(b) PEER-122, **Aspect ratio (H/D) = 8**

Dynamic Test : Experimental Specimen 9F1 & 9S1

El Centro Earthquake



9F1		
Specimen	Motion	Input Motion
COLUMN 9F1		Low Level Random
	*1	1/3 x El Centro
	2	2/3 x El Centro
	3	1.0 x El Centro
	4	1.5 x El Centro
	5	2.0 x El Centro
	6	2.5 x El Centro
	7	3.0 x El Centro
	8	3.5 x El Centro
9	4.0 x El Centro	

9S1

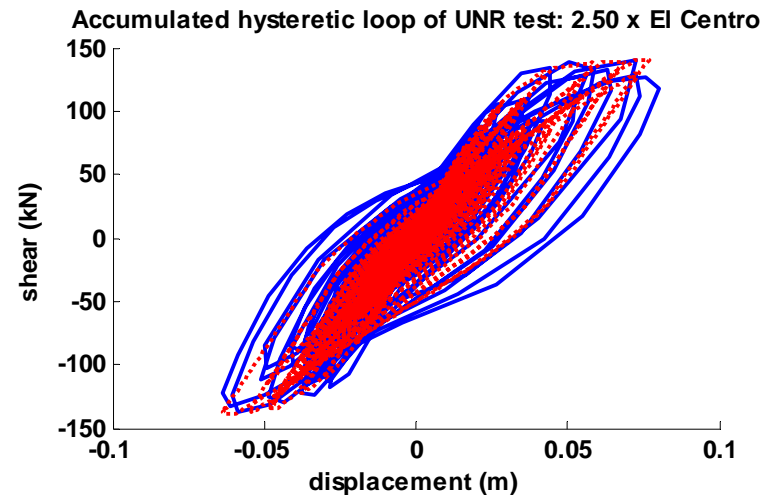
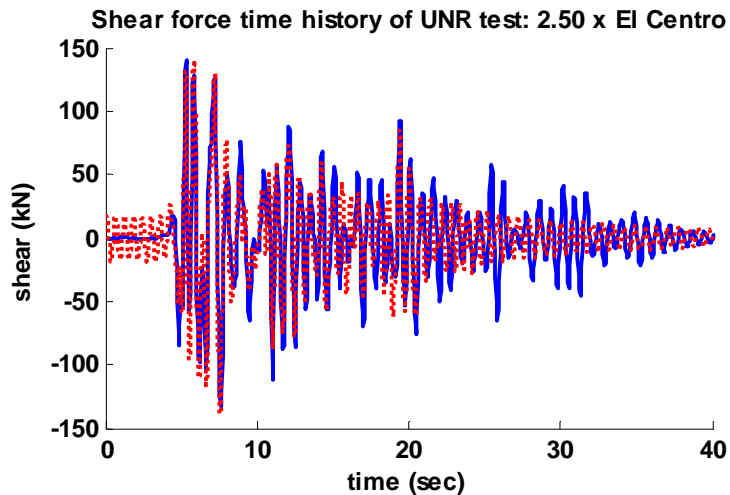
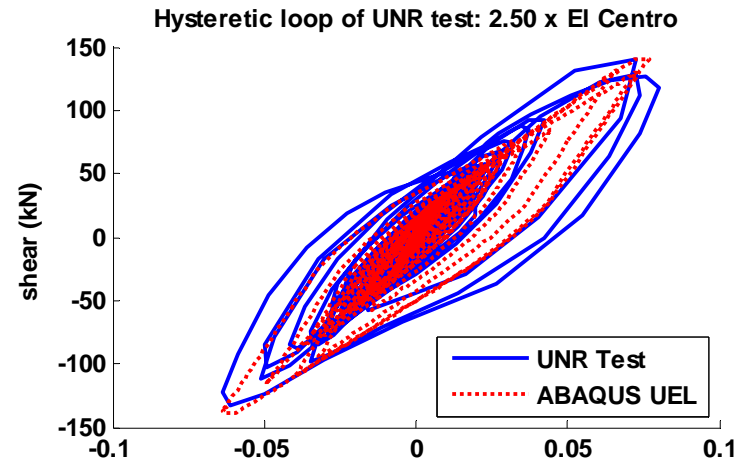
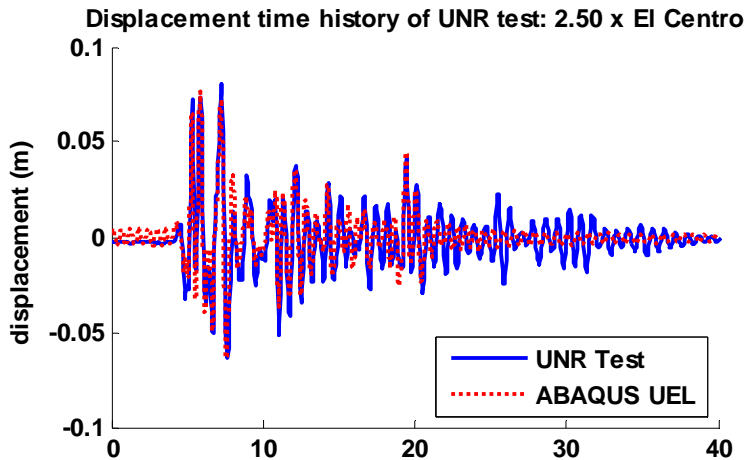
3.25 x El Centro

University of Nevada, Reno (Laplace et al. 1999)

	UNR MODEL
Scale	1/3
Aspect Ratio	4.5
Column Height	72 in.
Column Diameter	16 in.
Axial Load	80 kips
P/fcAg	0.1
Long. Steel Ratio	2%
Long. Bars	20 #4
Confinement	1/4 in. dia. wire
Spiral Pitch	1.5 in.
Spiral Ratio	1%
Concrete Cover	0.75 in.

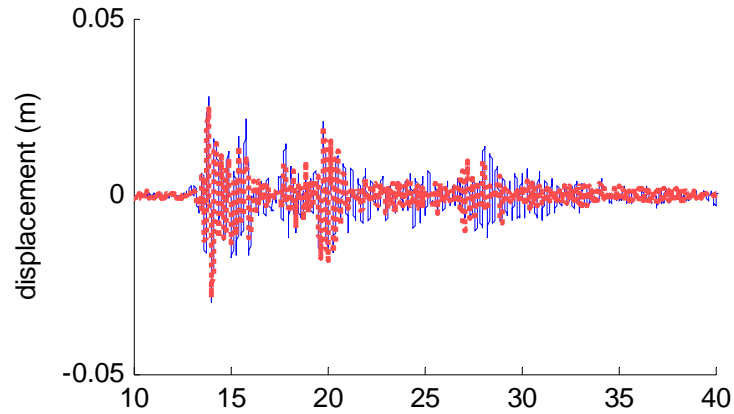
3.0

Hysteretic Loops of Column 9F1: 2.50x (6th Stage)

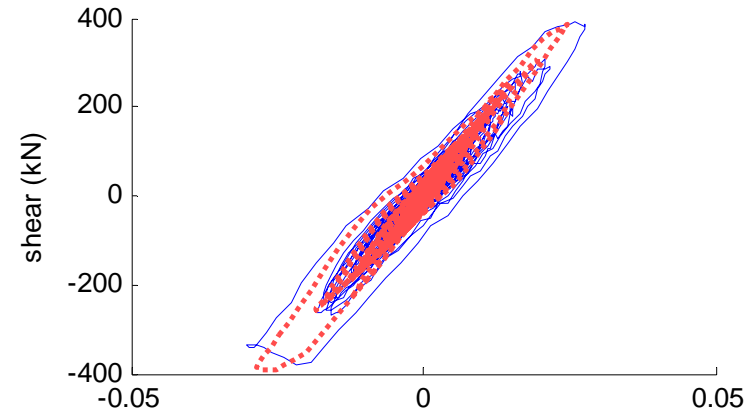


Stage VI : PGA = 2.5 x El Centro Earthquake record

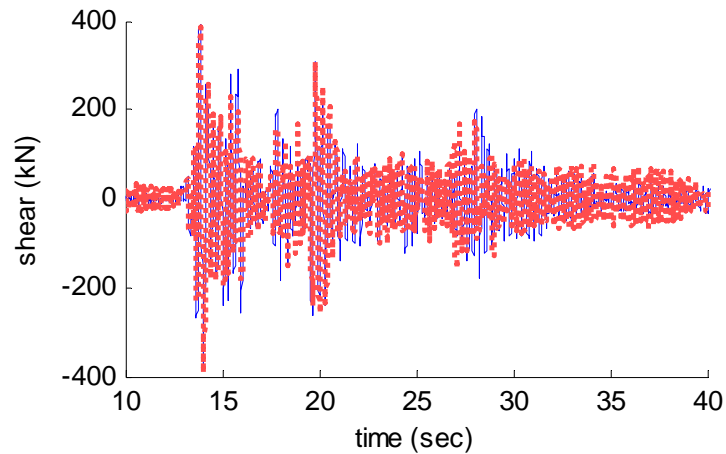
Hysteretic Loops of Column 9S1: 2.50x (6th Stage)



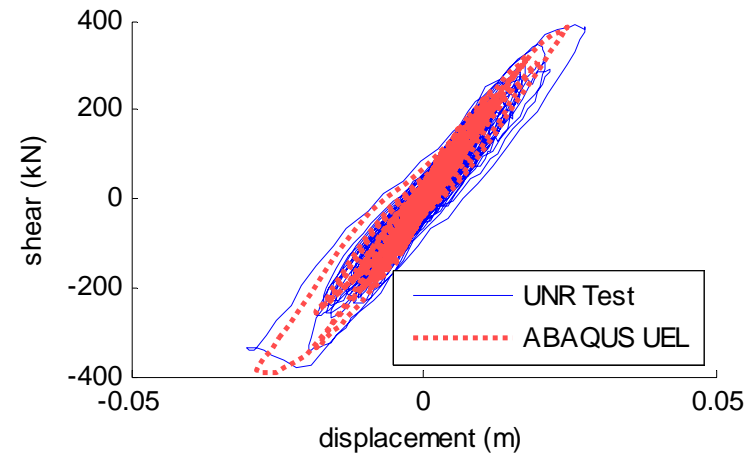
(a) Displacement time history



(b) Hysteretic response at current stage



(c) Shear force time history



(d) Accumulated hysteretic response

Stage VI : PGA = 2.5 x El Centro Earthquake record

Summary

- An analytical approach is introduced to generate the shear and flexure **primary curves** for RC column.
- Model defects in **shear hysteretic** rules are fixed; new equations are proposed and calibrated to model the **flexural hysteretic responses** of RC columns.
- The SFI model has been extensively validated against **cyclic tests and shake table tests**.
- Laboratory tests shows that **axial load** can significantly affect the shear and flexural responses of the columns.
- **Aspect ratio** (H/D ratio) is a measurement of the level of SFI.

Outline

- **Introduction**
 - Motivation & Objectives
 - Significance of Axial-Shear-Flexure Interaction
- **Shear-Flexure Interaction Hysteretic Model Under Constant Axial Load**
 - Generation of Primary Curves Considering Shear-Flexure Interaction
 - Improved Reloading/Unloading Hysteretic Rules
- **Inelastic Displacement Demand Model for Bridge Columns**
 - Modeling of Columns & Consideration of Ground Motions
 - Dimensional Analysis
- **Seismic Response Simulation of Bridges**
 - Site Specific Ground Motions
 - Soil-Structural Interaction
 - Nonlinear Behavior of Columns
- **Axial-Shear-Flexure Interaction Hysteretic Model Under Variable Axial Load**
 - Generation of Primary Curve Family
 - Stress Level Index & Two-stage Loading Approach
- **Conclusion**

Introduction

□ Motivation

- Adequate prediction on **displacement demand** is the key to conduct **performance-based design**
- Existing displacement demand models in general do not reflect the **realistic inelastic behavior** of RC columns
- Existing models do not consider the **combined actions**

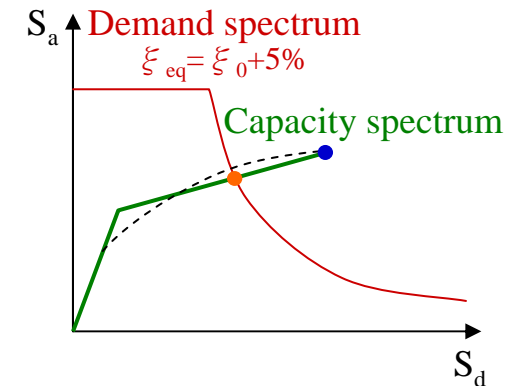
□ Objectives

- A **simplified displacement demand model** for RC columns
- A model that takes into account:
 - the effects of **shear-flexure interaction**,
 - column **structural properties** (strength and post-yield stiffness),
 - accumulated **material damage** (e.g. strength deterioration, stiffness degrading, and pinching behavior), and
 - (near-fault) **ground motion features**.

Quick Review of Existing Models

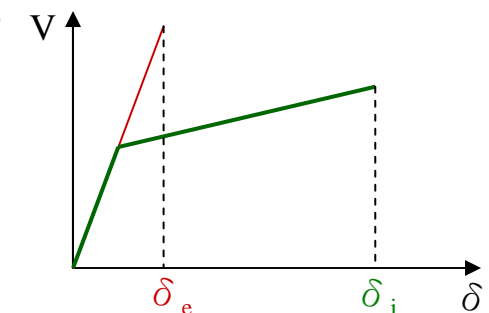
□ Capacity spectrum method (ATC-40)

- assuming a Trial Performance Point
- constructing the bilinear representation of capacity spectrum and the reduced 5% response spectrum based on the trial performance point
- in Acceleration-Displacement Response Spectra (ADRS) format (i.e., S_a versus S_d)
- iteration to find the converged **Performance Point**



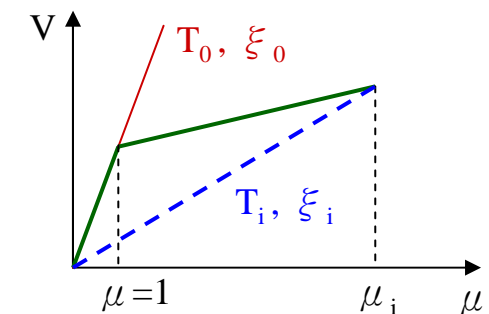
□ Inelastic displacement coefficient methods (FEMA 273, 356, 440)

- same initial stiffness & damping coefficient
- $\delta_i = C_0 \dots C_n \cdot \delta_e$
- estimating nonlinear inelastic displacement by multiplying elastic displacement of SDOF system with (several) modification factor(s)



□ Equivalent linearization methods

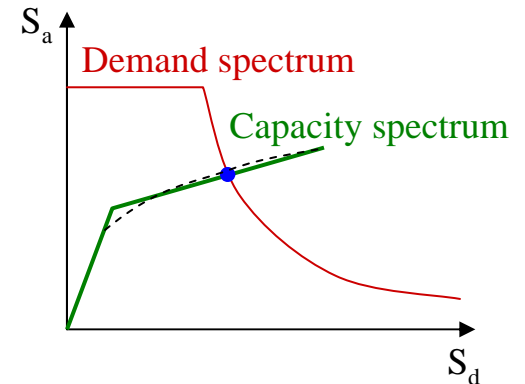
- secant stiffness & equivalent damping coefficient at given ductility level
- $T_i = f_1(\mu_i, T_0); \quad \xi_i = f_2(\mu_i, \xi_0)$
- estimating the nonlinear inelastic displacement using the elastic response spectrum of SDOF system with equivalent natural period and damping ratio



Deficiency of Existing Models

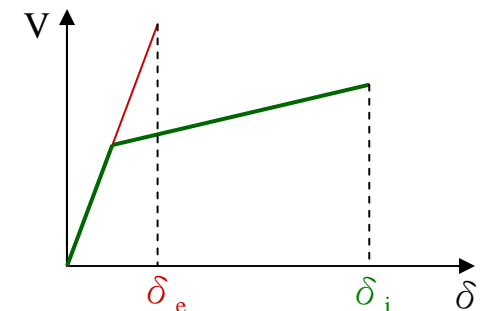
□ Capacity spectrum method (ATC-40)

- replacing the inelastic spectra with **highly damped elastic spectra** is questionable
- may not converge to the correct response



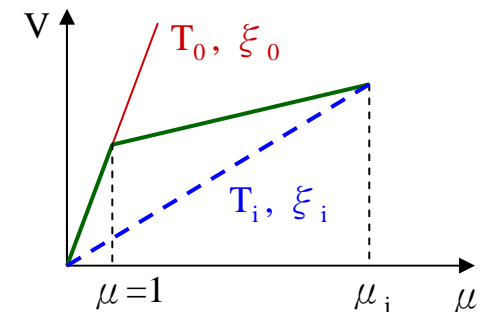
□ Inelastic displacement coefficient methods (FEMA 273, 356, 440)

- Most of the results were based on the responses of **elasto-plastic or bilinear SDOF systems** w/o the consideration of **material damage**



□ Equivalent linearization methods

- produce more accurate prediction in intermediate and long period ranges
- may either underestimate or overestimate the displacement in **short period ranges**

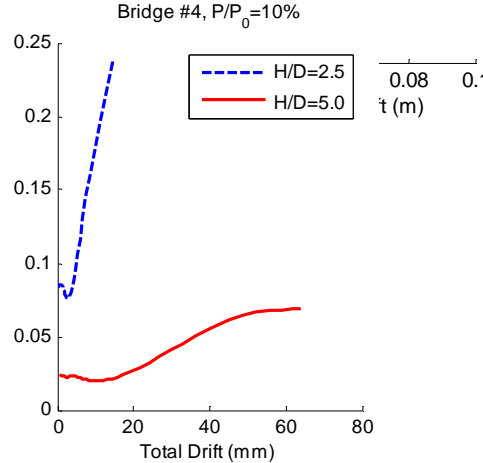
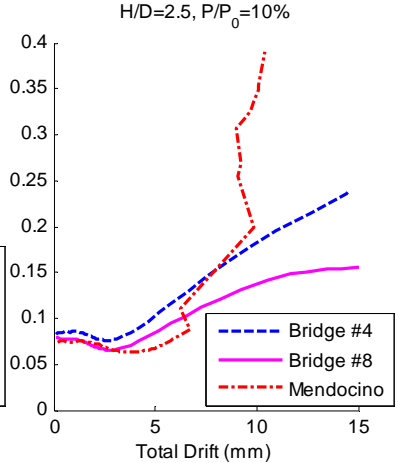
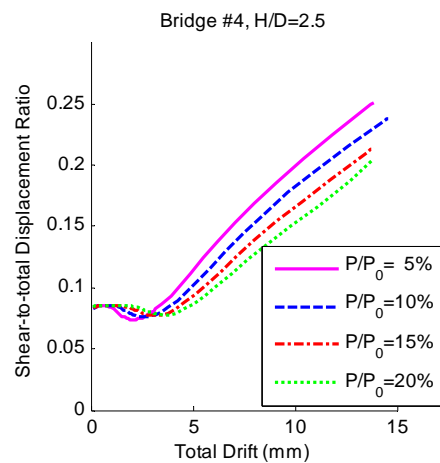
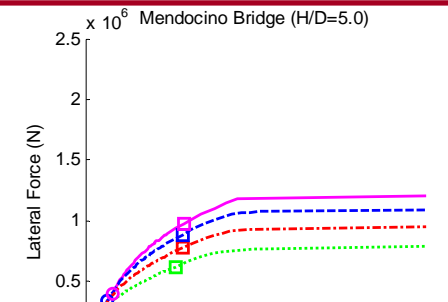
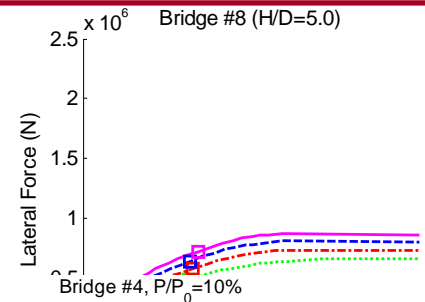
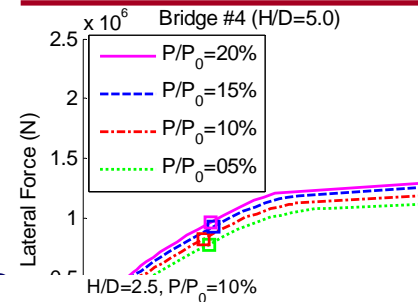
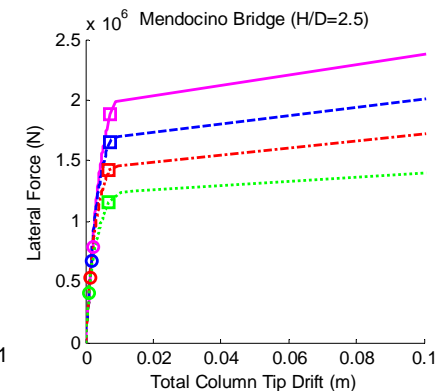
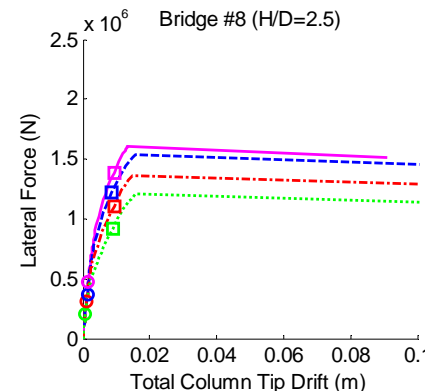
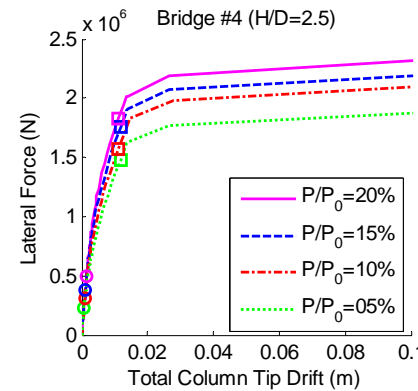


Effects of Combined Actions on Structural Responses

- ◆ 3 columns
- ◆ 2 aspect ratios
- ◆ 4 axial load levels

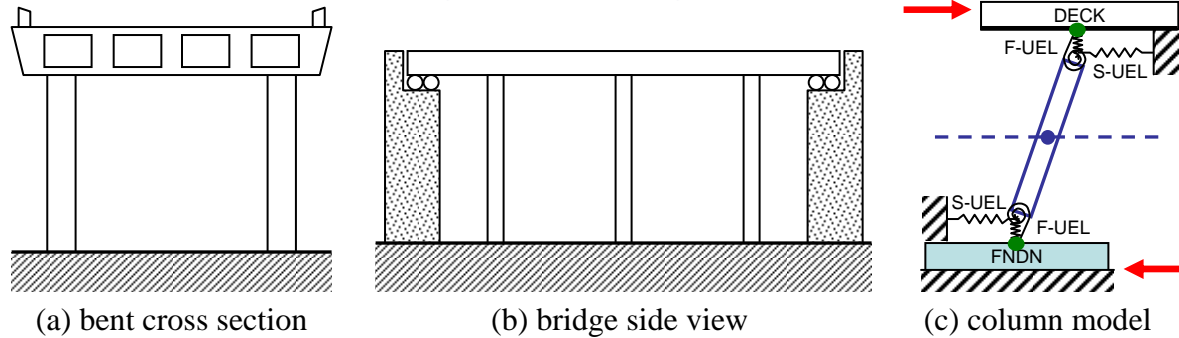
- Primary Curve
 - capacity
 - initial stiffness
 - post-yield K

- Shear-to-total Displ. Ratio



Modeling of Columns & Consideration of Ground Motions

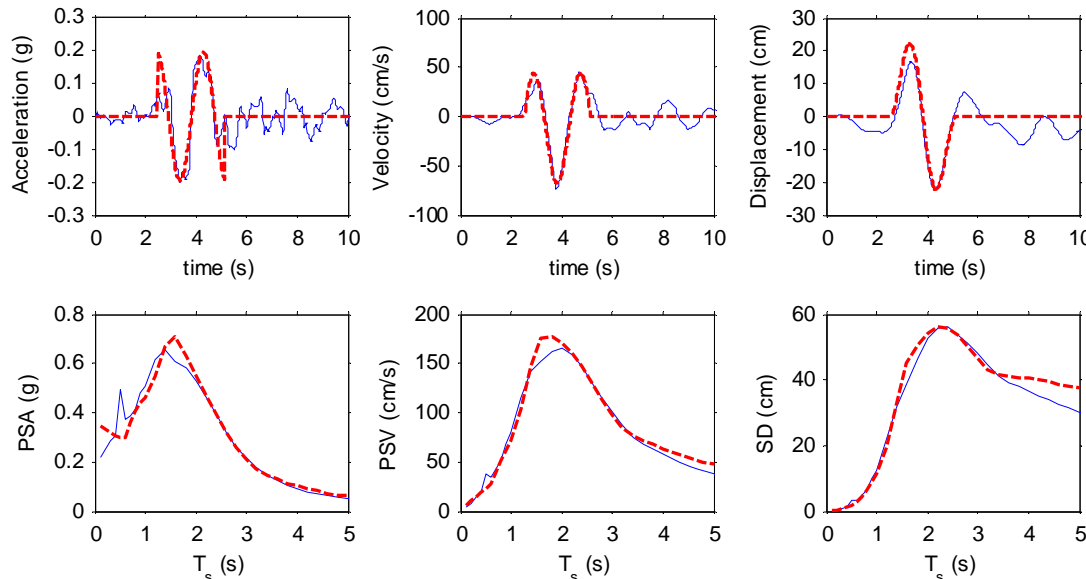
□ Structural modeling of bridge columns



The properties of the F-UEL and S-UEL are determined by:

- total primary curve;
- shear-to-total displacement ratio.

□ Pulse representation of near fault ground motions



Major characteristics of the identified pulse-type waveforms:

- Amplitude, a_p
- Frequency, ω_p

Dimensional Analysis & Similarity of Responses

□ Dimensional analysis

- utilizing the **characteristic length scale** (amplitude, a_p) and **time scale** (frequency, ω_p) of near-fault ground motions to normalize the input and output physical quantities.

□ Amplitude independent behavior of columns

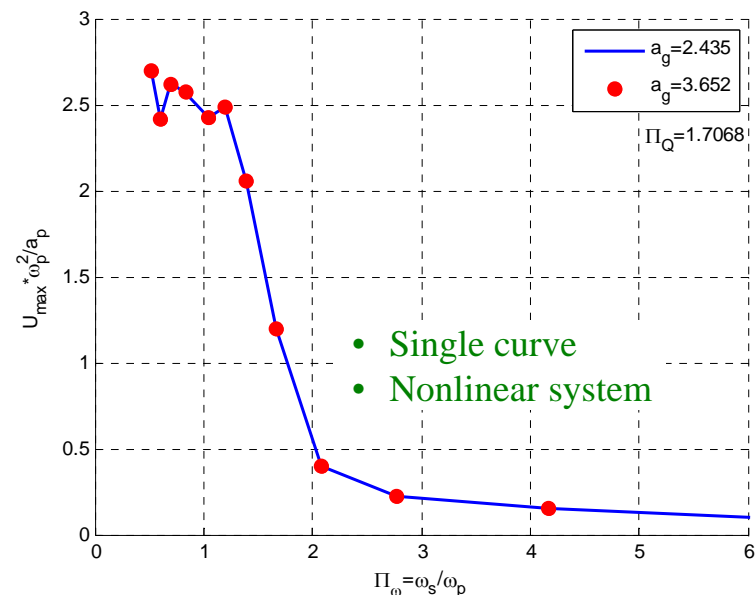
- normalized response of a **bilinear system** are independent of the amplitude of ground motions, showing better correlation.

$$\ddot{u} + 2\xi_s \omega_s \dot{u} + \omega_s^2 u_y \tilde{f}_s(u, \dot{u}) = -a_p g(\omega_p t)$$

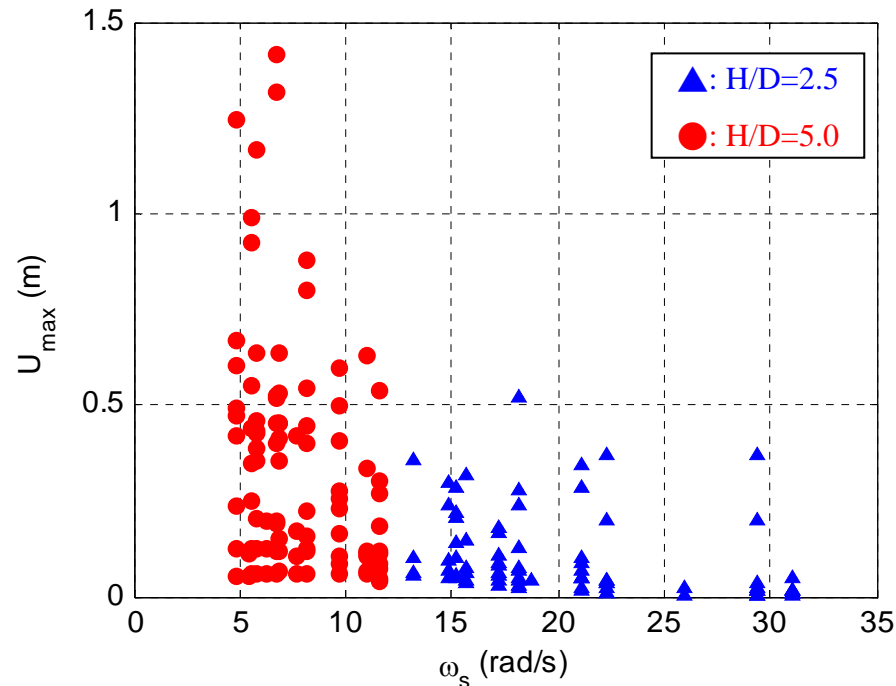
$$u_{\max} \equiv \max_t (|u(t)|) = f(\omega_s, \xi_s, u_y, \varepsilon_s, a_p, \omega_p)$$

Normalization by a_p & ω_p Number of independent variables is reduced by two.

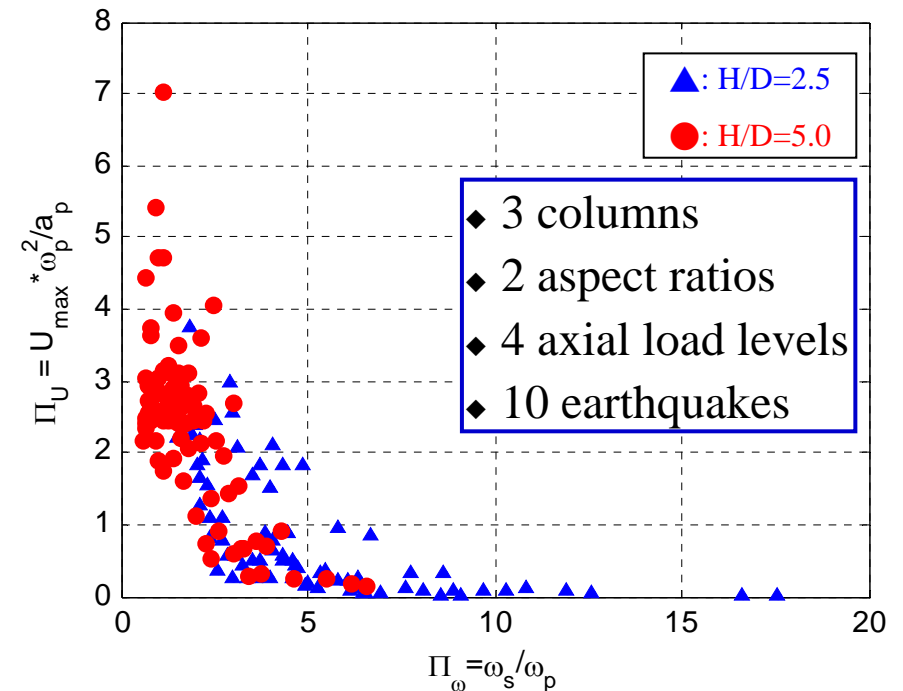
$$\Pi_u \equiv \frac{u_{\max}^{\max} \omega_p^2}{a_p} = \phi(\Pi_\omega, \Pi_\xi, \Pi_{u_y}, \Pi_\varepsilon) = \hat{\phi}(\Pi_\omega, \Pi_\xi, \Pi_Q, \Pi_\varepsilon)$$



Dimensionless Displacement Response of Columns



Response Spectrum in **Dimensional** Form

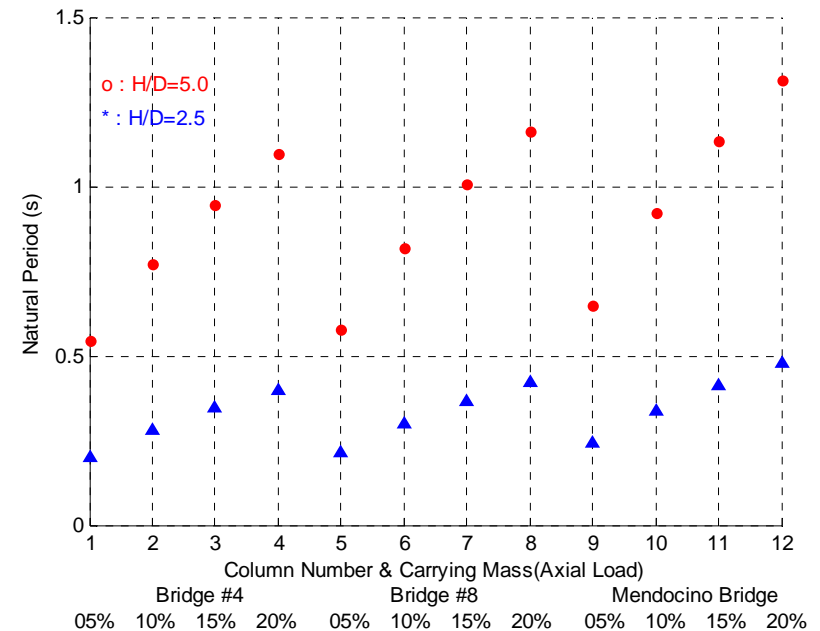


Response Spectrum in **Dimensionless** Form

- **No trend** can be found if the displacement demand is displayed in **dimensional** form.
- **A clear trend** emerges when the displacement demand is displayed in **dimensionless** form.

Significance of Aspect Ratio

- Aspect Ratio, defined as H/D in this study, is a measure of the **M/V ratio** (recall $M/V=H$ in a cantilever column) at the critical sections of a bridge column.
- Smaller the H/D ratio implies smaller the M/V ratio and therefore higher the **level of shear-flexure interaction**.
 - **Natural period** of a bridge column is also significantly affected by its aspect ratio.



Elastic periods of columns in simulation.

Significance of Nonlinearity Index , Π_{NL}

$$\Pi_{NL} \equiv \frac{m \cdot a_g}{Q_y} \left[\frac{1}{1 + k_p / (Q_y / u_y)} \right]$$

$m \cdot a_g$: a measure of max shear force imposed by earthquake

Q_y : a measure of the shear strength of bridge column

k_p : post-yield stiffness

Q_y / u_y : pre-yield stiffness

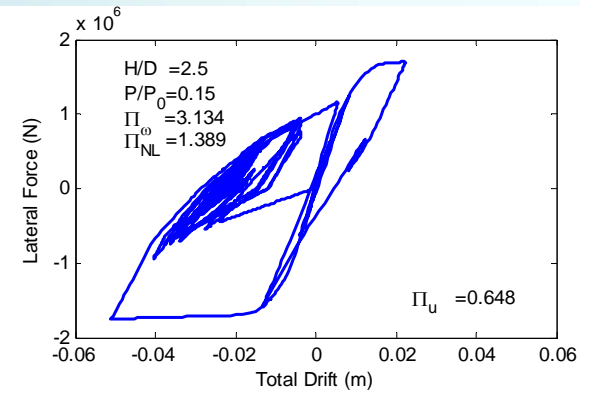
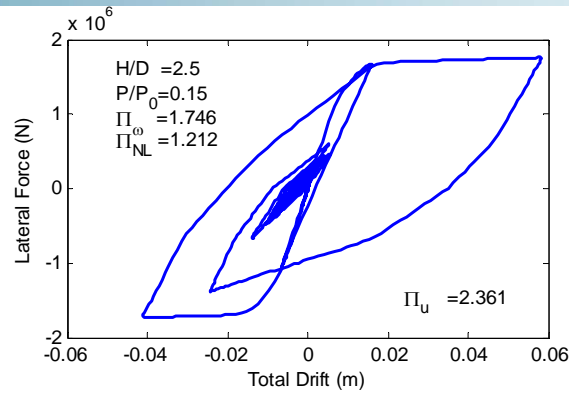
$\frac{1}{1 + \frac{k_p}{Q_y / u_y}}$: a measure of energy dissipation capability compared to elasto-plastic system

- Larger Π_{NL} implies more significant **nonlinear deformation**.

Dominant Dimensionless Parameters

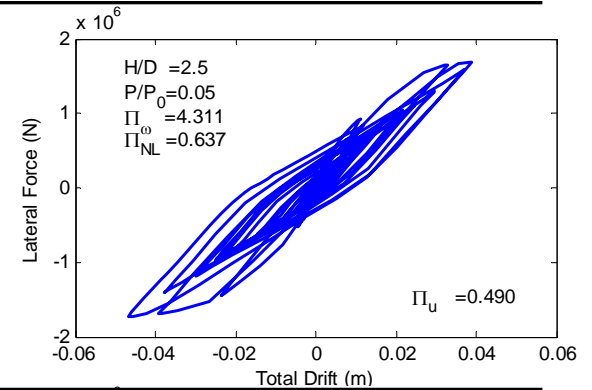
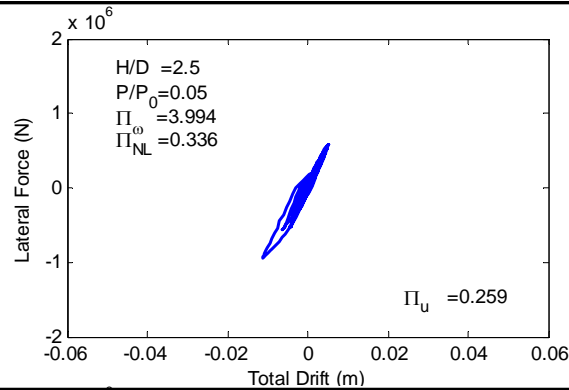
Frequency ratio

$$\Pi_{\omega} \equiv \omega_s / \omega_p$$

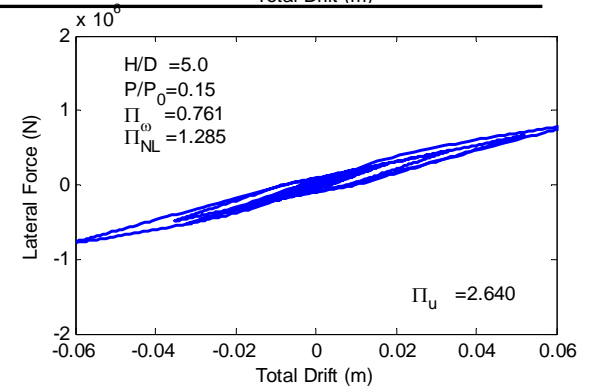
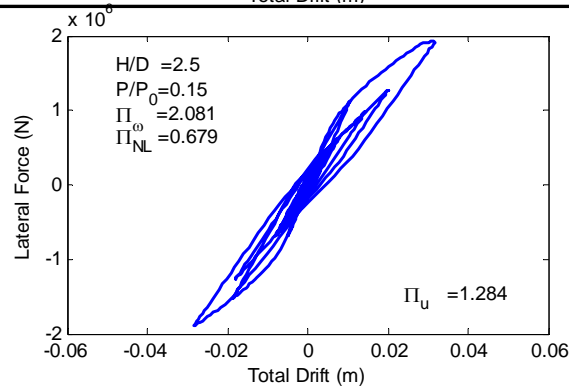


Nonlinearity index (new)

$$\Pi_{NL} \equiv \frac{m \cdot a_g}{Q_y} \left[\frac{1}{1 + k_p / (Q_y / u_y)} \right]$$



Aspect ratio, H/D

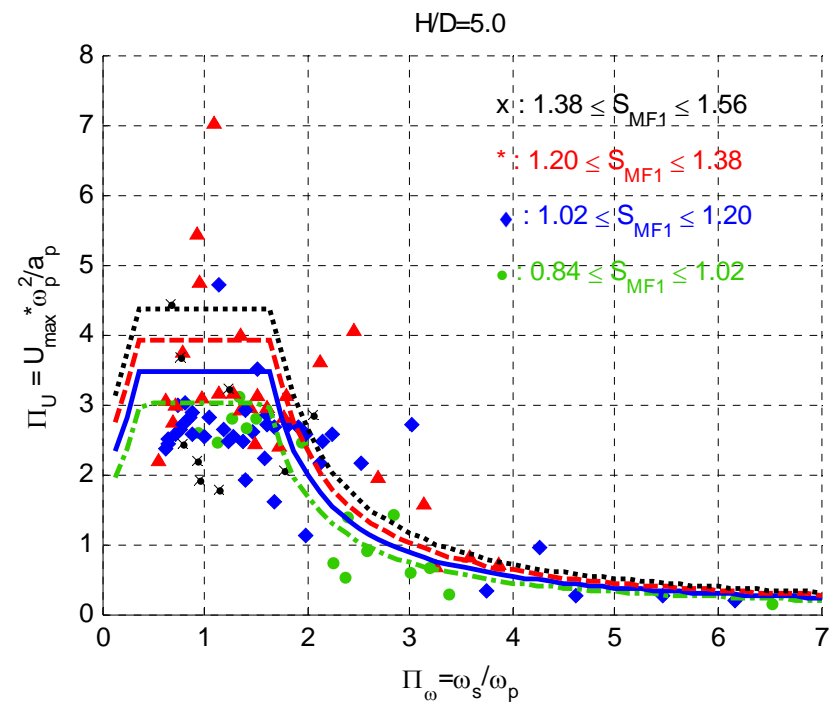
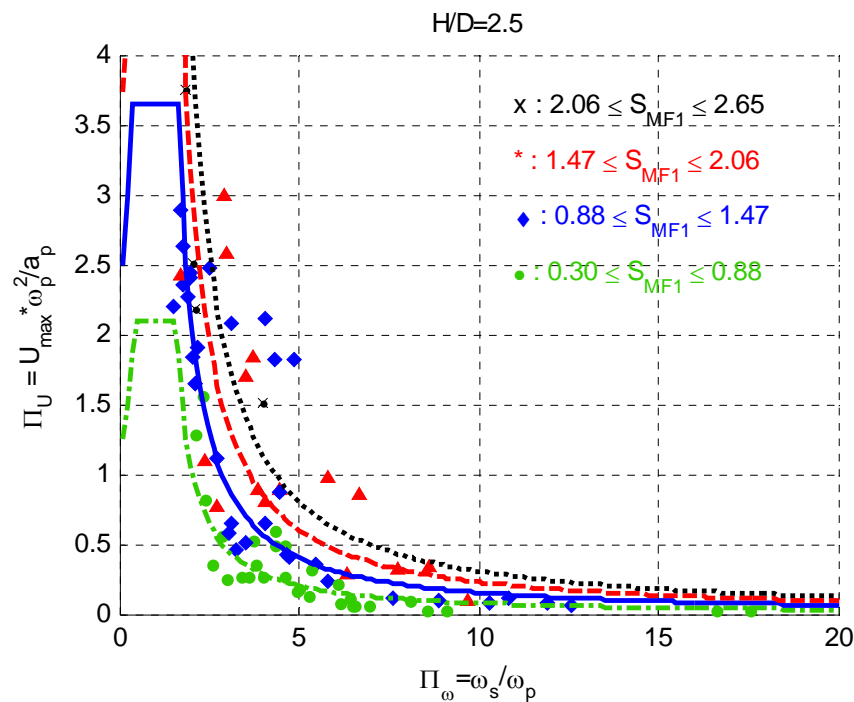


Proposed Displacement Demand Model

$$\Pi_u \equiv \frac{u_{\max} \cdot \omega_p^2}{a_p} = \frac{1.35}{|\Pi_\omega - 1.0|^{1.25}} \cdot S_{MF1} \leq 2.4 \cdot S_{MF1}$$

$$S_{MF1} = \Pi_{NL}^{C_{NL}} \quad (\text{Spectral Modification Factor})$$

$$\text{where } C_{NL} = 0.8\alpha^{-2} \quad \text{and} \quad \alpha = \frac{(H/D)}{2.5}$$



Model Validation

□ Inelastic displacement coefficient methods:

$$\Delta_{inelastic} = C_R \Delta_{elastic}$$

- By Ruiz-Garcia and Miranda (2003)

$$C_R = 1 + \left[\frac{1}{a(T/T_s)^b} - \frac{1}{c} \right] (R-1)$$

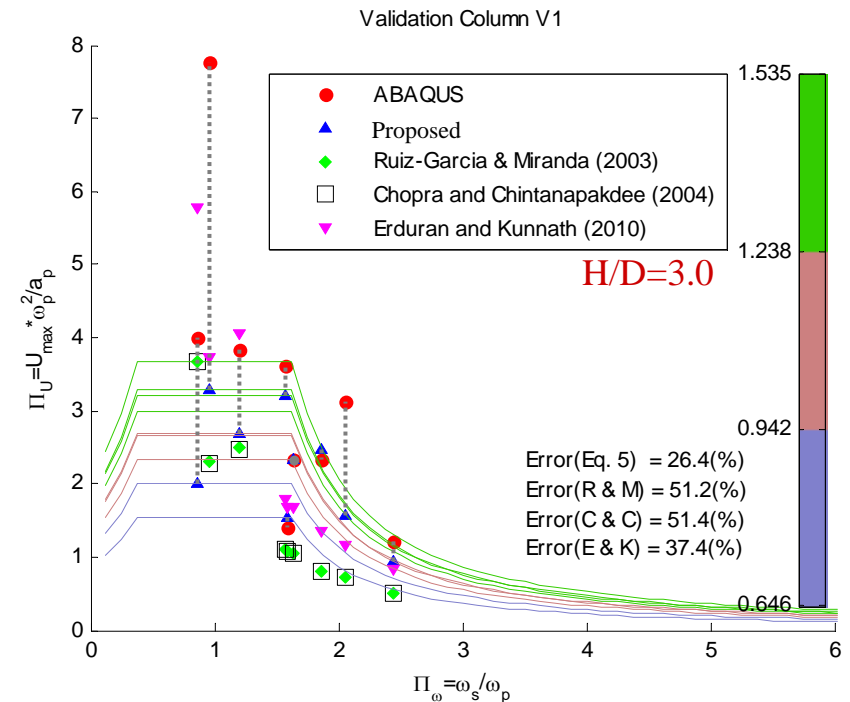
- By Chopra and Chintanapakee (2004)

$$C_R = 1 + \left[(L_R - 1)^{-1} + \left(\frac{a}{R^b} + c \right) \left(\frac{T}{T_c} \right)^d \right], \quad L_R = \frac{1}{R} \left(1 + \frac{R-1}{\alpha} \right)$$

□ Overall Error

- 26.4% -- Proposed model
- 51.2% -- Ruiz-Garcia and Miranda (2003)
- 51.4% -- Chopra and Chintanapakee (2004)
- 37.4% -- Erduran and Kunnath (2010)

$$e = \frac{1}{N} \sum_{i=1}^N \left| \frac{u_{predict}^i - u_{max}^i}{u_{max}^i} \right|$$



$$\Pi_u \equiv \frac{u_{max} \cdot \omega_p^2}{a_p} = \frac{1.35}{|\Pi_{\omega} - 1.0|^{1.25}} \cdot S_{MF1} \leq 2.4 \cdot S_{MF1}$$

$$S_{MF1} = \Pi_{NL}^{C_{NL}}$$

$$\text{where } C_{NL} = 0.8\alpha^{-2} \text{ and } \alpha = \frac{(H/D)}{2.5}$$

Summary

- Inelastic displacement responses of bridge columns are presented in **dimensionless form**.
- A dimensionless **nonlinearity index**, Π_{NL} is derived to take into account of the column strength, ground motion amplitude, and softening or hardening post-yield behavior.
- Normalized inelastic demand ($\Pi_u = u_{\max} \omega_p^2 / a_p$) is revealed to be strongly correlated to the **structure-to-pulse frequency ratio** Π_ω , the **nonlinearity index** Π_{NL} , and the **aspect ratio** H/D .
- A regressive equation is proposed to **directly** estimate the inelastic displacement imposed by earthquake motions.

$$\Delta_{inelastic} = C_R \cdot \Delta_{elastic}$$

- The proposed model can give dependable predictions with direct consideration of **structural and ground motion characteristics**.

Outline

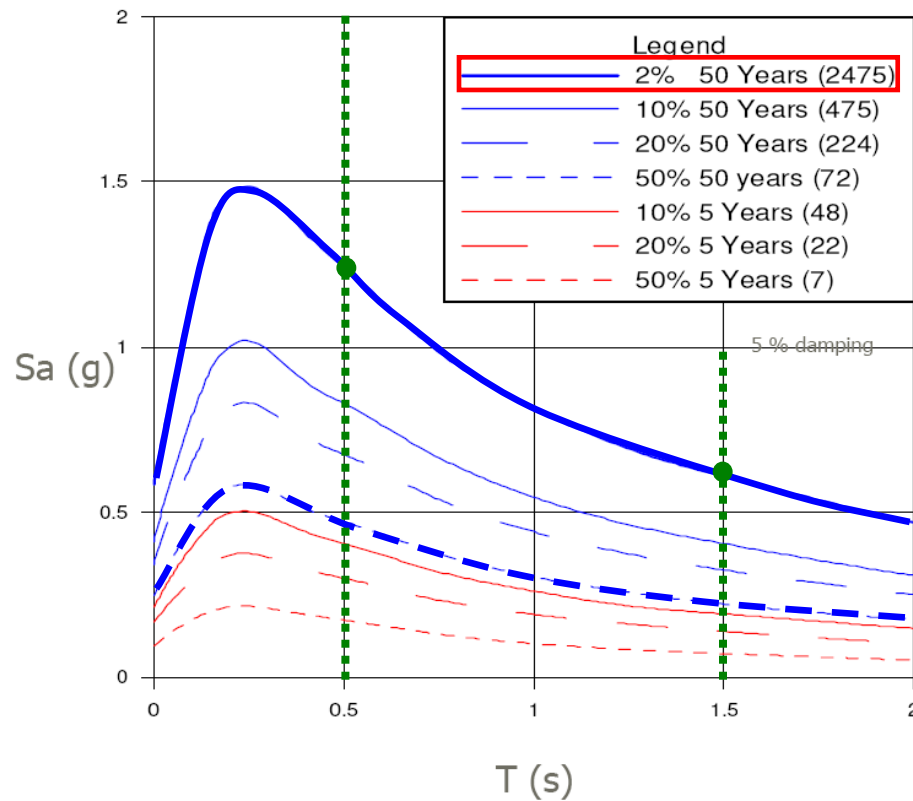
- **Introduction**
 - Motivation & Objectives
 - Significance of Axial-Shear-Flexure Interaction
- **Shear-Flexure Interaction Hysteretic Model Under Constant Axial Load**
 - Generation of Primary Curves Considering Shear-Flexure Interaction
 - Improved Reloading/Unloading Hysteretic Rules
- **Inelastic Displacement Demand Model for Bridge Columns**
 - Modeling of Columns & Consideration of Ground Motions
 - Dimensional Analysis
- **Seismic Response Simulation of Bridges**
 - Site Specific Ground Motions
 - Soil-Structural Interaction
 - Nonlinear Behavior of Columns
- **Axial-Shear-Flexure Interaction Hysteretic Model Under Variable Axial Load**
 - Generation of Primary Curve Family
 - Stress Level Index & Two-stage Loading Approach
- **Conclusion**

Factors Affecting Bridge Responses

<h2>Earthquake Features</h2>	
<h2>Structure Properties</h2>	<ul style="list-style-type: none"> • Deck (box girder) • Bent beam • Column • Spread footing • Foundation/ Embankment
<h2>Soil-Structure Interaction</h2>	<p>Three primary Soil-Structure Interaction effects (Stewart et al., 2004):</p> <ul style="list-style-type: none"> • flexible foundation effects • foundation damping effects • kinematic effects

Ground Motion Selection

Uniform Hazard Spectrum



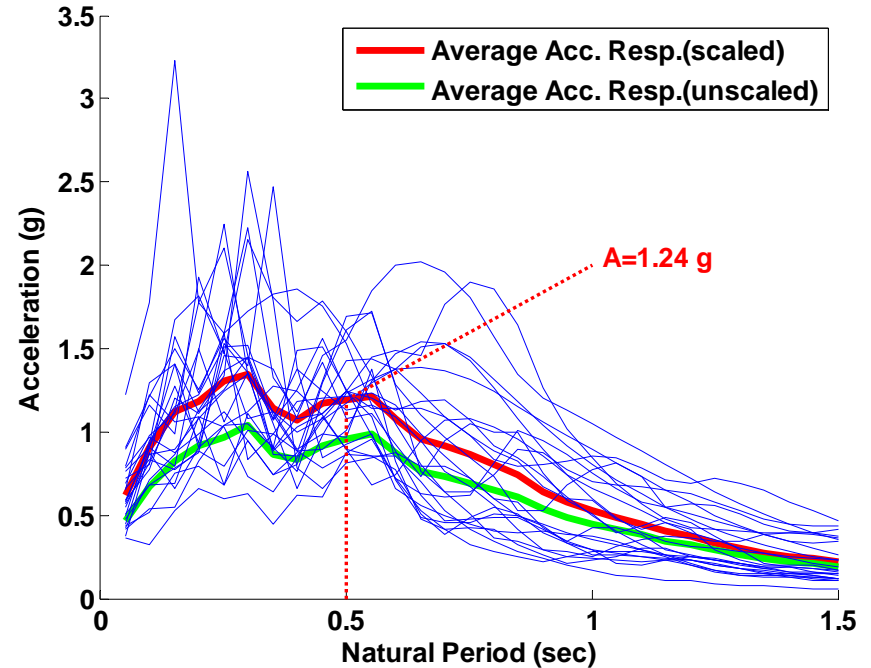
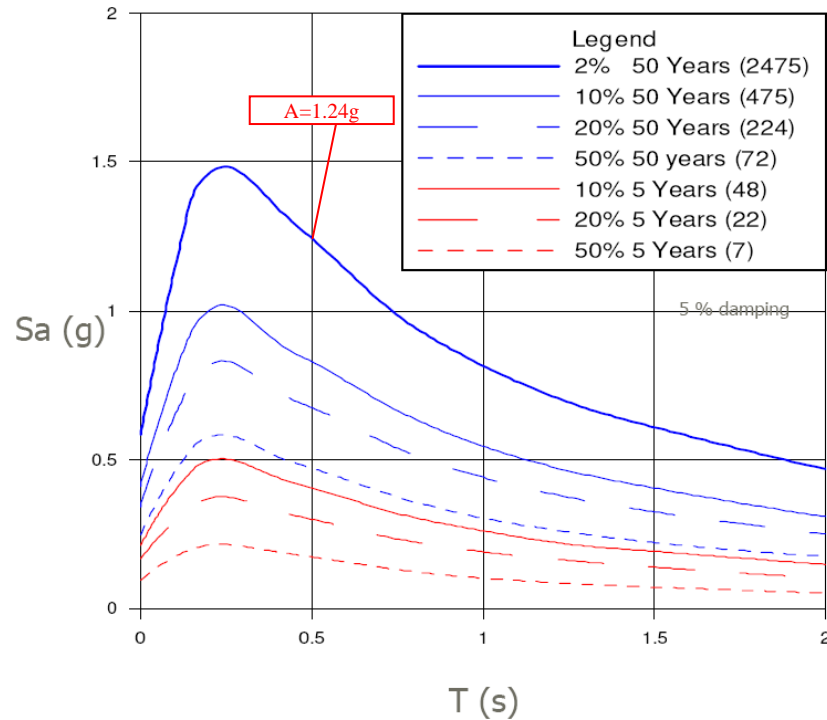
Uniform Hazard at LABMB Site

Structure Period (s)	Spectral Acceleration (g)	
	2% in 50 yrs	50% in 50 yrs
0	0.58	0.25
0.1	1.14	0.46
0.2	1.48	0.58
0.3	1.47	0.58
0.4	1.35	0.51
0.5	1.24	0.47
0.75	0.99	0.38
1.0	0.82	0.30
1.25	0.69	0.26
1.5	0.61	0.22
2	0.47	0.18

Note: 5% damping

Acceleration Spectra

For $T=0.5$ sec (FHWA Bridge #4 and Bridge Mendocino) :

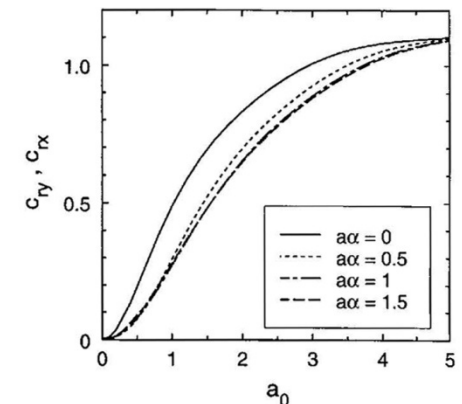
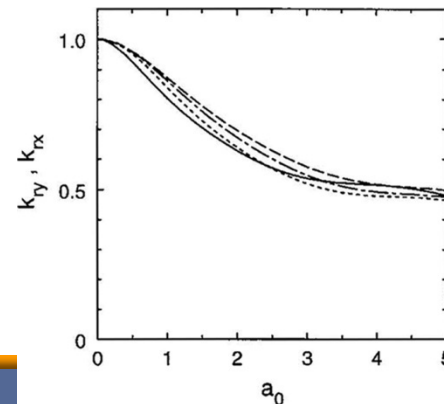
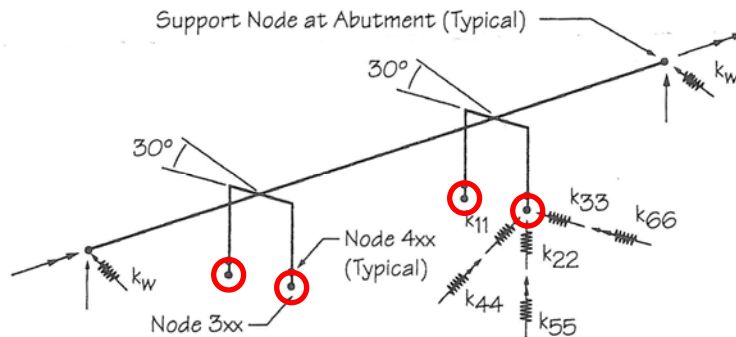


Formula of Dynamic Stiffness for Surface Foundation

Motion	Horizontal	Vertical	Rocking	Torsional
Equivalent radius, r_0	$\sqrt{\frac{A_0}{\pi}}$	$\sqrt{\frac{A_0}{\pi}}$	$\sqrt[4]{\frac{4I_0}{\pi}}$	$\sqrt[4]{\frac{2I_0}{\pi}}$
Poisson's ratio, ν	All ν	$\nu \leq \frac{1}{3}$	$\frac{1}{3} < \nu < \frac{1}{2}$	All ν
Wave velocity, V	$V_s = \sqrt{\frac{G}{\rho}}$	$V_p = \sqrt{\frac{E_c}{\rho}}$	V_p	V_s
Static stiffness, K_s	$8Gr_0$	$4Gr_0$	$\frac{8Gr_0^3}{3(1-\nu)}$	$16Gr_0^3$
High-frequency damping coeff., σ_∞	$2-\nu$	$1+\nu$	$\frac{3(1-\nu)}{32}$	3
	$\frac{\pi}{8}(2-\nu)$	$\frac{\pi}{4}\sqrt{\frac{2(1-\nu)^3}{1-2\nu}}$	$\frac{3\pi}{32}\sqrt{\frac{2(1-\nu)^3}{1-2\nu}}$	$\frac{3\pi}{32}$

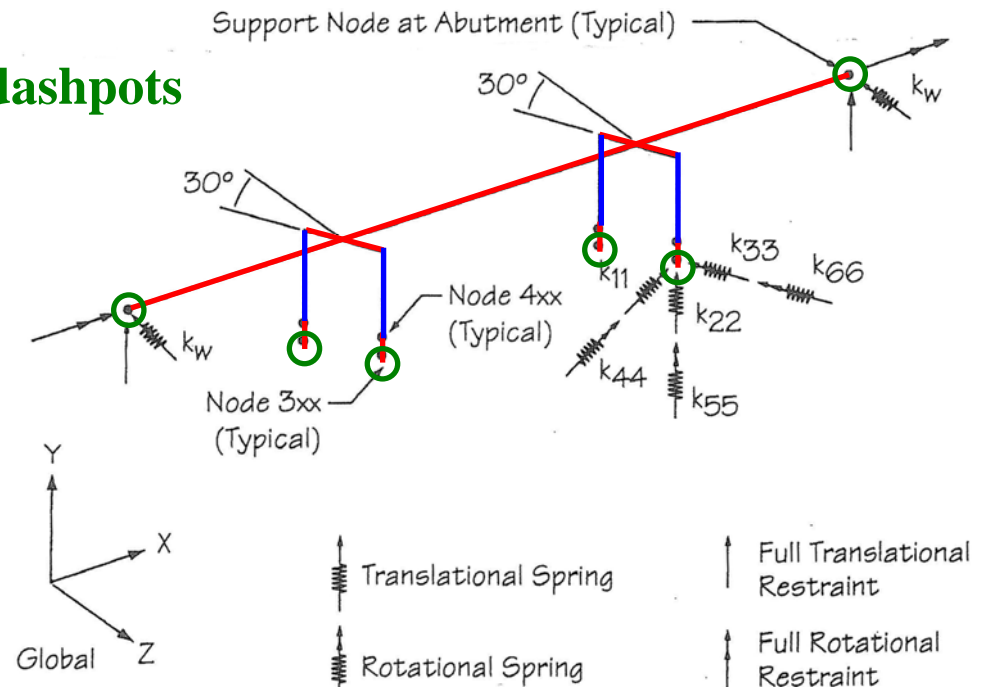
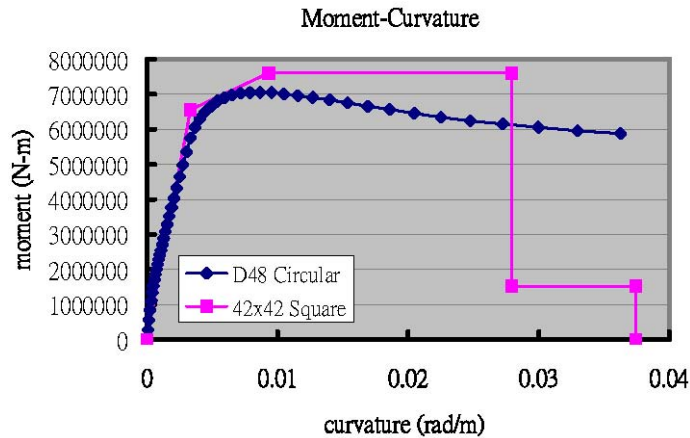
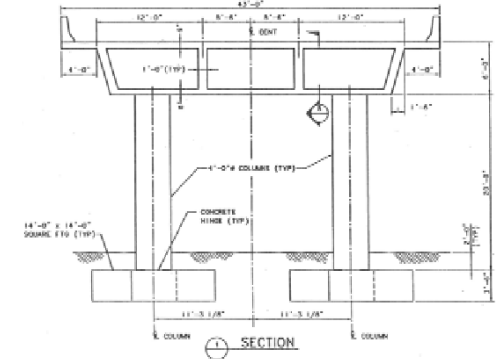
$$\bar{K}(\omega) = K_s * [k(a_0) + i * a_0 * \sigma_\infty * c(a_0)]$$

Dynamic stiffness and damping coefficients
-- by Vrettos (1999) [or use Gazetas (1991)]



Major Components of Stick Model

- Deck (box girder) → elastic beam
- Bent beam → rigid (very large I)
- Column → linear/nonlinear beam
- Spread footing → rigid (very large I)
- Foundation/ Embankment → equivalent linear springs and dashpots

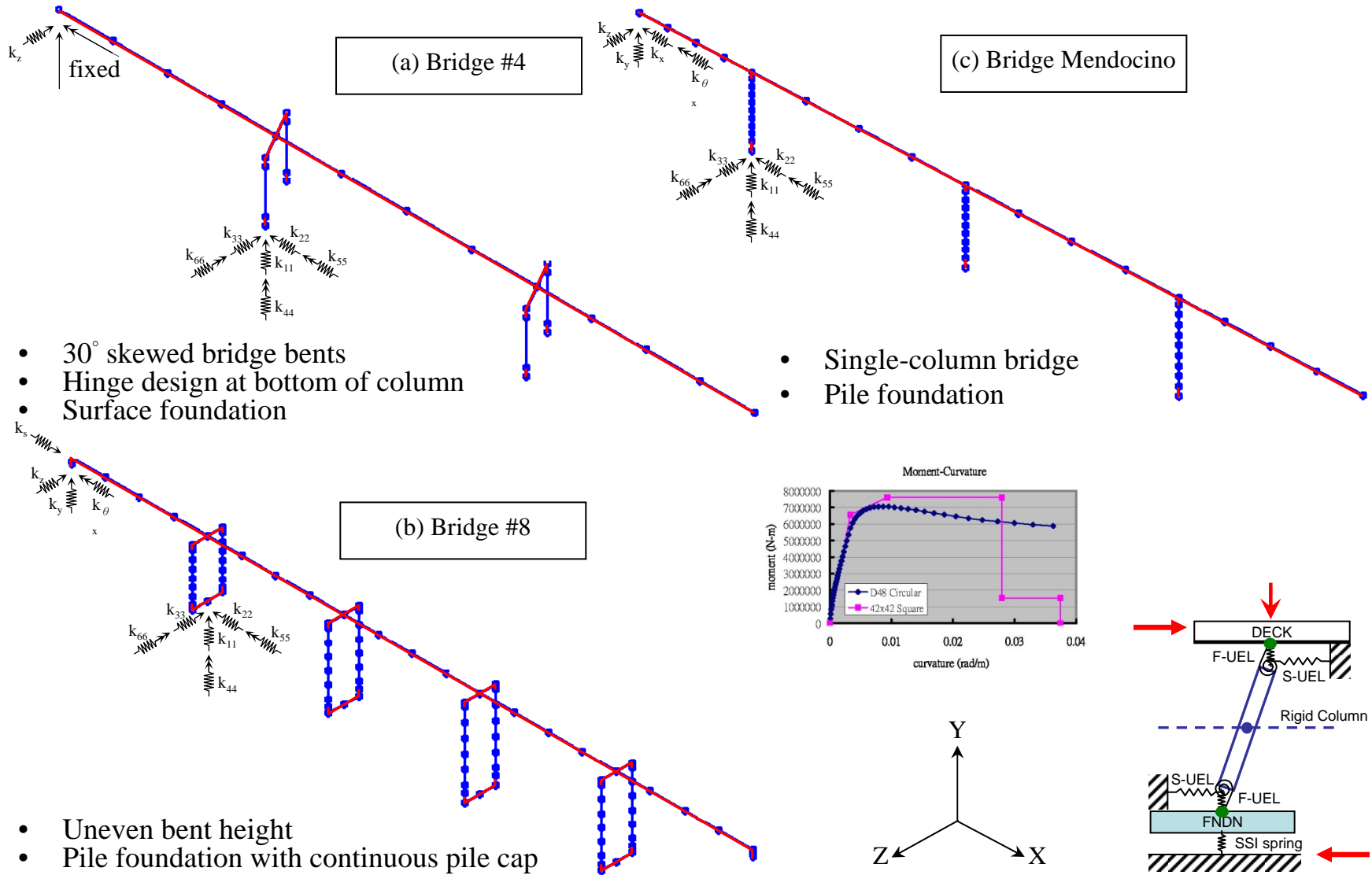


Prototype Bridges

Three box girder concrete bridges are selected as prototype bridges for preliminary analysis.

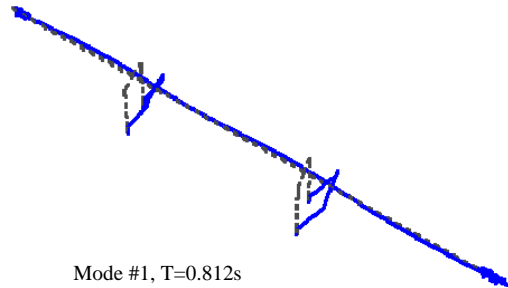
Structural Characteristics	FHWA Design Example #4 Bridge #4	FHWA Design Example #8 Bridge #8	Mendocino Ave. Overcrossing Bridge Mendocino (1963)
Span Length	Three-span continuous	Five-span continuous	Uneven, four-span continuous
Total Length	320 ft long	500 ft long	302 ft long
Pier Type	Two-column integral bent, monolithic at column top, pinned at base	Two-column integral bent (uneven height), monolithic at column top and base	Single column variable height, monolithic at column top and base
Abutment Type	Seat	Stub abutment with diaphragm	Monolithic
Foundation Type	Spread Footing	Pile Group	Pile Group
Expansion Joints	Expansion bearings & girder stops (shear keys)	Expansion bearings & girder stops	Expansion bearings & girder stops
Force Resisting Mechanism	[Longitudinal] intermediate bent columns & free longitudinal movement at abutments [Transverse] intermediate bent columns & abutments	[Longitudinal] intermediate bent columns and abutment backfill [Transverse] intermediate bent columns and abutment backfill	[Longitudinal] intermediate columns and abutment backfill [Transverse] intermediate columns and abutment backfill
Plan Geometry	30° skewed	Straight	Straight
Natural Period	~0.8 sec	~1.6 sec	~0.4 sec
Design Method	Old design (AASHTO provisions)	New design (LRFD guidelines)	Old design (AASHTO provisions)

Finite Element Bridge Models

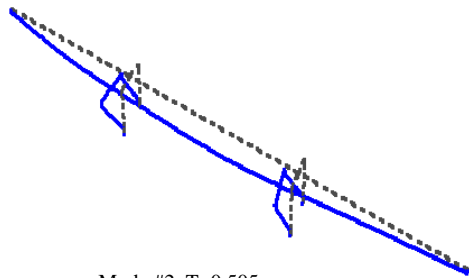


Mode Shapes of Prototype Bridges

Bridge #4

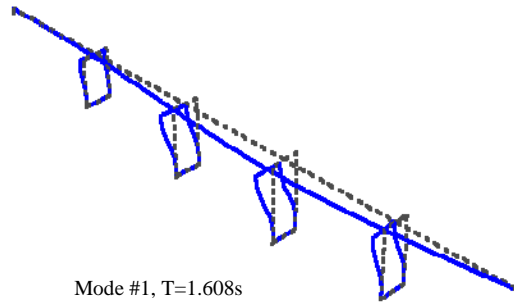


Mode #1, $T=0.812s$

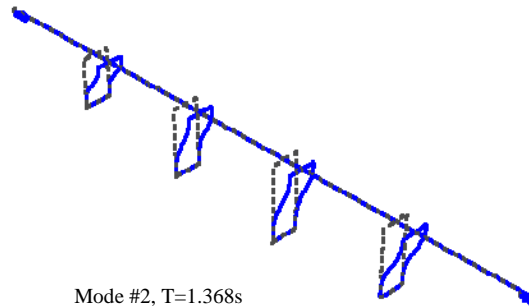


Mode #2, $T=0.505s$

Bridge #8

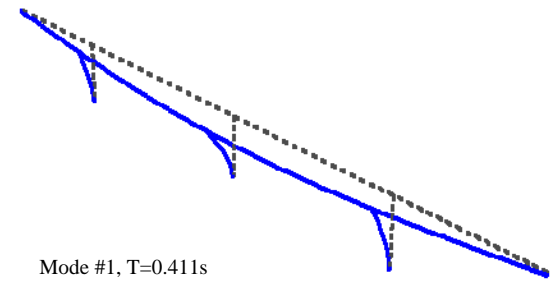


Mode #1, $T=1.608s$

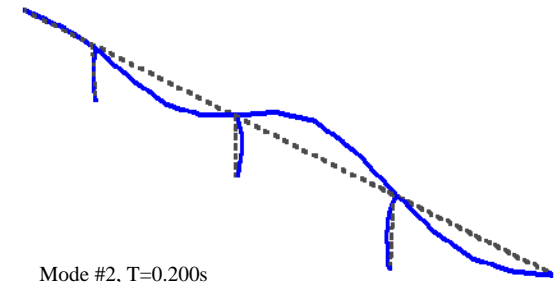


Mode #2, $T=1.368s$

Bridge Mendocino



Mode #1, $T=0.411s$

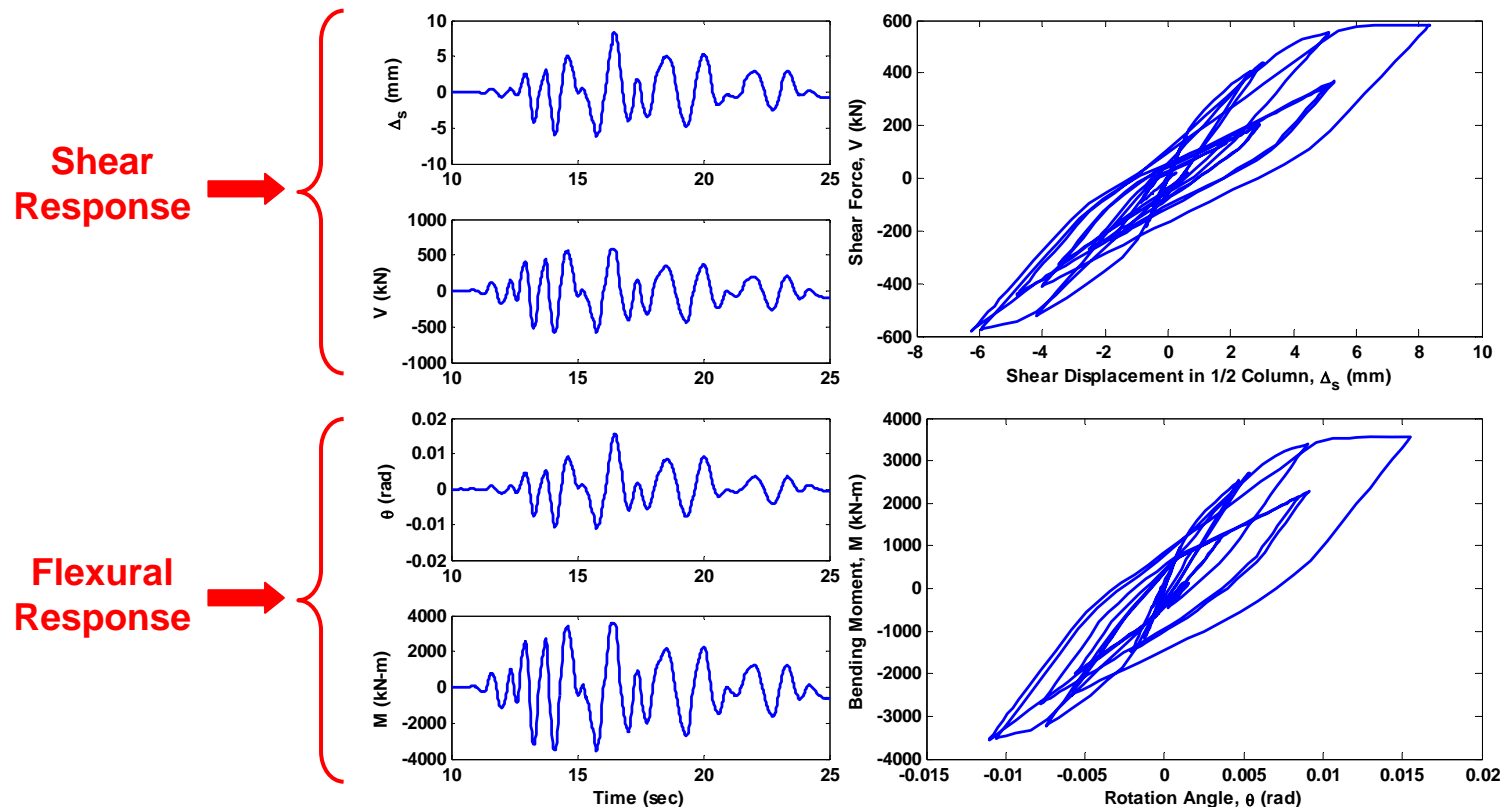


Mode #2, $T=0.200s$

Depends on the bridge structural characteristics, the first and second modes can be longitudinal mode, translational mode, or vertical mode, etc.

Shear and Flexural Responses in Bridge Columns

- The developed shear-flexural interaction (SFI) model and the implemented user element successfully model the nonlinear shear and flexural responses of the bridge (a MDOF system) under seismic loading

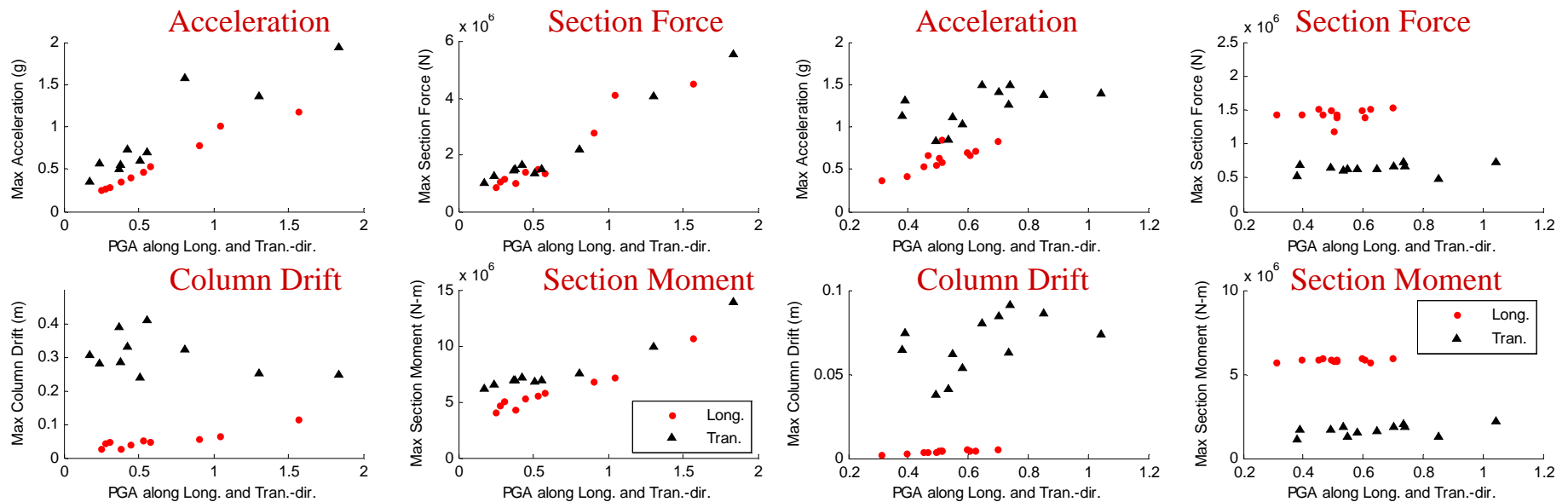
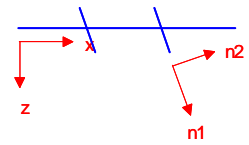


Shear and flexural responses in Bent 3 of Bridge #8 using UEL model

Nonlinear M- ϕ vs Shear-Flexural Interaction Model

Maximum Response Quantities of Bridge #8

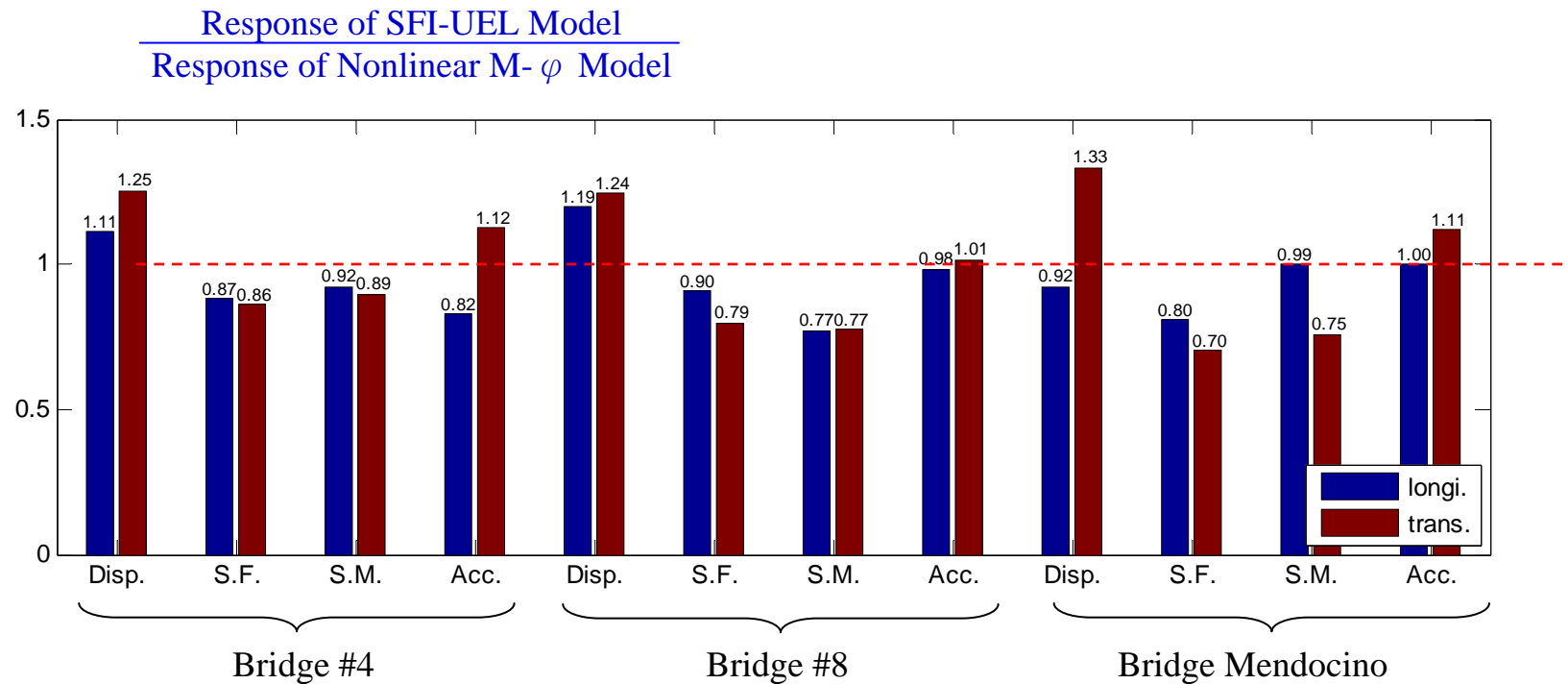
- With PGA increasing, the max acceleration and column drift also increase gradually. (ps. Bin 4 earthquakes are strong earthquakes.)
- Section forces and section moments may hit the capacity under these strong earthquakes and thus remain almost constant in the SFI model.
- All response quantities have experienced some change due to the consideration of the shear-flexural interaction of columns.



(a) using **nonlinear Timoshenko beam** (nonlinear M- ϕ) elements for columns

(b) using user-defined **shear-flexural interaction** elements (SFI-UEL) for columns

Summary for Bridge Response Simulation

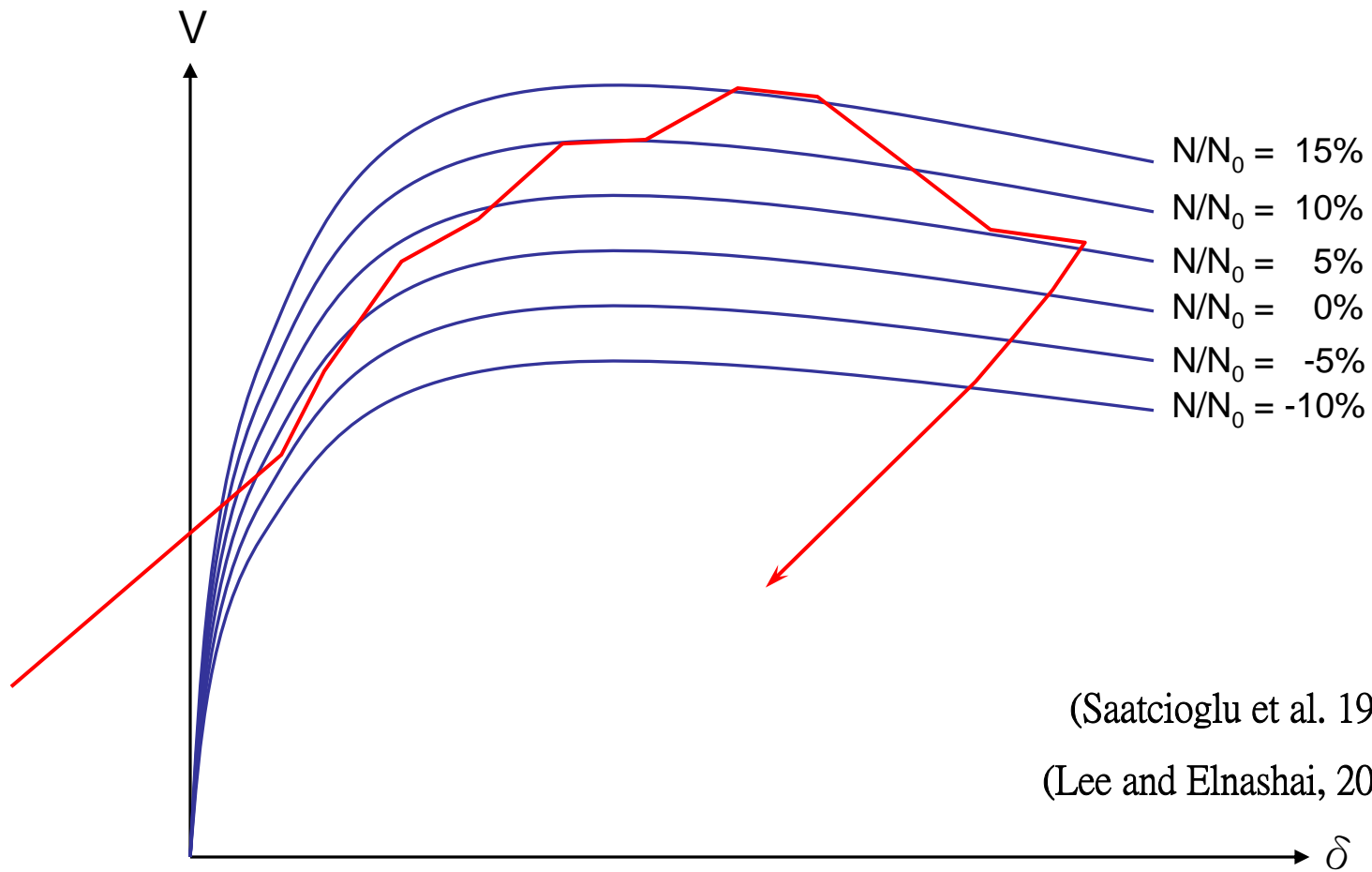


- The shear-flexural interaction effects of columns are similar, despite the different bridge structural and geometry characteristics.
- The general trends are :
 - larger drift demand (in SFI-UEL models than in nonlinear M- ϕ models)
 - smaller section forces and section moments

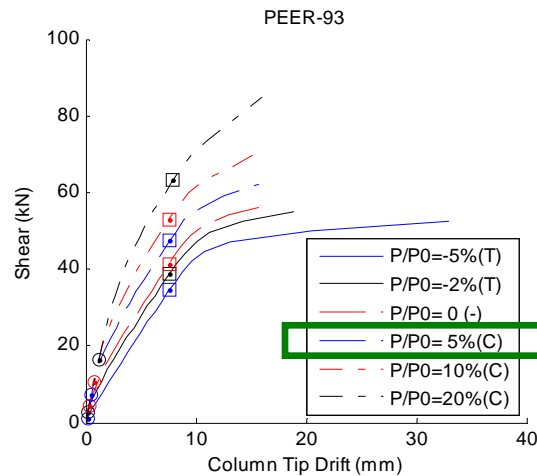
Outline

- **Introduction**
 - Motivation & Objectives
 - Significance of Axial-Shear-Flexure Interaction
- **Shear-Flexure Interaction Hysteretic Model Under Constant Axial Load**
 - Generation of Primary Curves Considering Shear-Flexure Interaction
 - Improved Reloading/Unloading Hysteretic Rules
- **Inelastic Displacement Demand Model for Bridge Columns**
 - Modeling of Columns & Consideration of Ground Motions
 - Dimensional Analysis
- **Seismic Response Simulation of Bridges**
 - Site Specific Ground Motions
 - Soil-Structural Interaction
 - Nonlinear Behavior of Columns
- **Axial-Shear-Flexure Interaction Hysteretic Model Under Variable Axial Load**
 - Generation of Primary Curve Family
 - Stress Level Index & Two-stage Loading Approach
- **Conclusion**

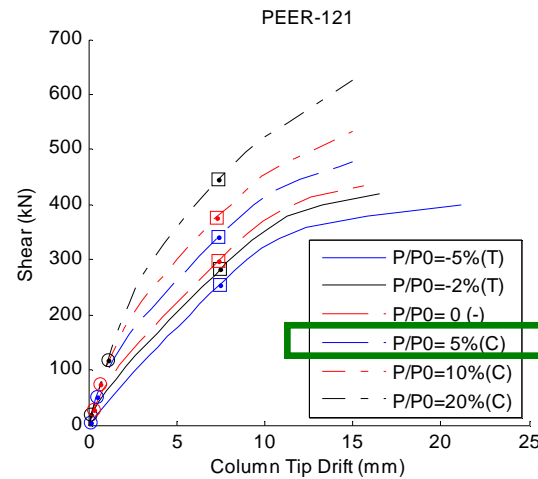
Shift of Primary Curve



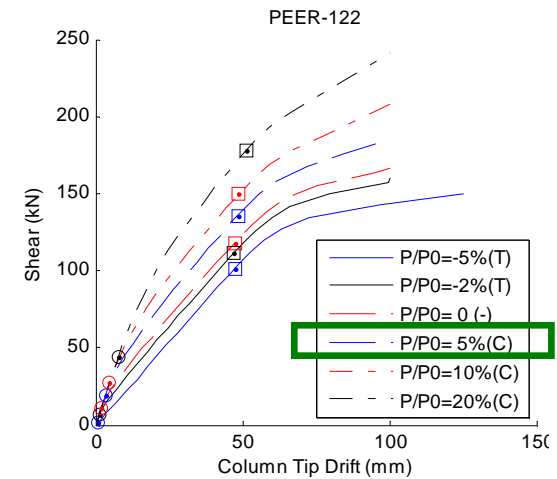
Effects of Axial Load Variation on Total Primary Curves



Kunnath et al.
H/D=4.5



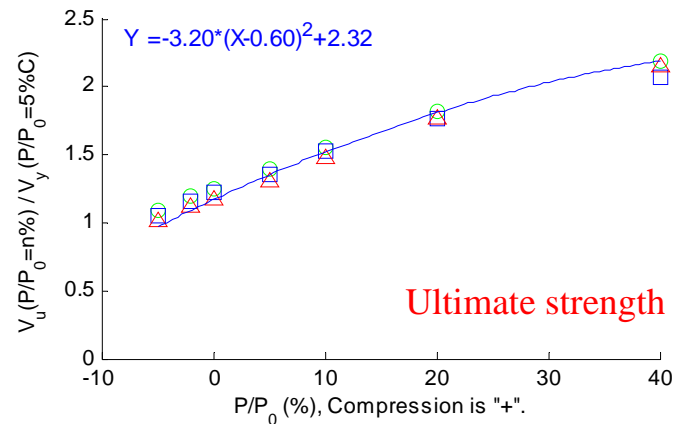
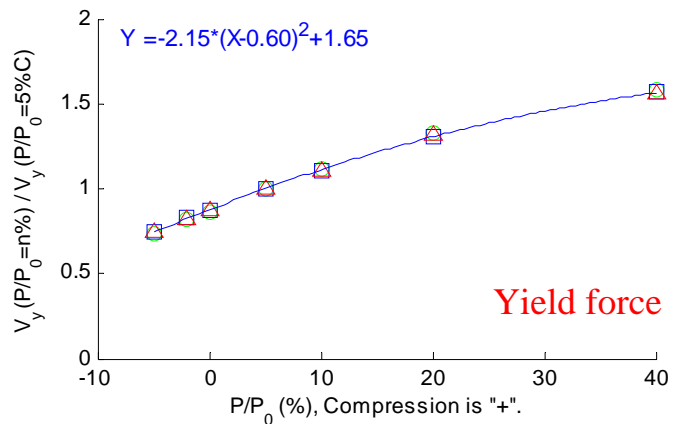
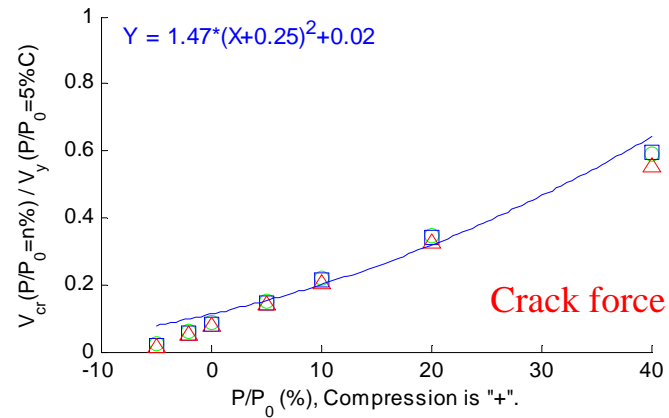
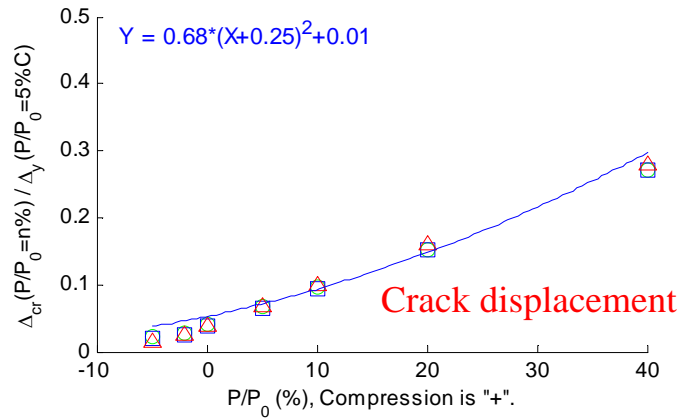
Calderone-328
H/D=3.0



Calderone-828
H/D=8.0

- ❑ Ultimate capacity and stiffness increase with compressive axial load level.
- ❑ Yielding displacement is almost fixed, regardless of applied axial load.
- ❑ Cracking point is getting smaller as axial force decreases, implying the column being relatively easy to be cracked.

Normalization of Primary Curves



$$\frac{\Delta_{cr}(P/P_0 = n\%)}{\Delta_y(P/P_0 = 5\%)} = 0.68 * \left(\frac{P}{P_0} + 0.25\right)^2 + 0.01$$

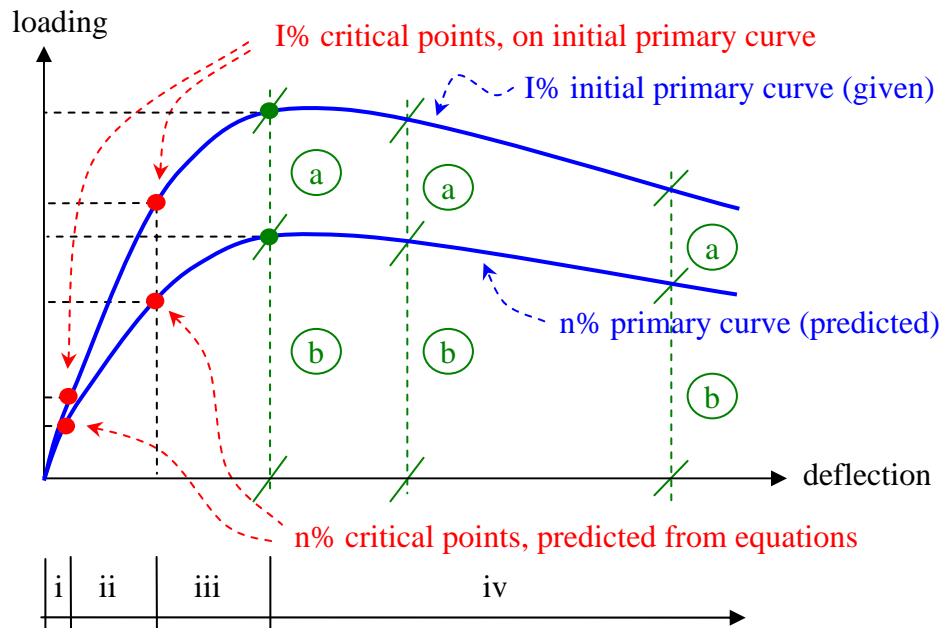
$$\frac{V_y(P/P_0 = n\%)}{V_y(P/P_0 = 5\%)} = -2.15 * \left(\frac{P}{P_0} - 0.60\right)^2 + 1.65$$

$$\frac{V_{cr}(P/P_0 = n\%)}{V_y(P/P_0 = 5\%)} = 1.47 * \left(\frac{P}{P_0} + 0.25\right)^2 + 0.02$$

$$\frac{V_u(P/P_0 = n\%)}{V_y(P/P_0 = 5\%)} = -3.20 * \left(\frac{P}{P_0} - 0.60\right)^2 + 2.32$$

Generation of Primary Curve Family

Objective: Generating the primary curves related to various axial load levels from a given primary curve subject to an initial axial load



(i) 0 → crack: straight line

$$DL = \text{def. level} \equiv \frac{\Delta_{(i)}^{I\%}}{\Delta_{cr}^{I\%}} \Rightarrow \Delta_{(i)}^{n\%} = DL * \Delta_{cr}^{n\%}$$

$$SL = \text{stress level} \equiv \frac{V_{(i)}^{I\%}}{V_{cr}^{I\%}} \Rightarrow V_{(i)}^{n\%} = SL * V_{cr}^{n\%}$$

(ii) crack → yield: interpolation

$$DL = \text{def. level} \equiv \frac{\Delta_{(ii)}^{I\%} - \Delta_{cr}^{I\%}}{\Delta_y^* - \Delta_{cr}^{I\%}}$$

$$SL = \text{stress level} \equiv \frac{V_{(ii)}^{I\%} - V_{cr}^{I\%}}{V_y^{I\%} - V_{cr}^{I\%}}$$

$$\Delta_{(ii)}^{n\%} = DL * (\Delta_y^* - \Delta_{cr}^{n\%}) + \Delta_{cr}^{n\%}$$

$$V_{(ii)}^{n\%} = SL * (V_y^{n\%} - V_{cr}^{n\%}) + V_{cr}^{n\%}$$

(iv) ultimate → failure: constant residual strength ratio

$$\text{ductility unchanged} \Rightarrow \Delta_{(iv)}^{n\%} = \Delta_{(iv)}^{I\%}$$

$$RSR = \text{residual strength ratio} \equiv \frac{V_{(iv)}^{I\%}}{V_u^{I\%}}$$

$$V_{(iv)}^{n\%} = RSR * V_u^{n\%}$$

(iii) yield → ultimate: interpolation

$$\text{ductility unchanged} \Rightarrow \Delta_{(iii)}^{n\%} = \Delta_{(iii)}^{I\%}$$

$$SL = \text{stress level} \equiv \frac{V_{(iii)}^{I\%} - V_y^{I\%}}{V_u^{I\%} - V_y^{I\%}}$$

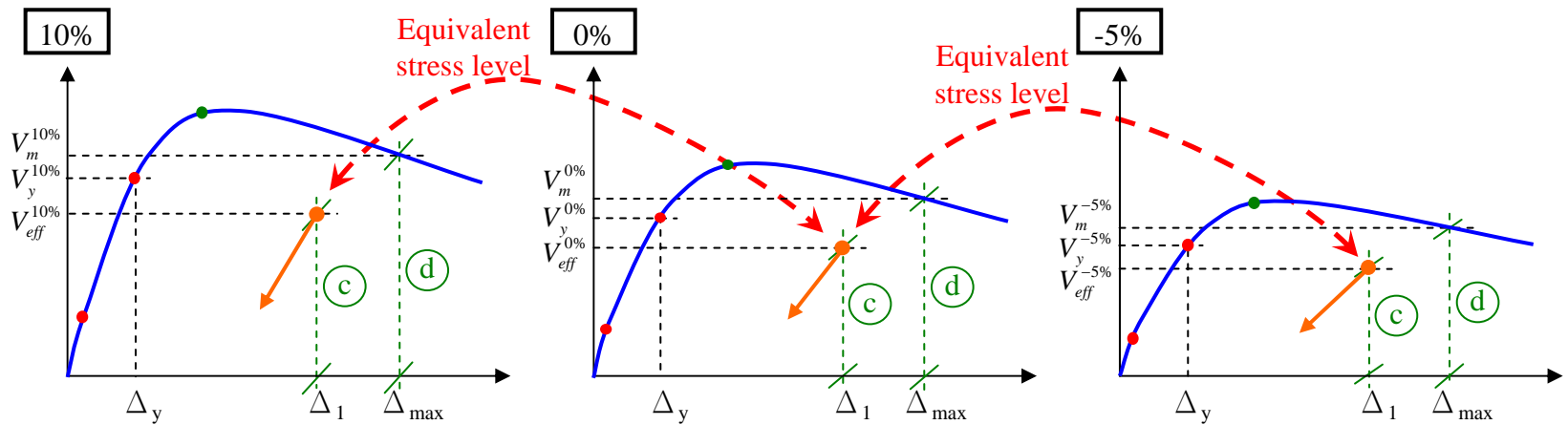
$$V_{(iii)}^{n\%} = SL * (V_u^{n\%} - V_y^{n\%}) + V_y^{n\%}$$

Stress Level Index & Two-stage Loading Approach

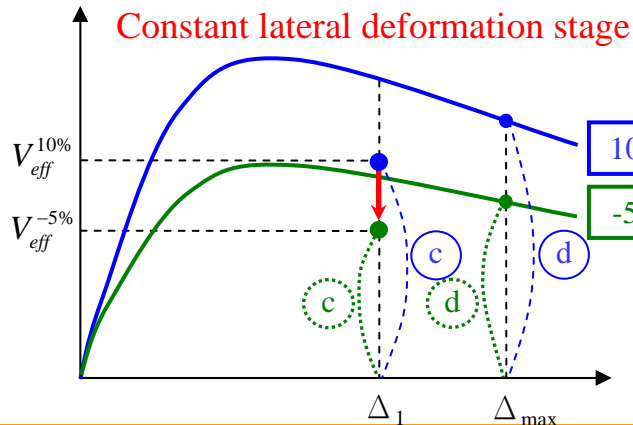
$$\text{Stress Level Index} \equiv \frac{\text{Effective Lateral Load, } V_{eff}}{\text{Lateral Capacity at } \Delta_{max}, V_m} = \frac{c}{d}$$

Assumption:

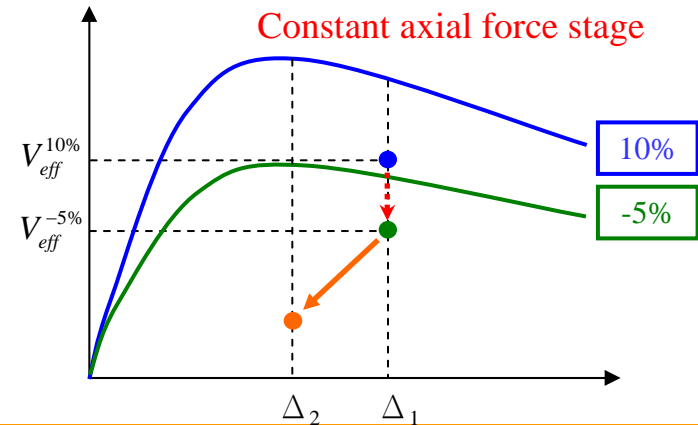
Effective stress level of a loaded column at fixed ductility is independent of axial load.



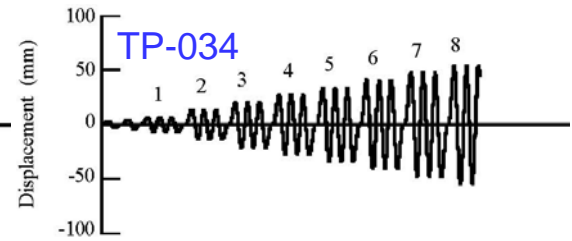
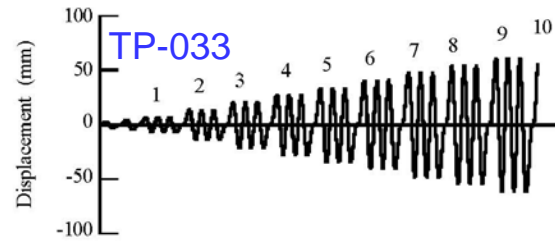
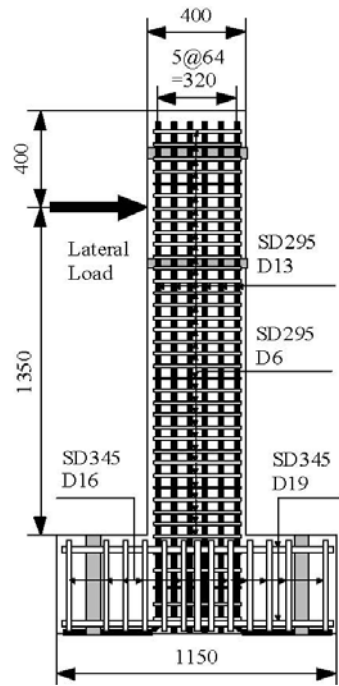
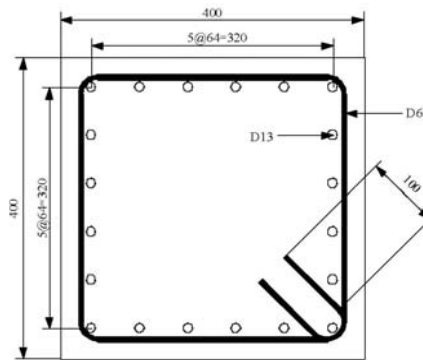
Keep Δ , change N: 10% \rightarrow -5%



Keep N, change Δ : $\Delta_1 \rightarrow \Delta_2$

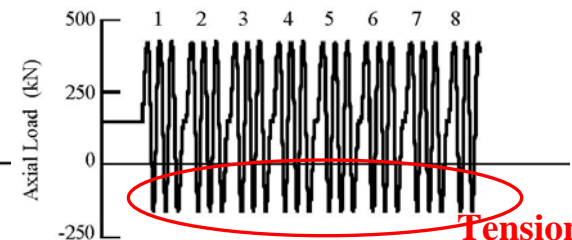
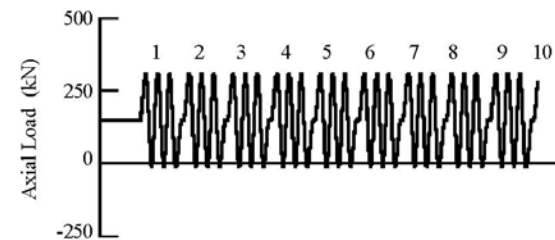


Cyclic Test: Experimental Program – TP031 ~ TP034



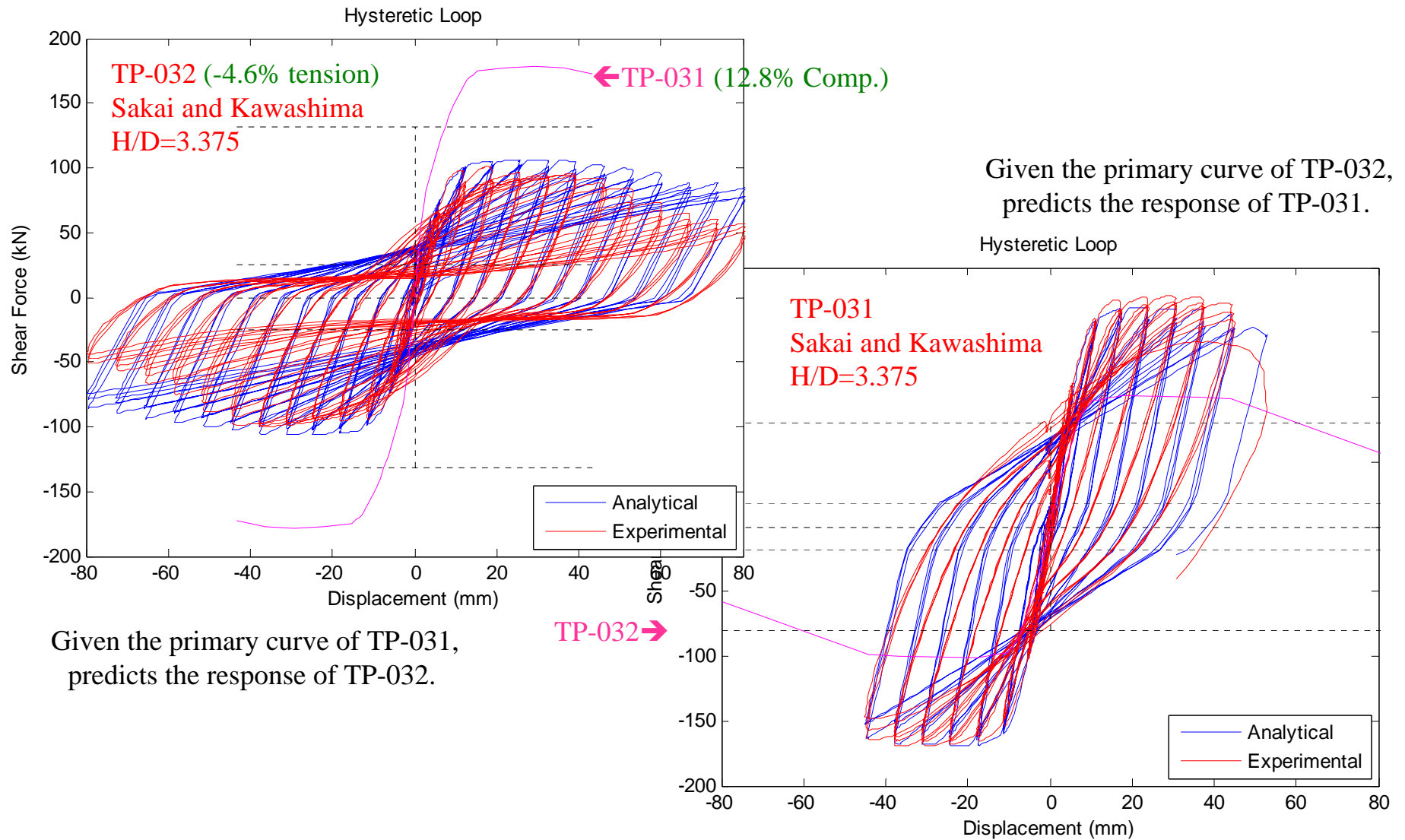
(i) Lateral Displacement

(i) Lateral Displacement

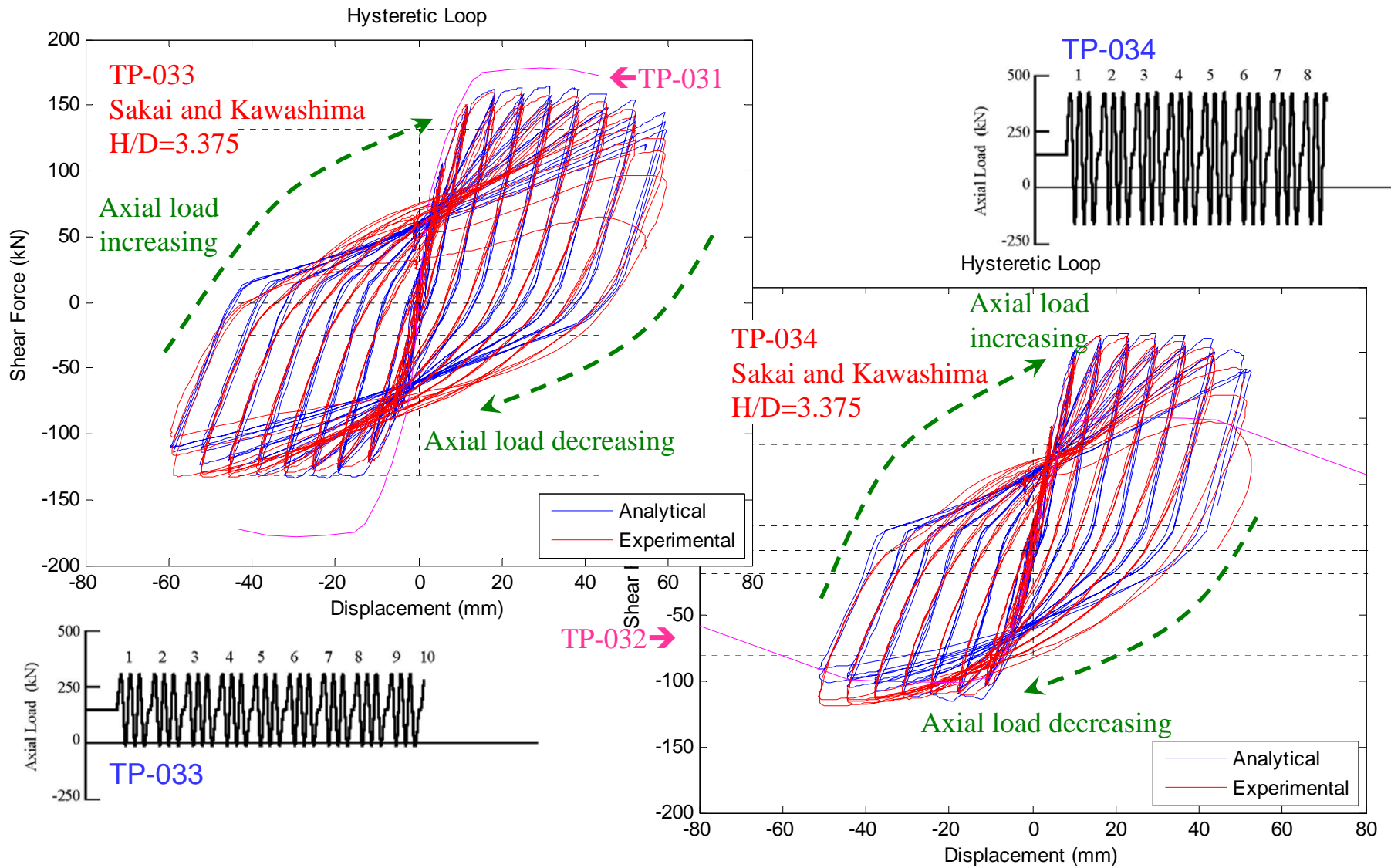


	TP-31	TP-32	TP-33	TP-34
ID in the Reference	CC	CT	V1	V2
Section	Square			
Section Size (mm)	400 × 400			
Effective Height h (mm)	1350			
Effective Depth d (mm)	360			
Aspect Ratio	3.75 = $\frac{\text{Height}}{\text{Diameter}}$			
Longitudinal Reinforcement Ratio (%)	1.58			
Volumetric Ratio of Tie Reinforcement ρ_v (%)	0.79			
Cylinder Strength of Concrete σ_{c0} (MPa)	22.9	23.0	22.9	23.0
Longitudinal Reinforcement	SD295A D13 (Yield Strength=374MPa)			
Tie Reinforcement	SD295A D6 (Yield Strength=363MPa)			
Axial Force (kN) (at the Bottom)	470 (3.0MPa) (Constant)	-170 (-1.0MPa) (Constant)	-10~310 (0~2.0MPa) (Varying)	-170~420 (-1.0~2.7MPa) (Varying)

Verification of Primary Curve Prediction

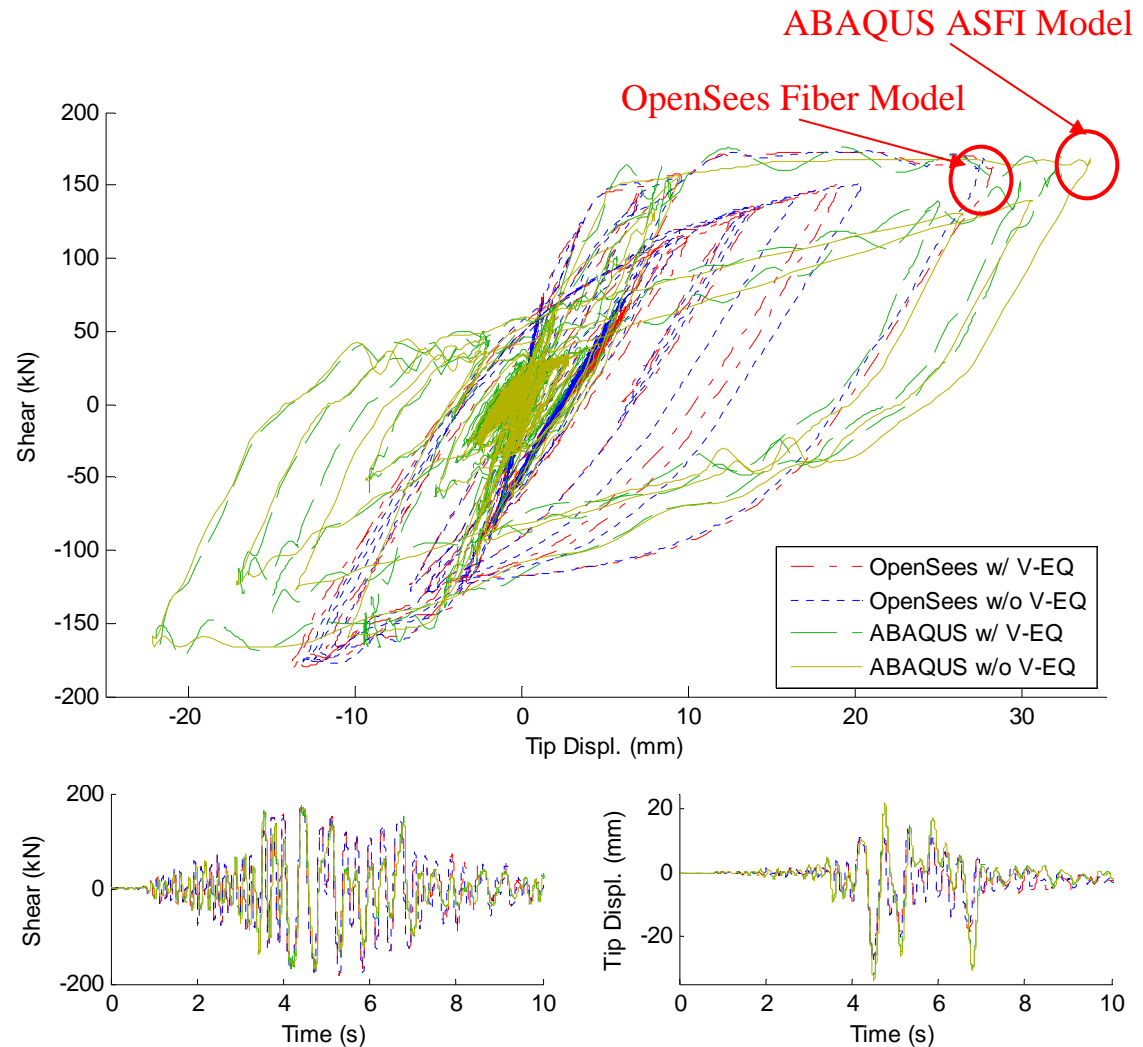


Verification of Mapping Between Different Axial Load Level



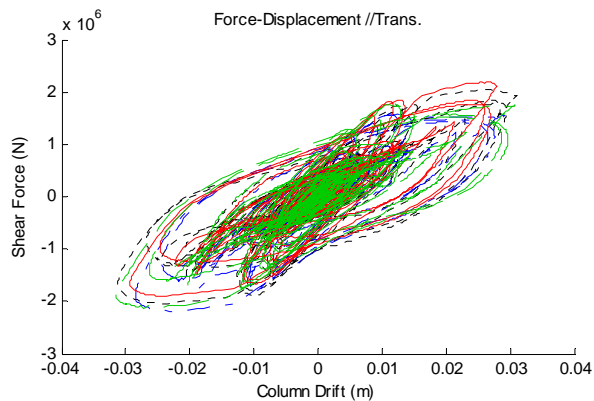
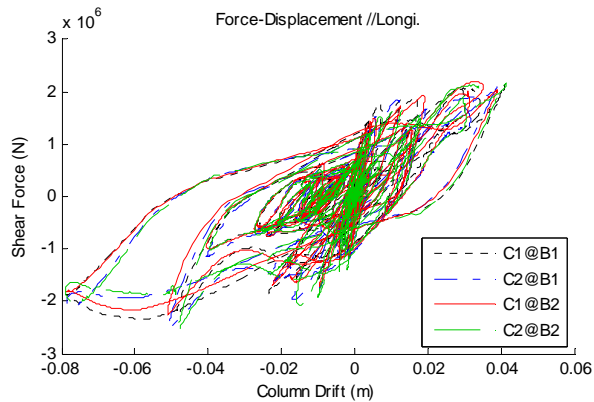
Dynamic Validation with Fiber Section Model

- Proposed ASFI model in general produces larger displacement demand than the fiber section model.
- Vibration frequencies of the two models agree with each other indicating reasonable prediction on the tangent stiffness of the proposed ASFI model.
- Considering only the SFI can yield good prediction on the displacement demand.

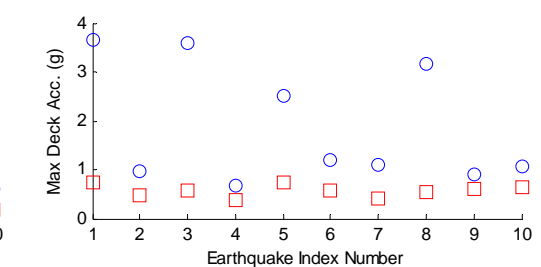
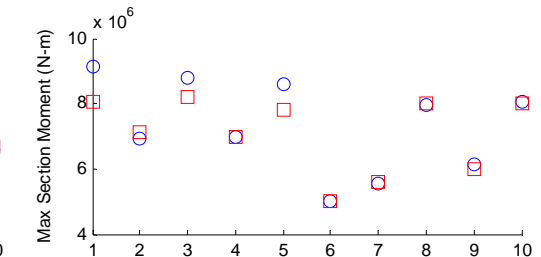
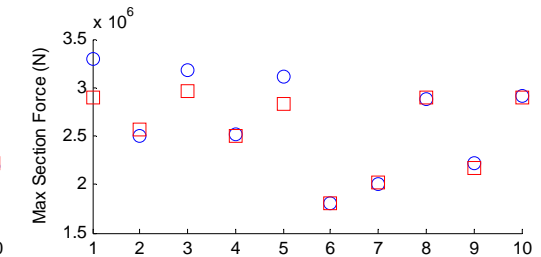
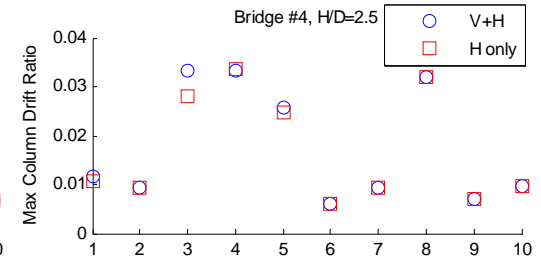
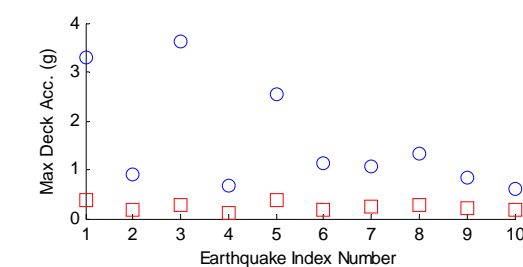
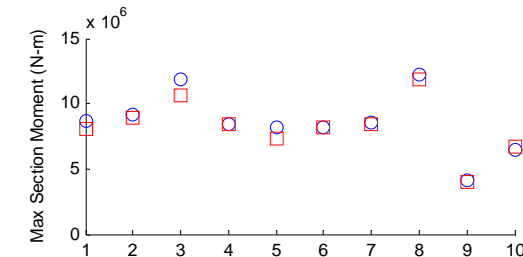
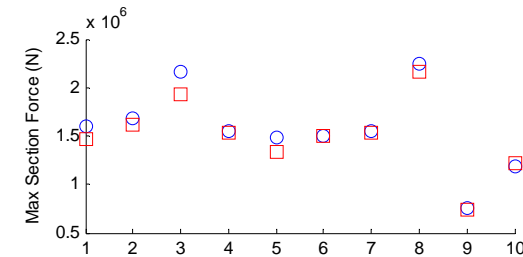
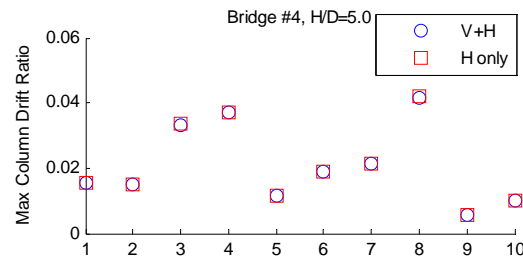


Bridge Responses Considering ASFI

Considering axial variation does not change overall bridge responses much.



Force v.s. total column drift (H/D=2.5)



Summary

- ❑ Axial load considerably affects the lateral responses of RC columns.
- ❑ **Primary curves** of the **same column under different axial loads** can be predicted very well by applying the normalized primary curve and parameterized critical points.
- ❑ Transition between loading branches corresponding to **different axial load** levels is made possible by breaking the step into two stages: **constant deformation stage** and **constant axial load stage**.
- ❑ Model verification shows that the proposed method is able to capture the effects of **axial load variation** on the lateral responses of RC columns.
- ❑ Dynamic analysis on individual bridge column and on prototype bridge system shows that considering axial load variation during earthquake events does **not** change the drift demand significantly.

Conclusion

- ❑ A plastic hinge type Shear-Flexure Interaction (SFI) model is proposed and fully calibrated in this study.
- ❑ The SFI model has been utilized to develop an inelastic displacement demand model for columns to facilitate the preliminary design of bridge columns.
- ❑ The SFI model can be incorporated into bridge systems, producing much improved seismic response assessment for bridges.
- ❑ The Axial-Shear-Flexure Interaction (ASFI) model built upon the SFI model is able to simulate the realistic behavior of RC columns under variable axial load.

Fragility Functions of Bridges Under Seismic Shaking and Lateral Spreading

Contributors:

Yili Huo (Ph.D. Student)

Professor Jian Zhang

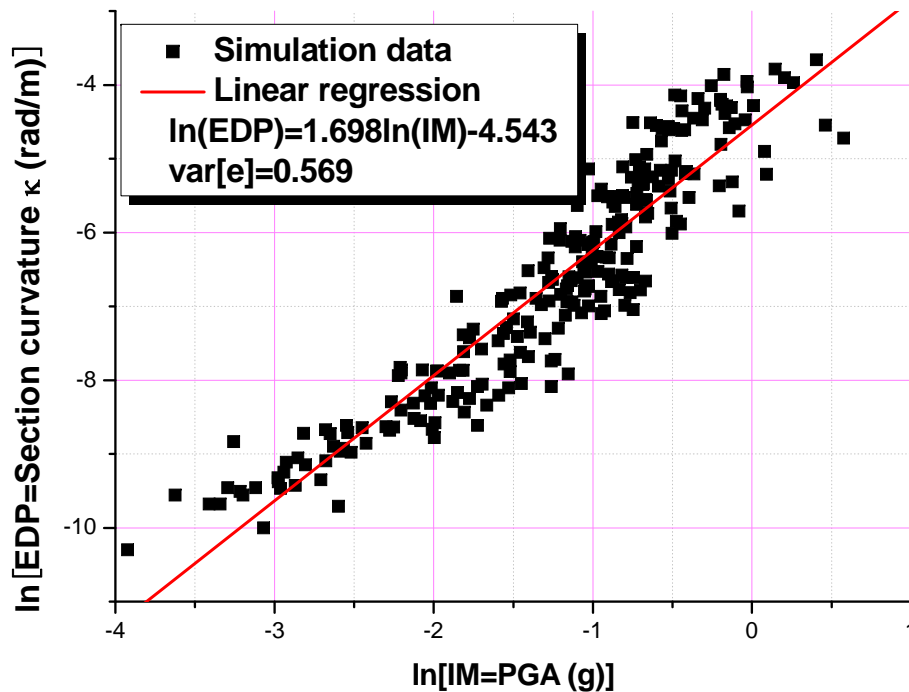
The research presented here was funded by PEER Transportation and Lifeline Programs

Outline

- **Fragility Functions of Bridges under Seismic Shaking**
 - **Methodology for deriving fragility functions**
 - Probabilistic Seismic Demand Analysis (PSDA)
 - Incremental Dynamic Analysis (IDA)
 - Composite Damage Index (DI)
 - **Effects of structural characterizations on fragility functions**
- **Fragility Functions of Bridges under Lateral Spreading**
 - **Uncertainties in soil and foundation properties**
 - **Monte Carlo Simulation**
 - **FOSM Method**
 - **Effects of Structural characterizations on fragility functions**

Probabilistic Seismic Demand Analysis (PSDA)

- Use un-scaled ground motions (“cloud” approach)



$$\ln(EDP) = \ln a + b \ln IM$$

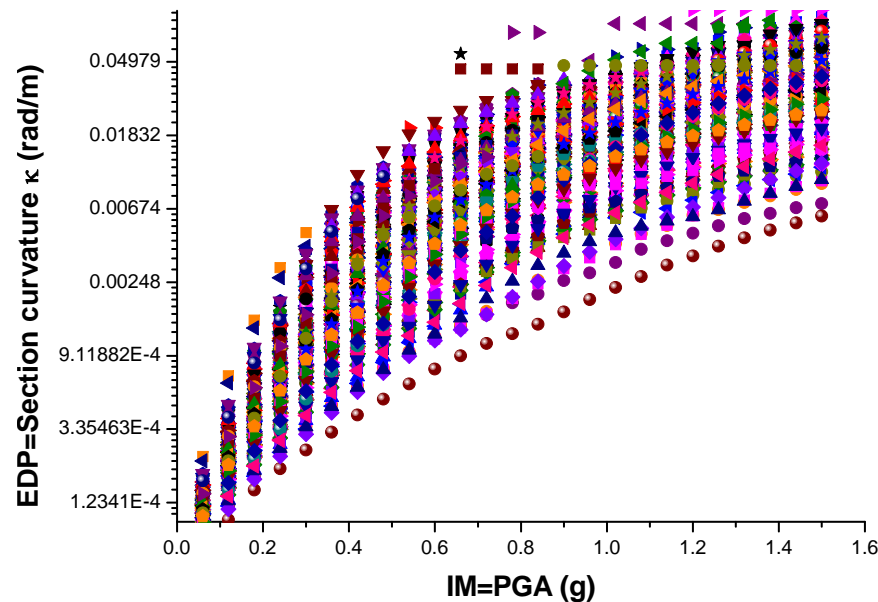
$$\text{var}[e] = \sqrt{\frac{\sum_{i=1}^n [\ln(EDP_i) - (a + b \ln IM_i)]^2}{n-2}}$$

- Assume normal or log-normal distribution

$$F(LS | im) = \Phi \left[\frac{(a + b \ln im) - \ln LS}{\text{var}[e]} \right]$$

Incremental Dynamic Analysis (IDA)

- Use scaled ground motions (“stripe” approach)



- Fragility function based on raw data

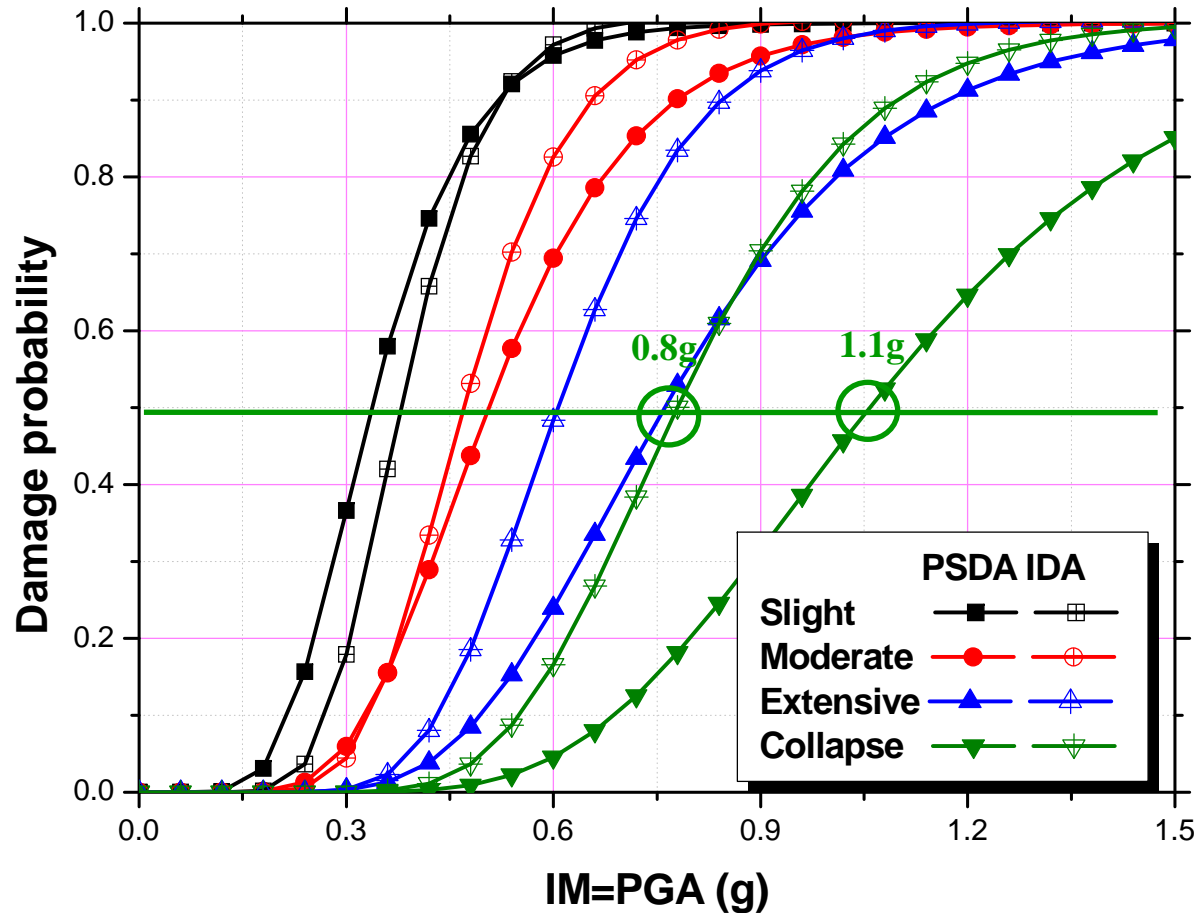
$$F(EDP > LS | im) = \frac{\text{number of cases } (EDP > LS | im)}{\text{total number of cases } (im)}$$

- Regress with normal or log-normal distribution

$$F(im | LS) = \Phi\left(\frac{im - \mu_{IM|LS}}{\sigma_{IM|LS}}\right)$$

$$F(im | LS) = \Phi\left(\frac{\ln(im) - \ln(\mu_{IM|LS})}{\xi_{IM|LS}}\right)$$

PSDA vs. IDA



Larger median \rightarrow Lower fragility \rightarrow Better Performance

Global Damage Index

□ Previous studies

- Not relate well with structure damage and hard to estimate
 - e.g. repairing cost by Mackie and Stojadinović (2006)
- Not theoretically correct for bridge
 - e.g. *DI* based on serial system assumption, Nielson and DesRoches (2007),

$$DS_{System} = \max(DS_{Pier}, DS_{Bearing})$$

$$p[Fail_{system}] = \bigcup_{i=1}^n p[Fail_{component-i}]$$

□ This study

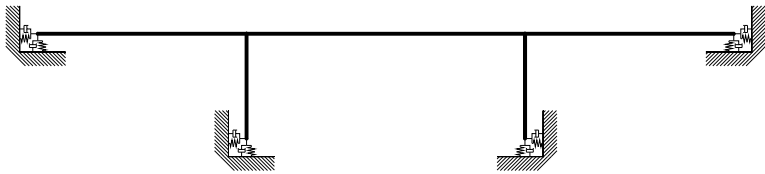
- Composite *DI*:

$$DS_{System} = \begin{cases} \text{int}(0.75 \cdot DS_{Pier} + 0.25 \cdot DS_{Bearing}) & DS_{Pier}, DS_{Bearing} < 4 \\ 4 & DS_{Pier} \text{ or } DS_{Bearing} = 4 \end{cases}$$

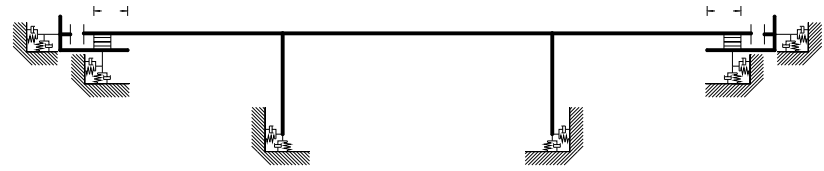
- Physically meaningful, with logical basis, and easy to compute.

Structure Configuration Characteristics

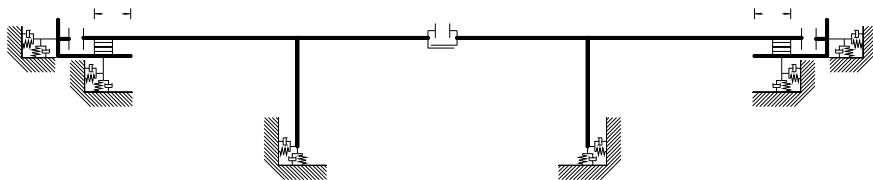
- Six models based on typical Caltrans bridges



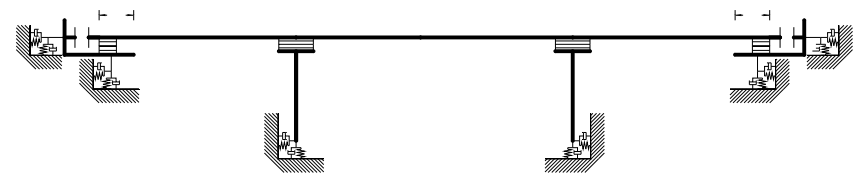
E1: Monolithic Abutment & Continuous



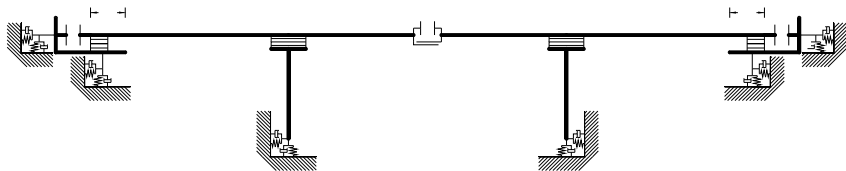
E2: Seat Abutment & Continuous



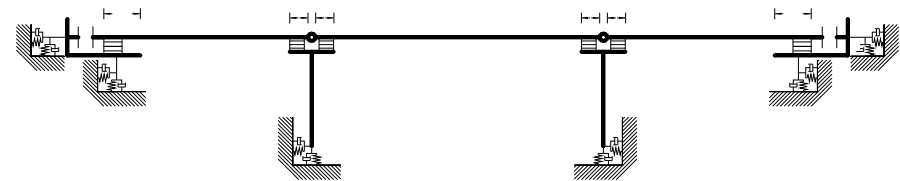
E3: Seat Abutment & Continuous (with expansion joint)



E4: Seat Abutment & Continuous (with pier isolation)

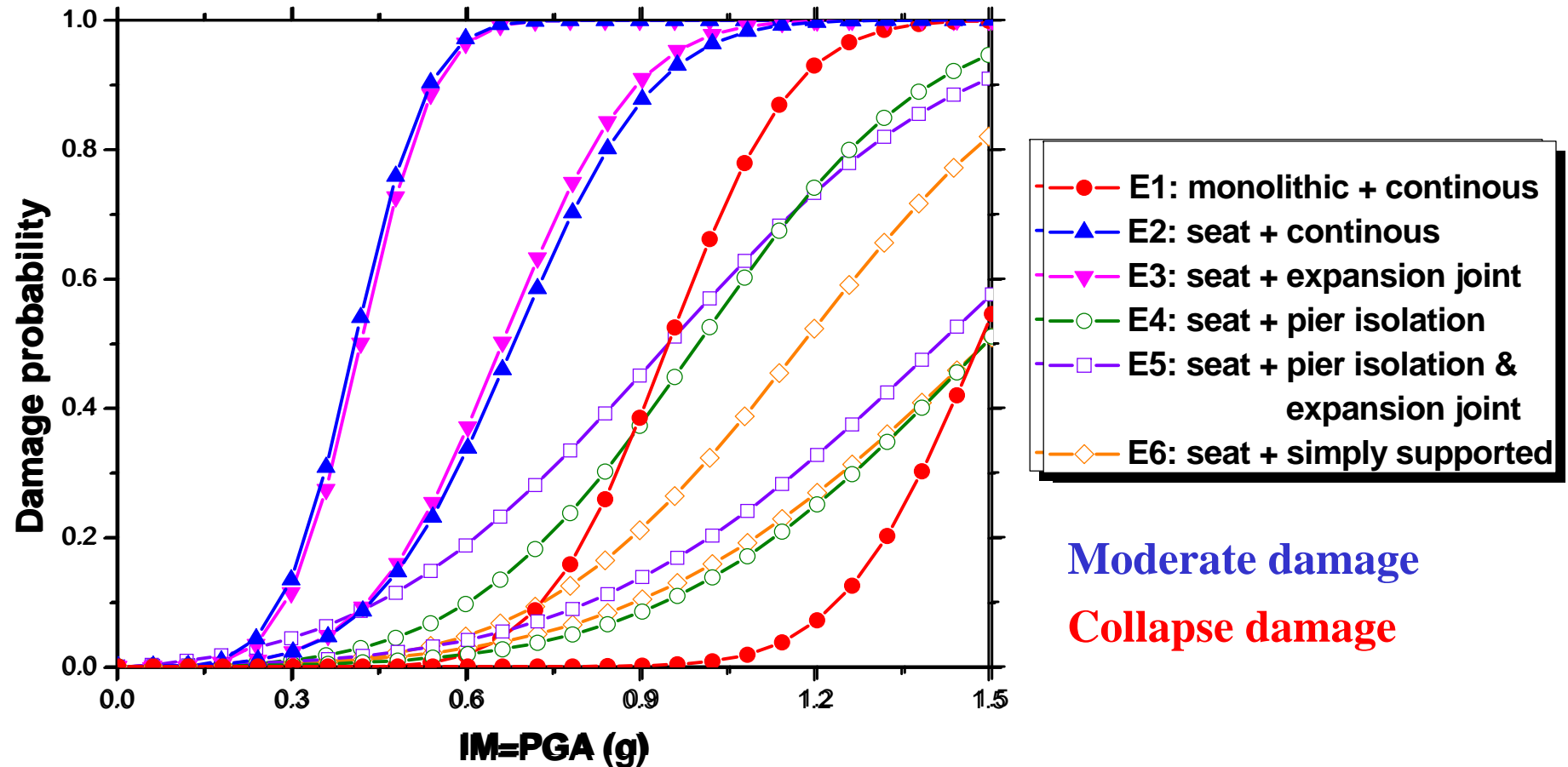


E5: Seat Abutment & Continuous (with expansion joint and pier isolation)



E6: Seat Abutment & Simply supported pin connection

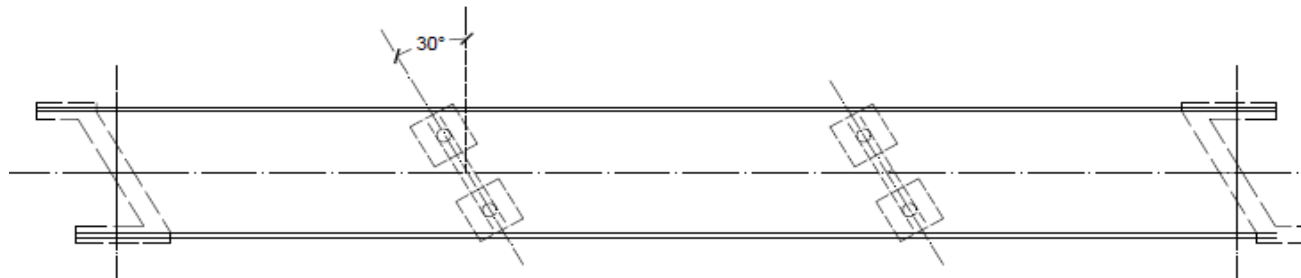
Fragility Results and Interpretation



- ❑ Seat-type abutments underperform monolithic abutments
- ❑ Seismic isolation is beneficial

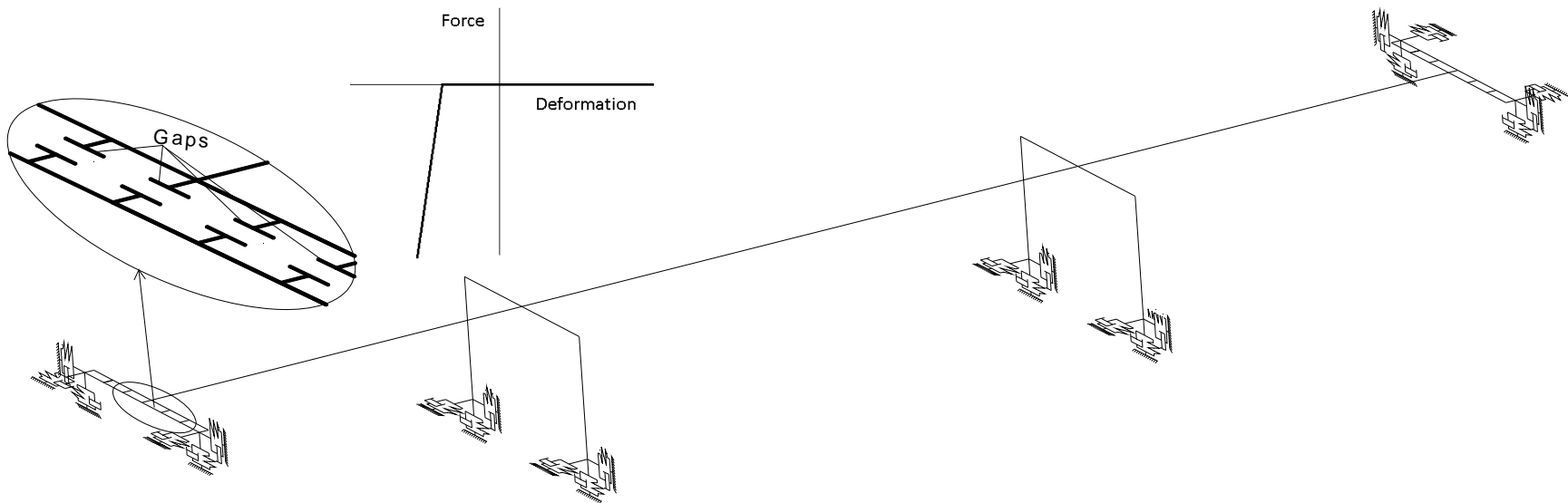
Coupled Pounding and Skew Alignment Behavior

- ❑ Pounding occurs between adjacent spans during earthquakes due to out-of-phase vibration
- ❑ Pounding results in acceleration spikes of bridge decks and local damages in various components
- ❑ Discrepancies on the pounding effects at the global level
 - Causes additional damages, with pounding force.
 - Reduces bridge damages, due to resonance disruption.
 - Either beneficial and detrimental, case sensitive.
 - Makes little global influence.
- ❑ Pounding may have prominent effects in skewed bridges



Modeling of Pounding

- Use gap element with various spacing
 - Insufficient spacing: with pounding potential
 - Sufficient spacing: without pounding potential

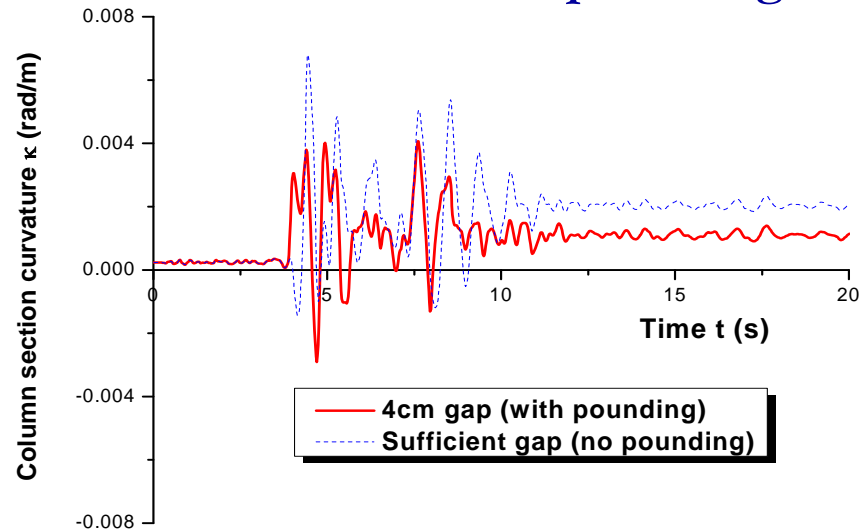


- Special attention to the source of out-of-phase vibration
 - Soil-structure interaction
 - Spatially varied motions

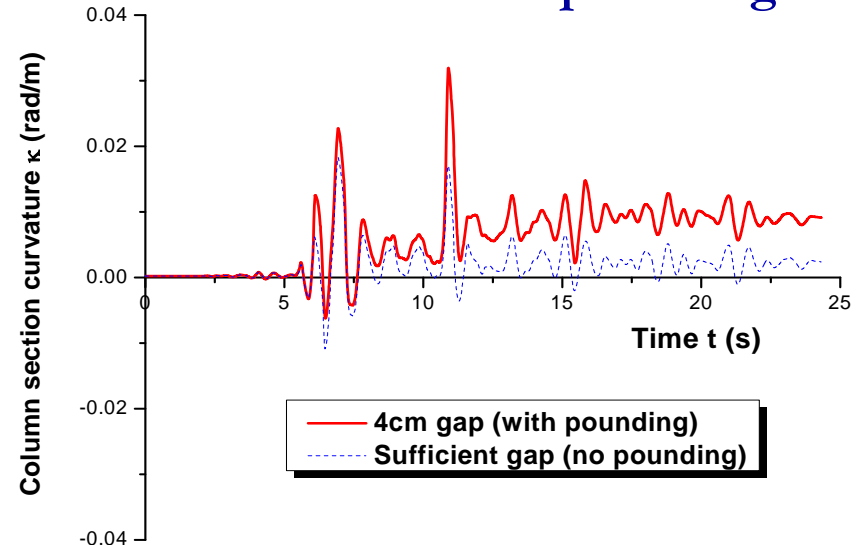
Necessity of Fragility Function Method

□ Deterministic case study

● Case 1: beneficial pounding



● Case 2: detrimental pounding

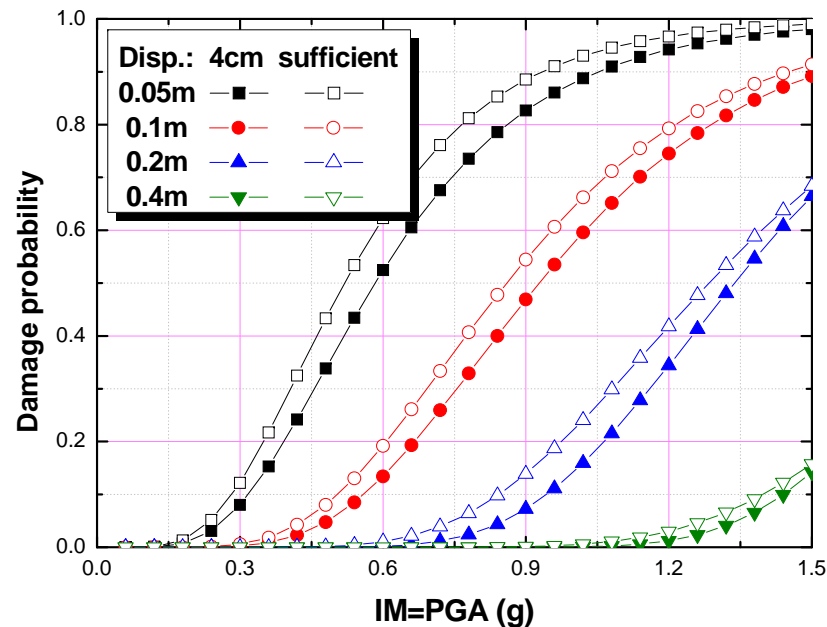


□ Fragility study

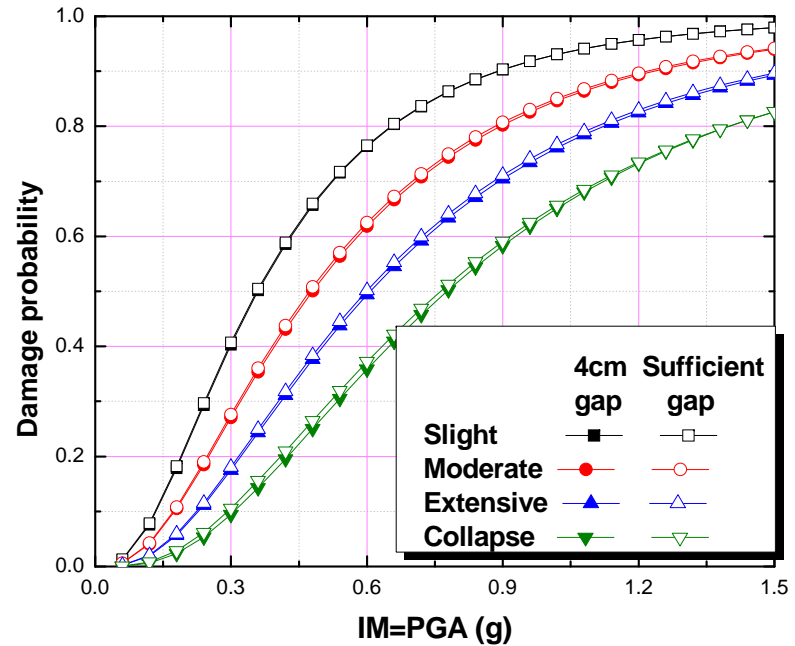
● Total 250×15 cases:

- 9.6% experiences beneficial pounding;
- 33.3% without pounding happening;
- 57.1% has detrimental pounding.

Pounding Behavior in Straight Bridge



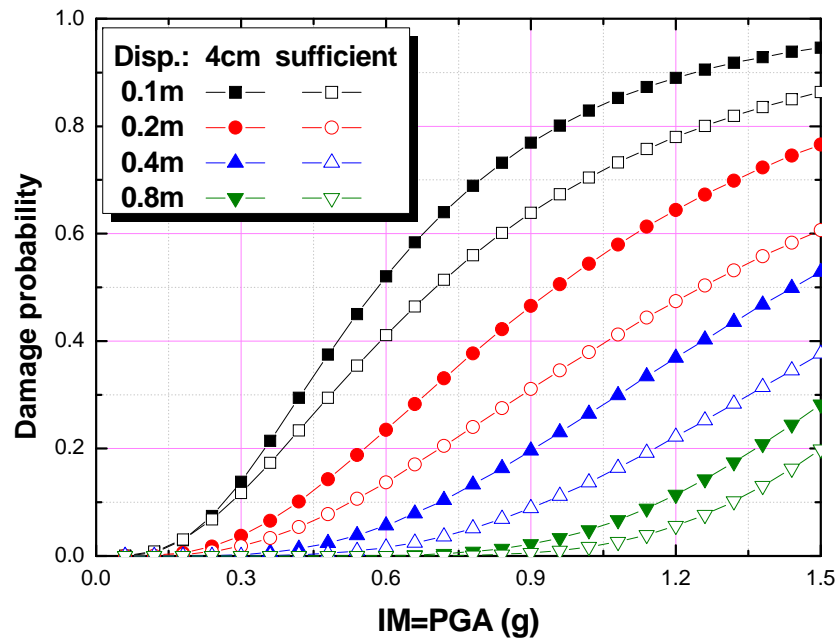
Longitudinal displacement



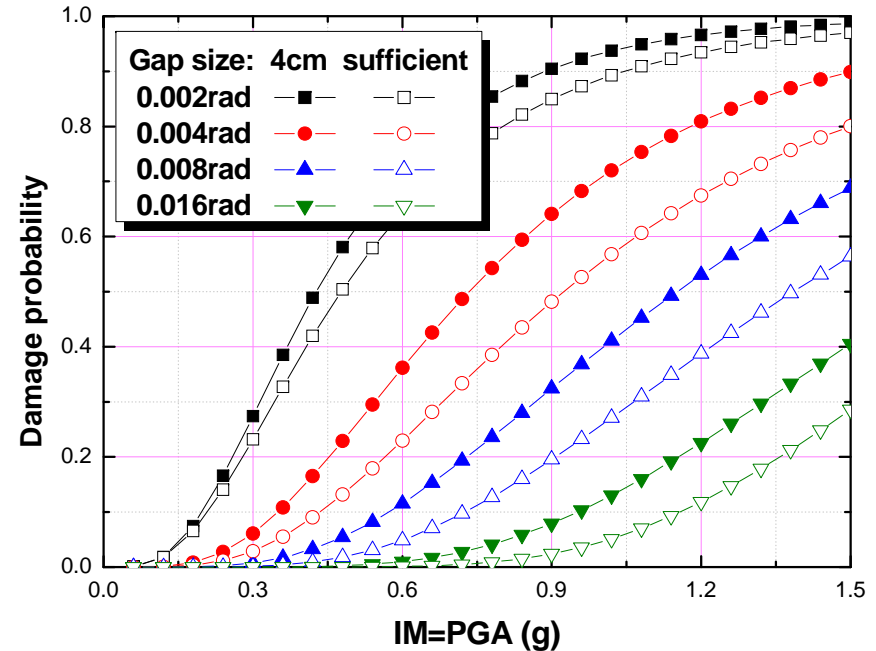
Pier damage

- ❑ Pounding reduces the longitudinal displacement.
- ❑ Pounding makes a little benefit in pier column.

Pounding Behavior in Skewed Bridge: Displacement

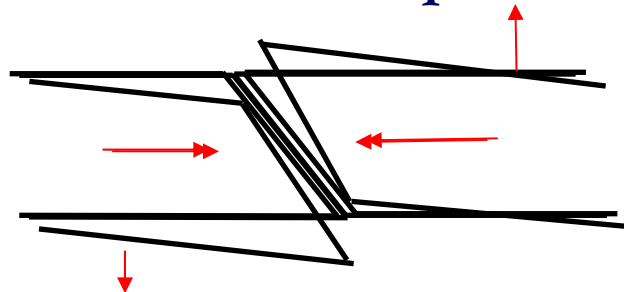


Transverse displacement

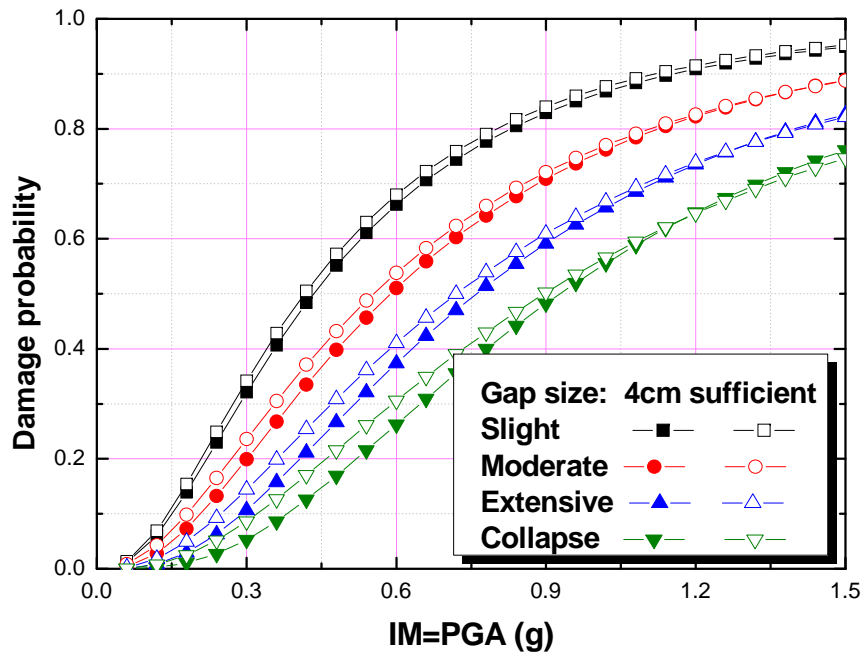


Deck rotation

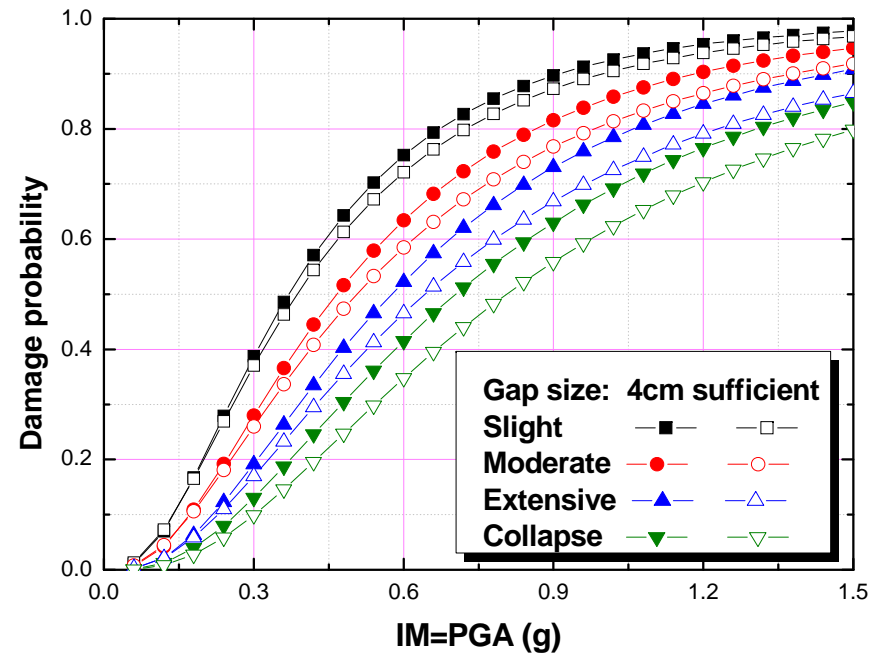
□ Pounding causes more transverse displacement and deck rotation.



Pounding Behavior in Skewed Bridge: Pier Damage



Left column



Right column

- ❑ With pounding, one of the pier columns damage is reduced a little bit, and the other one is increased.
- ❑ The total damage is increased.

Outline

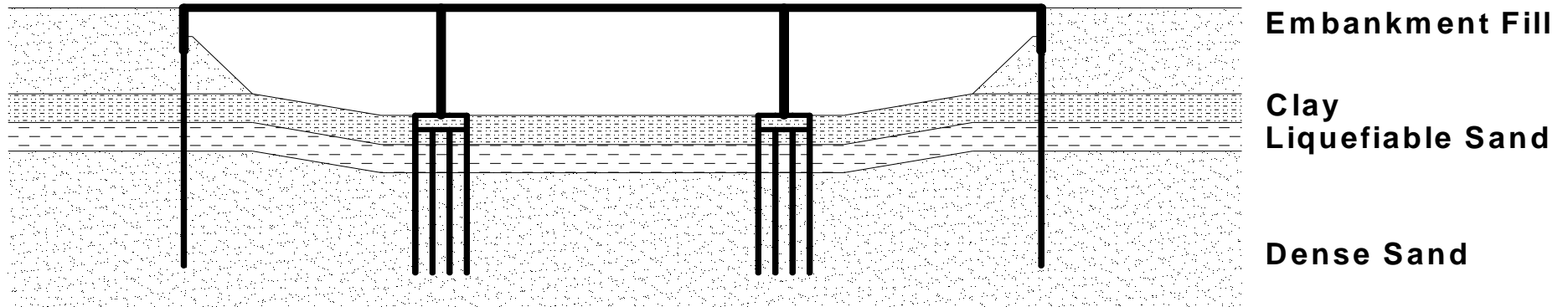
□ Fragility Functions of Bridges under Seismic Shaking

- Methodology for deriving fragility functions
 - Probabilistic Seismic Demand Analysis (PSDA)
 - Incremental Dynamic Analysis (IDA)
 - Composite Damage Index (DI)
- Effects of structural characterizations on fragility functions

□ Fragility Functions of Bridges under Lateral Spreading

- Uncertainties in soil and foundation properties
- Monte Carlo Simulation
- FOSM Method
- Effects of Structural characterizations on fragility functions

Probabilistic Parameters for Lateral Spreading



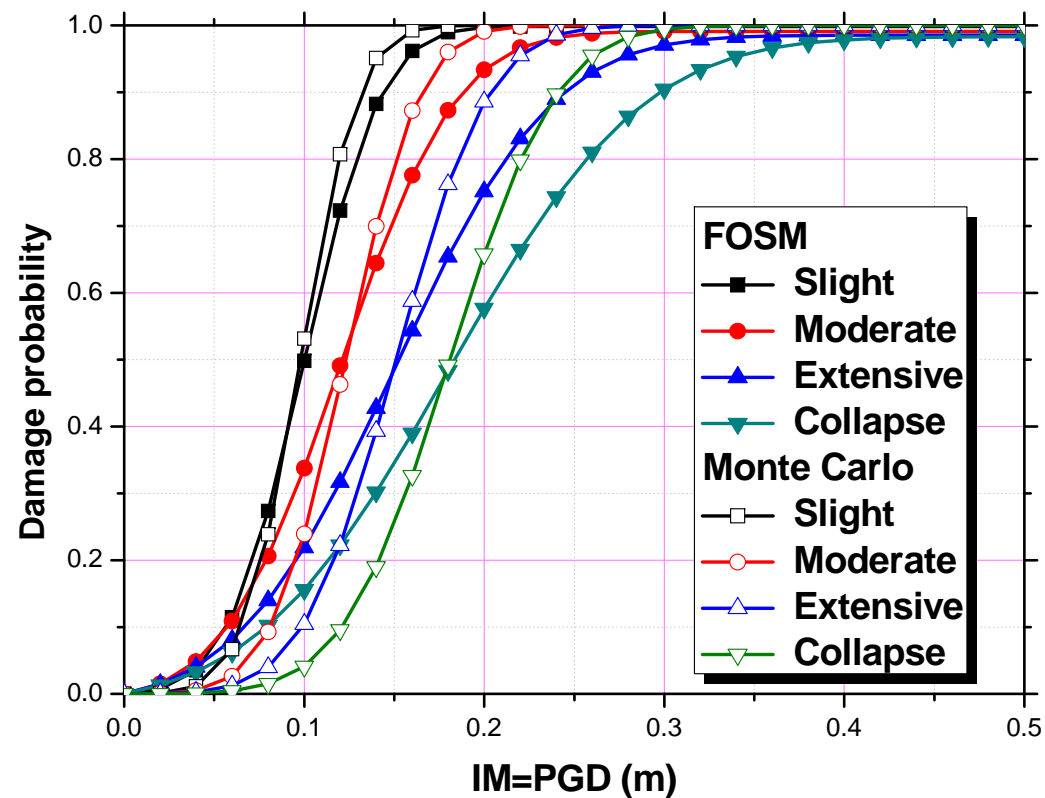
Parameter		Median	Negative Variation	Positive Variation	Distribution
Crust thickness	Embankment	6.0m	4.5m	7.5m	Normal
	Insitu clay	3.0m	1.5 m	4.5m	
Material strength		$\Phi'_{sand}=38^\circ$ $c'_{sand}=20$ kPa $c_{clay}=70$ kPa	Median \times 0.46	Median \times 2.17	Lognormal
$\Delta_{sand}/\Delta_{crust}$		0.5	0.16	0.84	Uniform
Liquefied sand m_p		0.050	0.025	0.075	Normal
y_{50} for p-y springs	Embankment	$y_{50}=0.20$ m	Median \times 0.5	Median \times 1.5	Normal
	Insitu clay	$y_{50}=0.05$ m			
Axial capacity		$Q_{tip}=1020$ kN	Median \times 0.5	Median \times 1.5	Normal
Inertia load		$a=0.4g$	$a=0.2g$	$a=0.6g$	Normal
Liquefied sand thickness		2.0m	1.0m	4.0m	Lognormal

Fragility Function Using Static Procedure

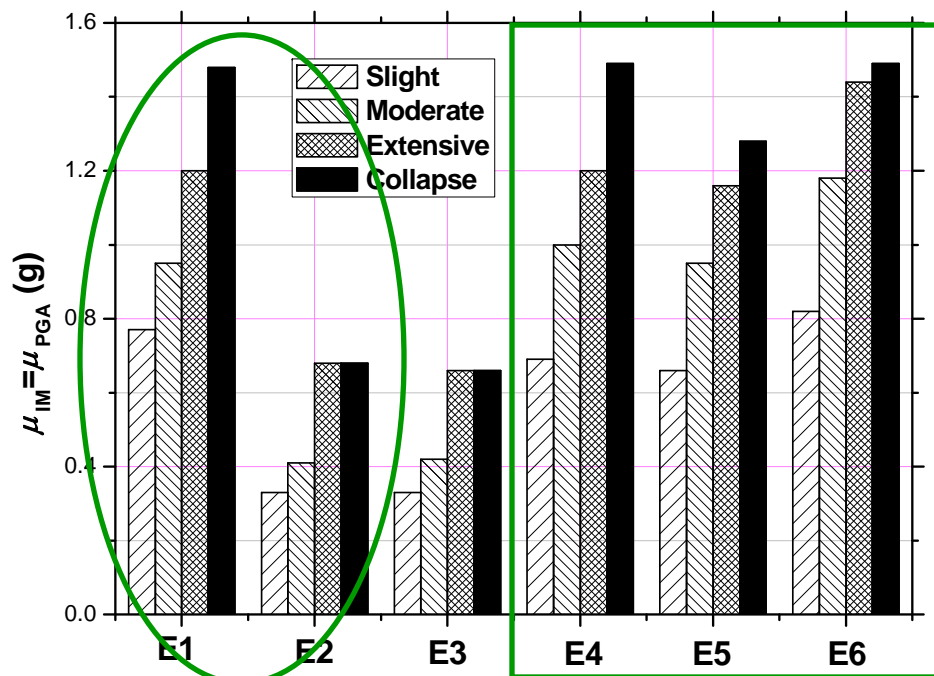
□ First order second moment (FOSM)

$$\mu_M = M(\mu_{x_1}, \mu_{x_2}, \dots, \mu_{x_n}) \quad \sigma_M = \sqrt{\sum_{i=1}^n \left(\frac{\partial M}{\partial x_i} \right)^2 \sigma_{x_i}^2}$$

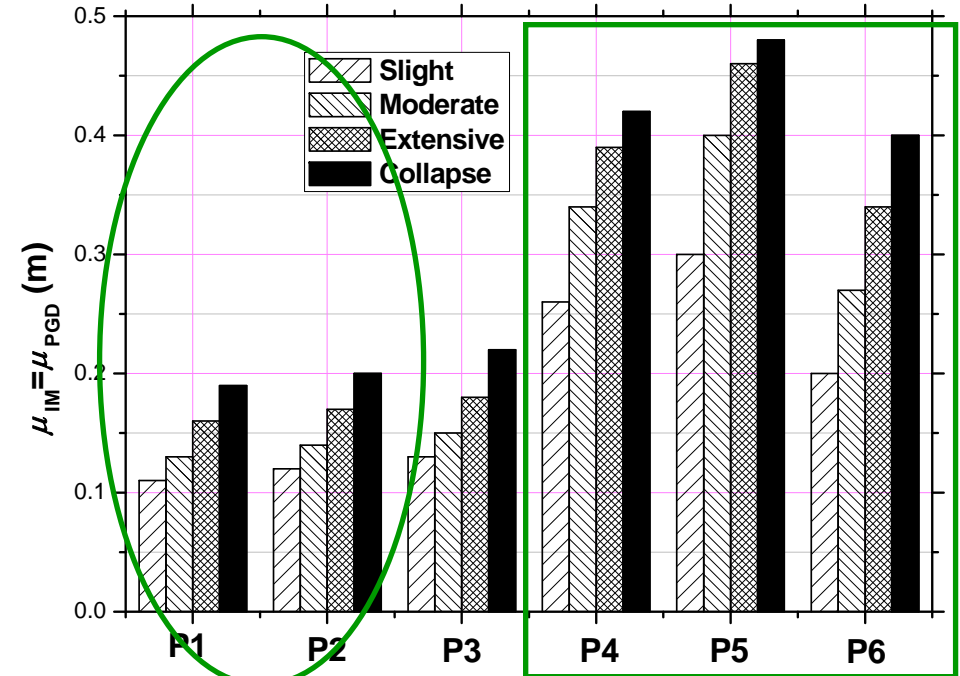
□ Monte Carlo



Effects of Structural Characterizations



Non-liquefaction cases



Liquefaction cases

- ❑ Some structure characteristics have different effects on bridge performance against seismic shaking and lateral spreading.
- ❑ Seismic isolation is consistently beneficial for both situations.

Optimum Seismic Isolation Design for Bridges Using Fragility Function Method

Contributors:

Yili Huo (Ph.D. Student)

Professor Jian Zhang

The research presented here was funded by PEER Transportation and Lifeline Programs

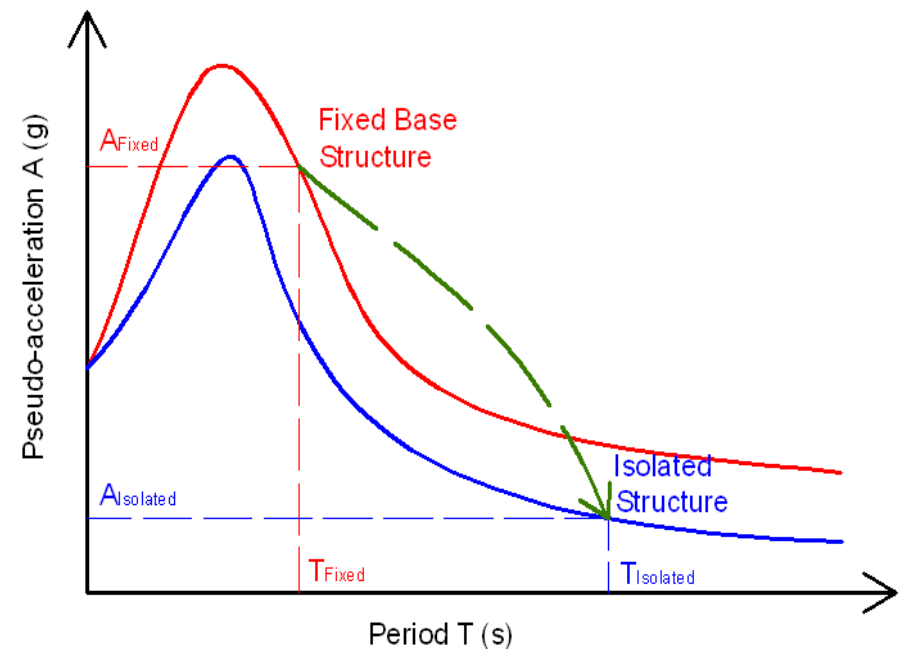
Background Information

□ Highway bridges

- Crucial component of transportation network
- Susceptible to damages under major earthquakes
- Significant direct and indirect economic impact

□ Seismic isolation can be used to improve seismic performance of bridges

- Lengthen the fundamental period of bridge to avoid the dominant frequency of earthquake input
- Provide additional damping into the bridge system



Issues in Seismic Isolation Design

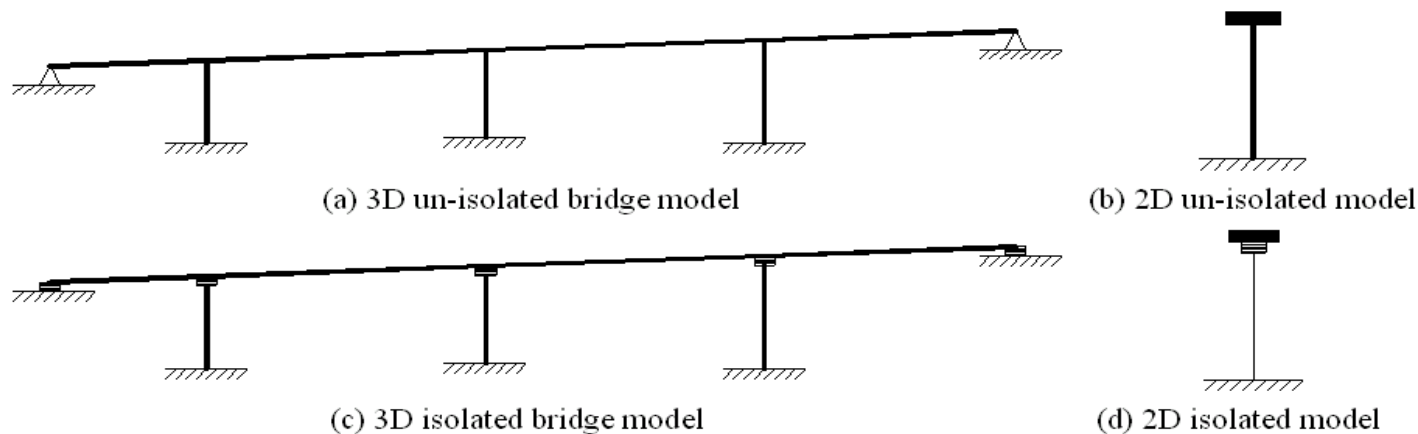
- ❑ Isolation devices possess various mechanical properties
 - Highly nonlinear, sometimes frequency dependent
- ❑ Seismic responses of isolated bridges depend on
 - Structural/geotechnical parameters
 - Ground motion characteristics
 - Mechanical properties of isolators
- ❑ Selection of isolation parameters to achieve the optimum design should consider:
 - Uncertainties in ground motions
 - Variability of structural characteristics
 - System level performance (soil-structure interaction etc.)
 - Performance objectives



Fragility Function Method

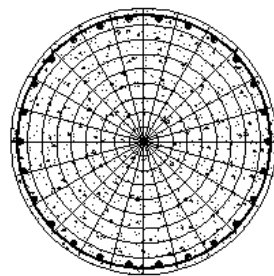
Numerical Model of Bridge

□ Prototype Bridge: Mendocino Overcrossing

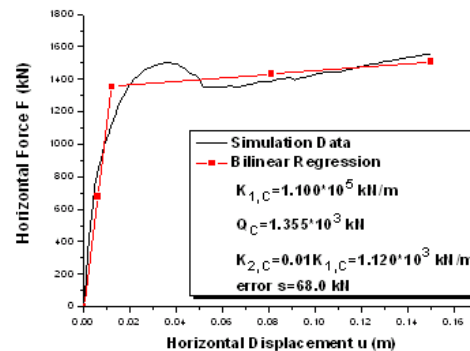


□ Structural elements in OpenSees

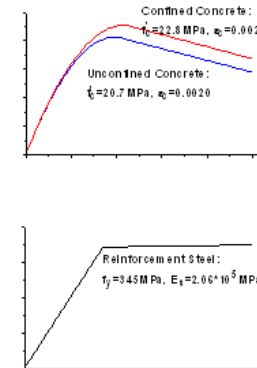
- Fiber section element for pier column; Elastic beam element for deck



(a) Fiber section



(b) Force-displacement relation

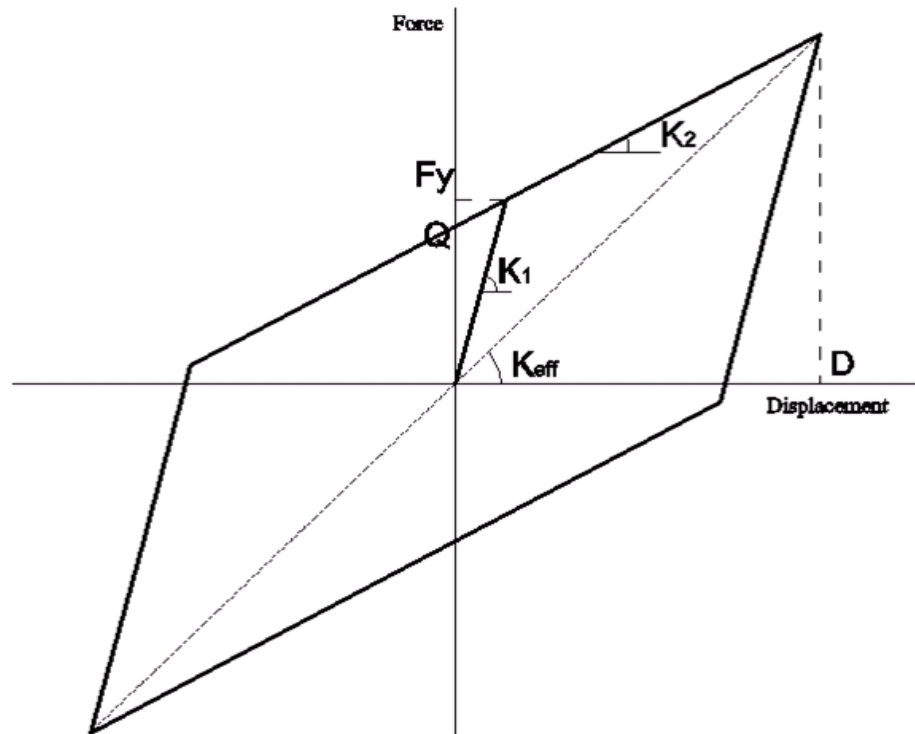


(c) Material properties

Numerical Model of Isolation Devices

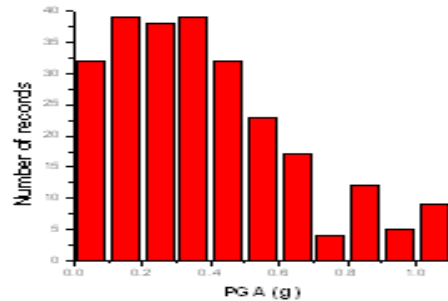
- Most common types of isolation devices
 - Elastomeric Rubber Bearing (ERB)
 - Lead Rubber Bearing (LRB)
 - Friction Pendulum System (FPS)
- Mechanical properties of isolation devices

	$K_1 = NK_2$ ($N = 5 - 15$)
ERB	Q : From hysteresis loop
	$K_2 = GA / \sum t_r$
	$K_1 = NK_2$ ($N = 15 - 30$)
LRB	$F_y = f_y A_{Lead}$
	$K_2 = (1.15 \sim 1.20) GA / \sum t$
	$K_1 = NK_2$ ($N = 50 - 100$)
FPS	$Q = \mu W$
	$K_2 = W / R$

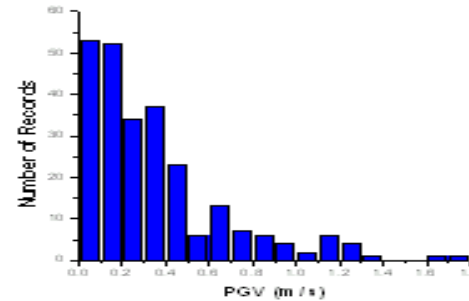


Earthquake Hazard Definition

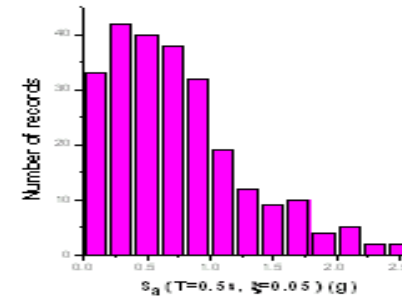
□ Selection of earthquake records: 250 ground motions



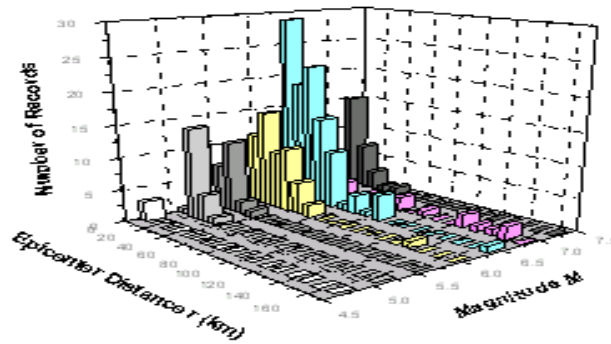
(a) PGA



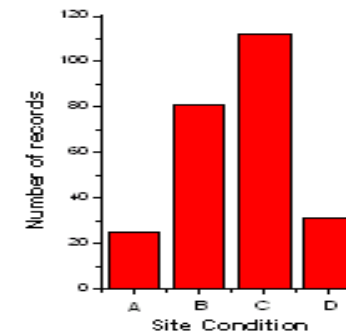
(b) PGV



(c) S_a ($T=0.5s, \zeta=0.05$)



(d) (M, r)



(e) Site Condition

Properties of selected earthquake records

□ Intensity Measure: Peak ground Acceleration (PGA)

- PGA is proved as one of several good *IMs*: *PGA*, *PGV*, *S_a(T)* etc.
- Structure-dependent *IMs* are not fair for comparing structure capacity.
- PGA is more widely used in engineering practical and hazard analyses.

Structural Damage Index Definition

□ Structural damage

- Damage states: slight, moderate, extensive and collapse (Hazus 1999)
- Component level *EDP* and *LS*: pier and bearing

	EDP or DI definition	Slight damage (DS=1)	Moderate damage (DS=2)	Extensive damage (DS=3)	Collapse damage (DS=4)
Pier column (Choi et al, 2004)	Section ductility μ	$\mu > 1$	$\mu > 2$	$\mu > 4$	$\mu > 7$
Bearing	Shear strain γ	$\gamma > 100\%$	$\gamma > 150\%$	$\gamma > 200\%$	$\gamma > 250\%$

- System level: composite DI

- Serial assumption: (Nielson and DesRoches, 2007)

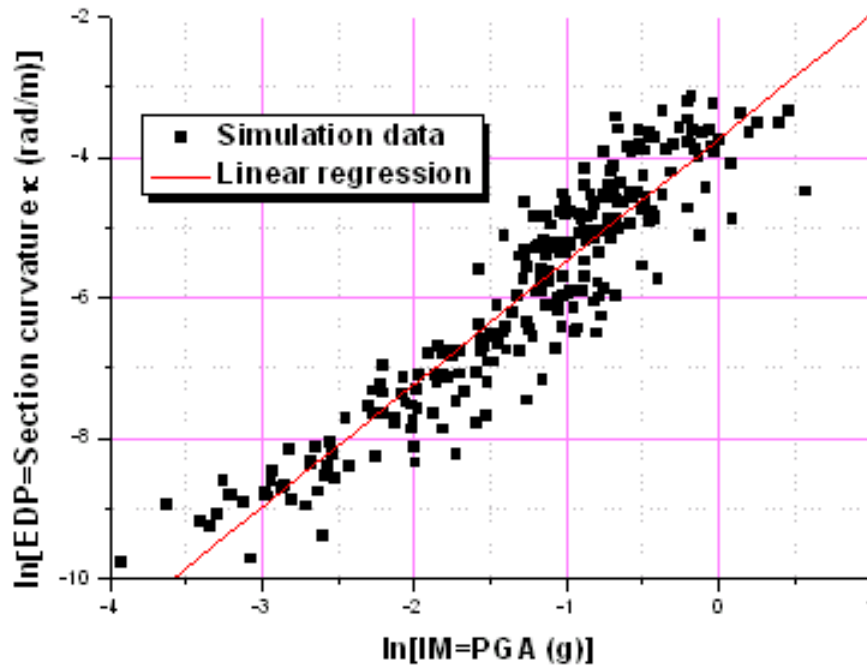
$$DS_{System} = \max(DS_{Pier}, DS_{Bearing})$$

- Parallel assumption: $DS_{System} = \min(DS_{Pier}, DS_{Bearing})$

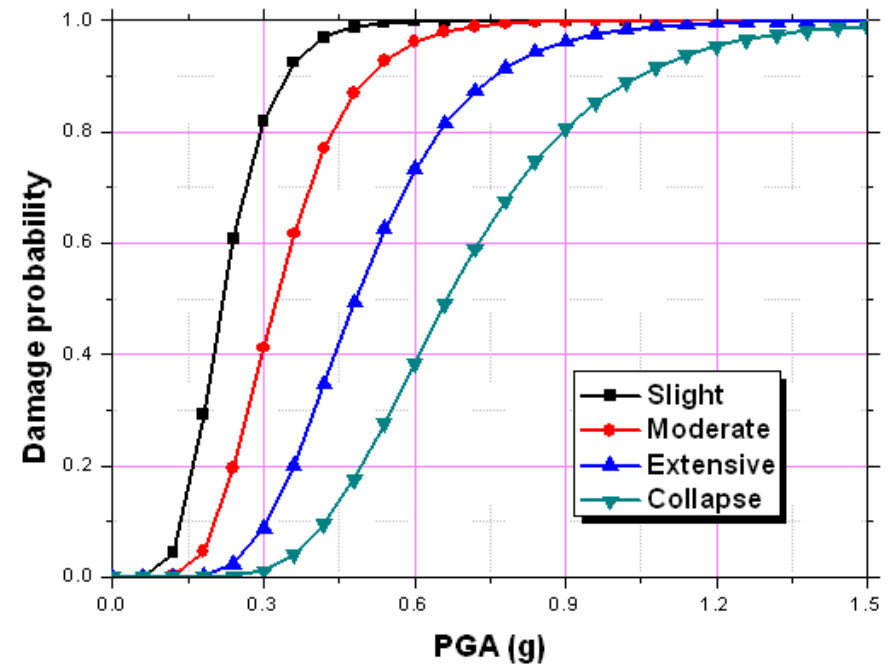
- Composite DI (this study): considering different importance of components

$$DS_{System} = \begin{cases} \text{int}(0.75 \cdot DS_{Pier} + 0.25 \cdot DS_{Bearing}) & DS_{Pier}, DS_{Bearing} < 4 \\ 4 & DS_{Pier} \text{ or } DS_{Bearing} = 4 \end{cases}$$

PSDA Fragility Analysis of Un-Isolated 3D Model



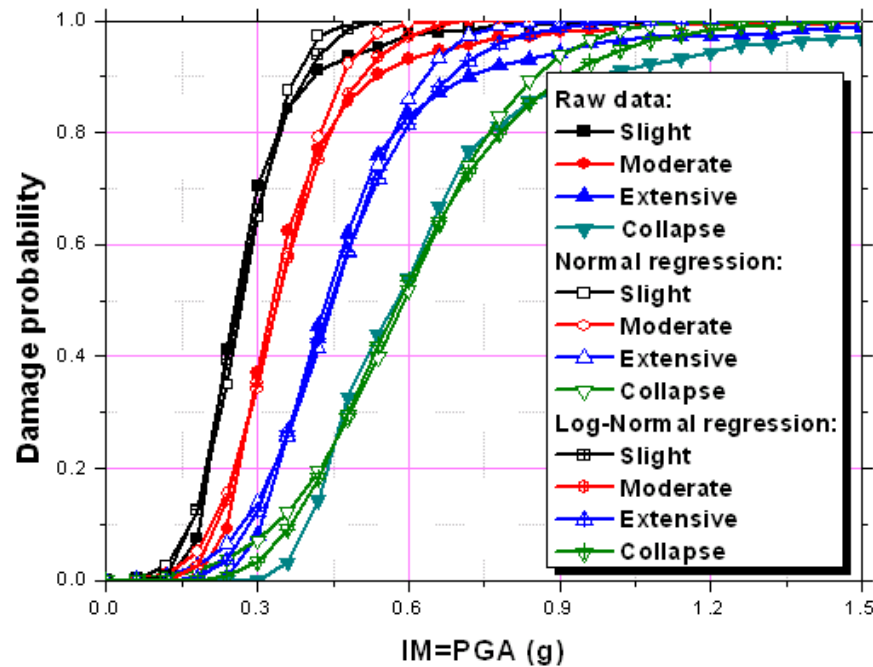
Data and Regression



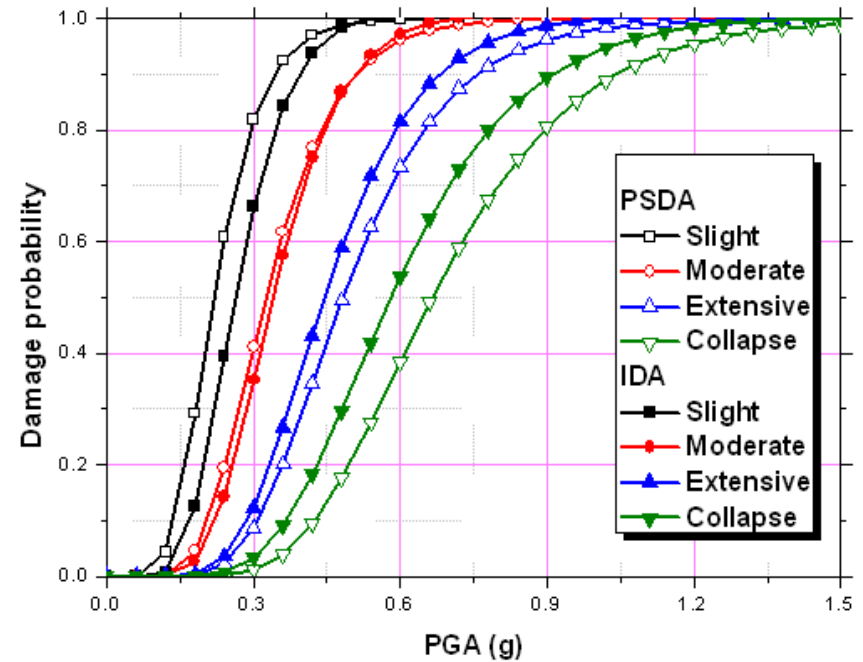
Fragility Curves

	Slight damage ($DS=1$)	Moderate damage ($DS=2$)	Extensive damage ($DS=3$)	Collapse damage ($DS=4$)
LS (rad/m)	$1.673e-3$	$3.346e-3$	$6.692e-3$	$11.711e-3$
$\ln(LS)$	-6.393	-5.700	-5.007	-4.447
μ_{IM} (g)	0.22	0.32	0.48	0.66

IDA Fragility Analysis of Un-Isolated 3D Model



IDA curves and regression



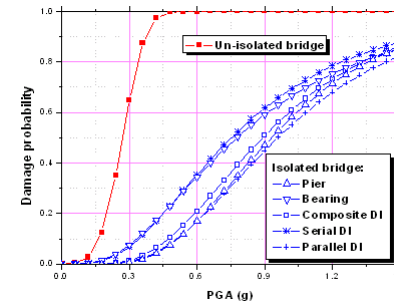
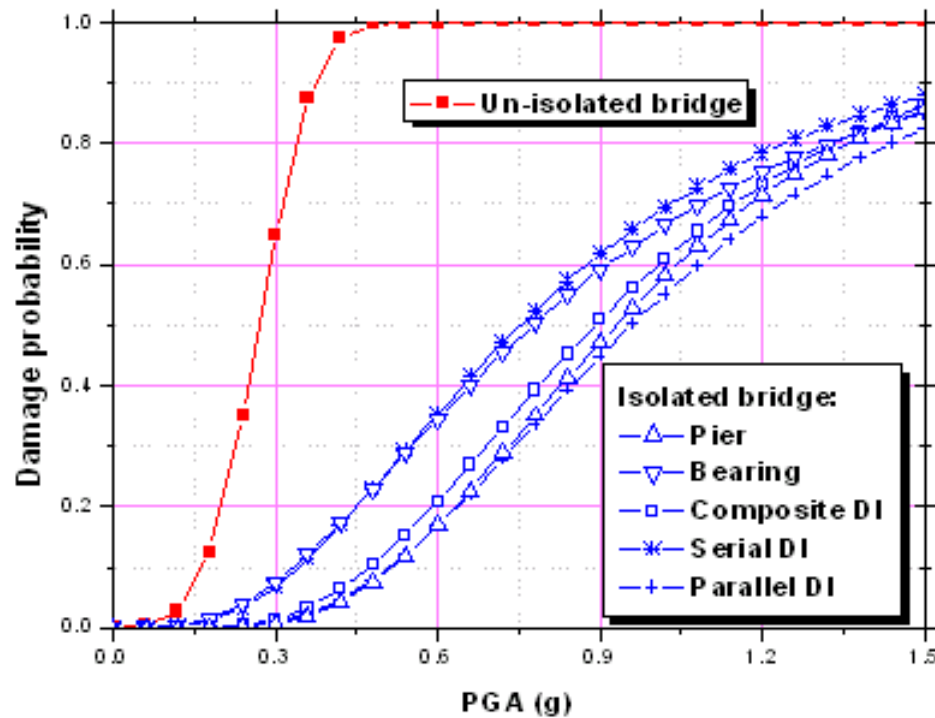
PSDA vs. IDA

□ Mean IM for achieving specified damage states

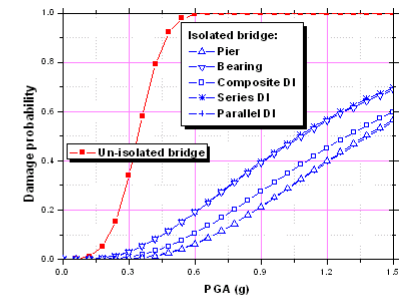
		$DS=1$	$DS=2$	$DS=3$	$DS=4$
PSDA	$\lambda_{IM}(g)$	0.22	0.32	0.48	0.66
	$\xi_{EDP/IM}$	0.61	0.61	0.61	0.61
IDA	$\lambda_{IM}(g)$	0.30	0.37	0.48	0.61
	ξ_{IM}	0.30	0.30	0.32	0.34

Fragility Analysis of Isolated 3D Model (IDA)

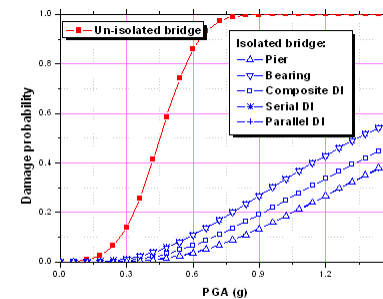
- Isolation design: $K_{1,B}/K_{1,C}=0.65$, $Q_B/Q_C=0.85$, $K_{2,B}/K_{1,B}=1/50$



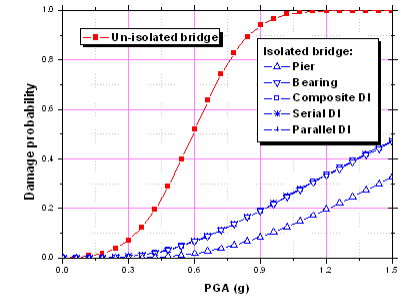
(a) Slight damage



(b) Moderate damage



(c) Extensive damage



(d) Collapse damage

- Isolation significantly reduces bridge damages.
- Composite *DI* is needed for global damage state

Effect of Q_B and $K_{1,B}$

□ Parametric study

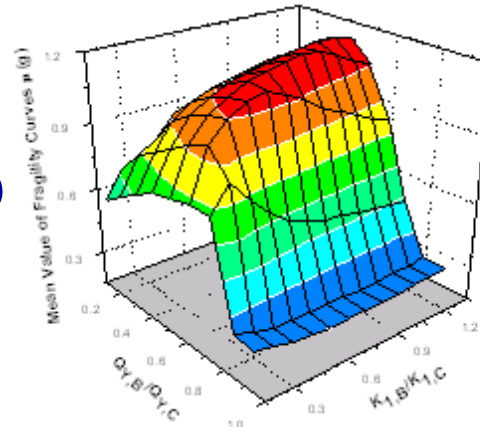
- $N=K_{1,B}/K_{2,B}$:
10, 30, 50, 70 (ERB-FPS)
- $K_{1,B} : 0.15-1.65K_{1,C}$
- $Q_B : 0.15-0.95Q_C$

□ Optimal values ($N=30$)

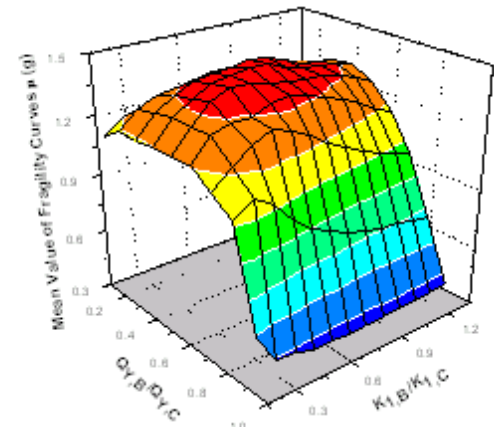
(Peak point of the surfaces)

$$K_{1,B}/K_{1,C}=0.85$$

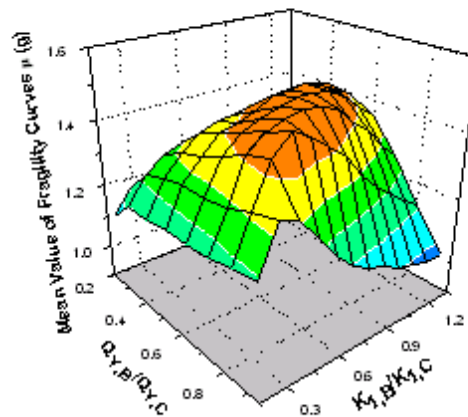
$$Q_B/Q_C=0.55$$



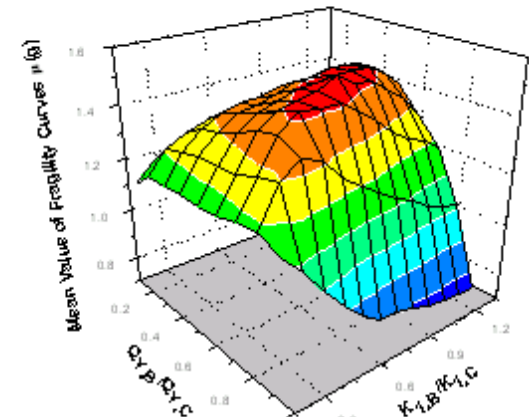
(a) Slight damage



(b) Moderate damage



(c) Extensive damage



(d) Collapse damage

$N=30$

Optimal Parameters of Q_B and $K_{1,B}$

□ Optimal parameters

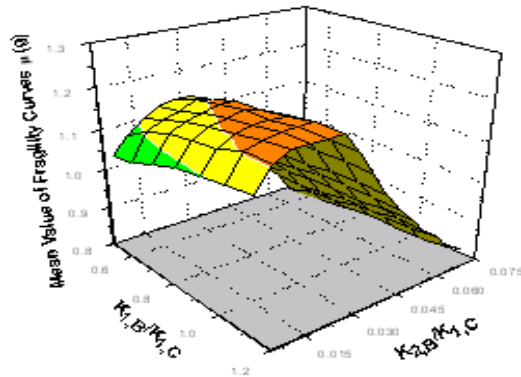
Stiffness ratio $N=K_{2,B}/K_{1,B}$		10	30	50	70
Slight	Q_B/Q_C	0.45	0.55	0.55	0.55
	$K_{1,B}/K_{1,C}$	0.35	0.85	1.25	1.55
Moderate	Q_B/Q_C	0.45	0.45	0.45	0.45
	$K_{1,B}/K_{1,C}$	0.25	0.65	1.05	1.35
Extensive	Q_B/Q_C	0.45	0.45	0.65	0.65
	$K_{1,B}/K_{1,C}$	0.35	0.85	1.15	1.55
Collapse	Q_B/Q_C	0.45	0.65	0.65	0.65
	$K_{1,B}/K_{1,C}$	0.35	0.75	1.15	1.65

□ Discussion

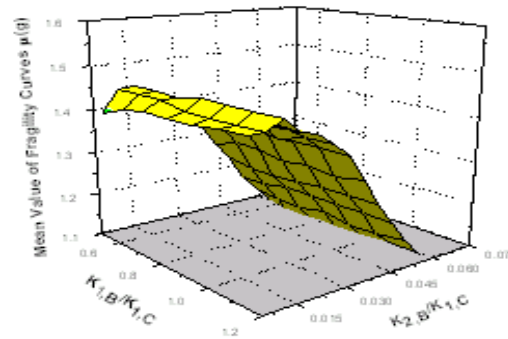
- Q_B is around $0.55Q_C$.
- Optimal $K_{1,B}$ increase with N . Since $K_{2,B}=K_{1,B}/N$, probably there is an optimal $K_{2,B}$ but $K_{1,B}$ is not important.

Effect of $K_{1,B}$ and $K_{2,B}$

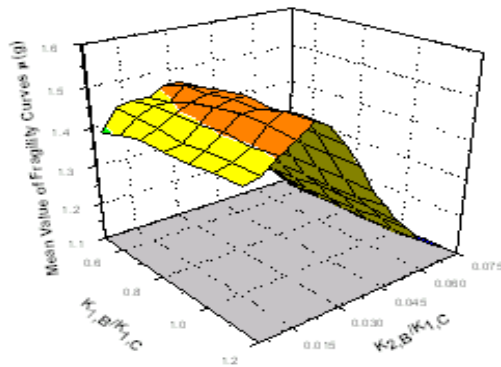
- $Q_B=0.55Q_C$ and vary $K_{2,B}$, $K_{1,B}$ independently



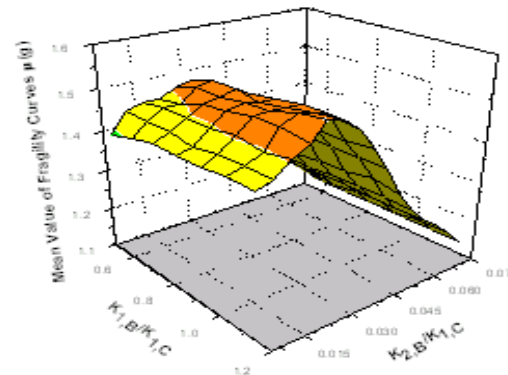
(a) Slight damage



(b) Moderate damage



(c) Extensive damage



(d) Collapse damage

- $K_{1,B}$ has no obvious influence if $Q_B=0.55Q_C$ and $K_{1,B}$ is in the range $0.4-1.2K_{1,C}$. Optimal $K_{2,B}$ is about $0.025K_{1,C}$.

Optimal Isolation Design Based-on Structural Period

□ Structures with other periods

Structural periods T (s)		0.35	0.45	0.55	0.65	0.75
Slight	Q_B/Q_C	0.55	0.55	0.65	0.75	0.85
	$K_{2,B}/K_{1,C}$	0.028	0.035	0.038	0.038	0.042
Moderate	Q_B/Q_C	0.55	0.55	0.65	0.65	0.75
	$K_{2,B}/K_{1,C}$	0.028	0.025	0.038	0.025	0.028
Extensive	Q_B/Q_C	0.55	0.75	0.55	0.85	0.85
	$K_{2,B}/K_{1,C}$	0.035	0.025	0.032	0.032	0.035
Collapse	Q_B/Q_C	0.55	0.75	0.55	0.85	0.85
	$K_{2,B}/K_{1,C}$	0.038	0.025	0.028	0.035	0.035

□ Optimal design depends on structural properties and can be achieved by: $K_{1,B}=0.4-1.2K_{1,C}$, $Q_B=0.55-0.85Q_C$, $K_{2,B}=0.025-0.040K_{1,C}$.

Conclusions

- ❑ Fragility functions of un-isolated and isolated bridges are generated using PSDA and IDA methods based on nonlinear time history analyses.
- ❑ The seismic isolation reduces the damage probability both in pier columns and bridge system as measured by a composite DI that effectively captures the system-level damages.
- ❑ Extensive parametric study was carried out under the fragility analysis framework to evaluate the damage potential of isolated bridges with various isolation devices.
- ❑ Characteristic strength and post-yielding stiffness of isolation devices exhibit optimal values to minimize the damage probability of bridges while elastic stiffness is not as important if kept in a reasonable range.

Thank you!